CLINICAL IMPLEMENTATION OF 4-DIMENSIONAL RADIOTHERAPY FOR TREATMENT OF LUNG CANCER

Klinische implementatie van 4-dimensionale radiotherapie
voor de behandeling van longkanker

René Widjai Marcel Underberg

Clinical implementation of 4-dimensional radiotherapy for treatment of lung cancer

Address for correspondence
René Underberg
Department of Radiation Oncology
VU University medical center
De Boelelaan 1117
1081 HV Amsterdam
E-mail: rwm.underberg@vumc.nl

VRIJE UNIVERSITEIT

Clinical implementation of 4-dimensional radiotherapy for treatment of lung cancer

ACADEMISCH PROEFSCHRIFT

ter verkrijging van de graad Doctor aan
de Vrije Universiteit Amsterdam,
op gezag van de rector magnificus
prof.dr. L.M. Bouter,
in het openbaar te verdedigen
ten overstaan van de promotiecommissie
van de faculteit der Geneeskunde
op woensdag 1 november 2006 om 13.45 uur
in het auditorium van de universiteit,
De Boelelaan 1105

door

René Widjai Marcel Underberg

geboren te Gainesville, Florida, Verenigde Staten van Amerika

promotoren: prof.dr. S. Senan

                prof.dr. B.J. Slotman

copromotor: dr. F.J. Lagerwaard

Voor en dankzij Ashra en mijn lieve ouders

Contents

C h a p t e r

1

Introduction and outline of the thesis

Cancer in The Netherlands

Cancer remains a major health problem. In The Netherlands around 70.000 new cases were diagnosed in 2000 and approximately 38.000 patients died from cancer [1]. Lung cancer is one of the most deadly types in both males and females. It accounts for a significant part of all cancer cases with an incidence rate of 52.4 per 100.000 in 2002, and can be regarded as a disease of the elderly, as the peak-incidence is found at the age of 70-74. Therefore, ageing of the population is expected to result in an increase in the incidence of lung cancer.

Radiotherapy

Radiotherapy is an important modality in the treatment of cancer. It is estimated that 50% of all cancer patients undergo radiotherapy as part of their treatment. Radiotherapy can be applied as a single (local) treatment modality. It can be used following surgery to destroy cancer cells that were not removed, or prior to surgery to "shrink" a previously inoperable tumor to enable surgical excision. Chemotherapy and radiation therapy may also be combined for the effective treatment of cancer. Finally, radiotherapy can be used to relieve symptoms of incurable cancer, such as bleeding or pain.

External beam radiotherapy

The current routine for external beam radiotherapy planning and delivery is commonly referred to as 3-dimensional conformal radiotherapy (3DCRT). 3DCRT makes use of multiple radiation fields that are closely tailored to the shape of the planning target volume to deliver a homogeneous dose, while limiting the radiation dose to surrounding normal tissues [2-4]. Many steps are involved in the external beam radiotherapy process, and the overall accuracy can be affected by errors at each step. In many cases immobilization devices are used to establish reproducible patient positioning during treatment planning and daily treatments [5]. Next, a computerized tomography (CT) scan of the region of interest is performed in the patient's treatment position in order to use the 3D anatomy for treatment planning. The planning CT scan is usually acquired during normal free-breathing as patients commonly undergo daily irradiation under the same condition. Digitally reconstructed radiographs (DRR) are generated from the CT dataset, and can be used as a template for verification of the patient's position during treatment. To define a common point of reference between

the actual anatomy and its 3D representation ink marks are made on the patient's skin (tattoos). Furthermore, ink marker lines are placed on the patient's skin with use of the laser alignment system. The CT data is imported into the treatment planning software. The radiation oncologist then contours the gross tumor volume (GTV). This consists of all clinically macroscopic disease, including that which is visible on imaging modalities [6], and (if indicated) the adjacent organs at risk (OAR) on all axial CT images.

Several safety margins must be added to the GTV in order to establish adequate treatment (Figure 1). These margins account for microscopic tumor extension (clinical target volume; CTV) and geometric uncertainties such as patient movement, positioning uncertainties, and organ motion (planning target volume; PTV) [5, 7, 8]. The International Commission on Radiation Units and Measurements (ICRU) Report 62 [9] furthermore recommends the use of an internal target volume (ITV) to account for variations in size, shape, and position of the CTV (Figure 2). Information about the amount and nature of the CTV motion is essential for the determination of the internal margin size.

Figure 1. Illustration of different target volumes derived from the GTV
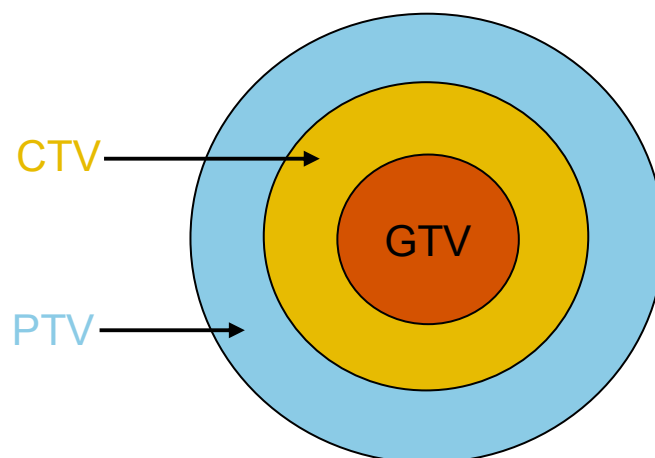
Figure 2. Target definition according to the recommendations in ICRU Report 62 [9]
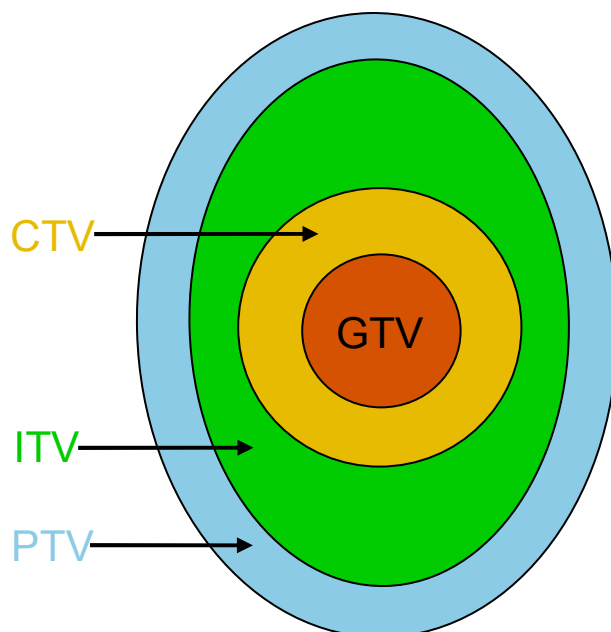
Based on the PTV and OAR's, a treatment plan is generated by optimizing the number of beams used, the beam angles, beam weights and beam energies. A treatment plan is regarded optimal when a homogeneous dose delivery to the target volume is possible, without exceeding the maximum tolerance dose of normal structures [6, 9]. The patient's treatment can commence after a suitable treatment plan is approved. Electronic portal image devices (EPID's) are frequently used to verify the accuracy of daily patient treatment. EPID's are generated using the exit radiation dose in order to obtain 2-dimensional images of the patient's anatomy, and accuracy of patient setup is determined by comparison with DRR's.

The ultimate goal is to exactly reproduce the entire setup, i.e. the patient's positioning during CT scanning and the beam geometry that was generated with treatment planning, in order to deliver the prescribed dose to the intended anatomy.

Geometric uncertainties in radiotherapy
In recent years, radiotherapy treatment planning has increasingly used conformal techniques, and a high level of geometric accuracy is required to ensure delivery of the prescribed dose to the target volume. The most important causes of geometric

uncertainties in radiotherapy are 1) variations in delineation of target volumes, 2) setup errors, and 3) organ motion. Errors arising from these geometric uncertainties can be divided into systematic errors, which are repeated during all fractions, and random errors, which can vary between treatments fractions. As random errors will point in different directions for different fractions, they generally have a smaller impact upon the delivered dose than systematic errors. Random errors will cause blurring of the dose distribution [10], and lead to a small decrease in the dose at the edge of the high-dose region. However, systematic errors result in suboptimal tumor doses, because they are repeated during all fractions.

Geometric errors in target volume delineation are systematic errors and can be introduced by factors such as suboptimal imaging protocols [11], interobserver variation [12, 13] or inter-institution variation [14]. Setup errors both have a random and a systematic component, such as limited reproducibility of patient positioning due to skin motion with respect to the internal anatomy [15]. Organ and tumor motion is also an important source of geometric uncertainty [16, 17] and is the cause of both random and systematic errors. Lung tumor mobility has been reported to range from 0.6-25 mm, with motion of 10 mm or more reported in 28% of patients [18].

Approaches to address tumor mobility in radiotherapy planning
There are essentially four approaches to address the problem of tumor mobility in radiotherapy planning: 1) Use of an ITV based on 3D tumor mobility that is present during quiet respiration; 2) Breath holding-techniques; 3) Respiratory gating; and 4) Tumor-tracking. All these approaches have the aim to generate individualized target volumes.

All tumor mobility can be used to derive a planning target volume by performing multiple CT scans during quiet or forced respiration, and fusing the separate target volumes to generate an ITV [19, 20]. Furthermore, recent work has shown that the mobility of peripheral lung tumors can be fully characterized with a single 'slow' CT scan and a 5 mm expansion of the ITV [21]. However, use of the 'slow' CT technique is only applicable to tumors located in lung tissue because of the high contrast between tumor and normal lung tissue, and not for mediastinal structures [22].

A second approach to tumor mobility would be to control the target motion by attempting to actively or passively influence respiration-induced movements, which is typified by approaches such as deep-inspiration breath-hold (DIBH) [23] or active breathing control (ABC) [24]. However, up to 40% of patients with lung cancer cannot tolerate breath-holding [23].

A third approach is respiratory gating, where radiation is delivered only during a pre-defined part of the respiratory cycle in which the tumor exhibits relatively little mobility. Clinical experience with gating for liver tumors has shown that reductions in treatment margins are possible [25].

The final approach to tumor motion is the use of tracking and control systems to monitor tumor position, and to continuously adapt radiation fields during free breathing. Fiducial markers that are implanted in, or adjacent to, hepatic and lung lesions have been used for fluoroscopic tracking of the target volume during radiotherapy [26]. However, the insertion of markers carries all the risk of an invasive procedure and markers are often placed next to instead of in the tumor. The placement of at least 3 tumor markers is required to identify rotational movements [27], but this is seldom possible.

4-dimensional radiotherapy

A potential solution for the problem of respiration-induced mobility is 4-dimensional radiotherapy, in which respiratory movement is accounted for during imaging, planning and treatment execution [28]. This approach requires a respiration-correlated CT (4DCT) scan in which changes in position and shape of the internal anatomy of a patient are quantified as a function of the respiratory cycle. The corresponding respiratory phase at the time of image acquisition is digitally 'stamped' on each CT image. Once the 4DCT scan is performed, 4D software automatically sorts the images into individual 3D image sets, each representing the entire patient's anatomy during a single respiratory-phase. This enables tumor and organ movement to be visualized, and utilized for determination of individualized margins for treatment planning. Such an approach can be combined with breath-holding, gated irradiation and can also be used to generate target volumes in which all respiration-induced mobility is incorporated.

Aims of this thesis

This thesis describes the early clinical evaluation of 4DCT scanning using a multi-slice CT, in order to optimize target definition in non-small cell lung cancer (NSCLC). The geometric and dosimetric outcomes of target definition in stage I NSCLC using three different CT scanning protocols, including 4DCT, are evaluated in Chapter 2. The use of 4DCT scans increases by ten-fold or greater the amount of data that are used for generating target volumes. As manual GTV delineation in up to ten 4D datasets significantly adds to the clinical workload, the use of post-processing tools was evaluated for rapid ITV generation (Chapter 3). 4DCT datasets enable tumor and normal organ mobility to be visualized as a function of the breathing cycle, thereby enabling respiratory gating to be performed in order to reduce target volumes. Chapter 4 describes the benefits of respiratory gating in extracranial stereotactic radiotherapy (ESRT) for medically inoperable stage I NSCLC, as well as simple approaches to identify patients that are suitable for this type of treatment.

ESRT enables delivery of biological effective doses of up to 180 Gy to stage I lung tumors. As target definition has to be optimal during the entire course of ESRT, the impact of inter-fractional changes of the target volume is characterized in Chapter 5.

4DCT scans also enable characterization of mobility of the hilus and the mediastinal lymph nodes, thereby permitting 4D respiration-gated radiotherapy for locally advanced lung cancer. Currently, radiotherapy for stage III NSCLC is characterized by large target volumes, as population-based margins are added to the CTV to account for organ mobility and patient setup errors during treatment. In Chapter 6 the geometric and dosimetric consequences of 4D respiratory gating in stage III NSCLC are evaluated in order to establish accurate dose delivery and limit the risk of treatment-related toxicity.

References

1. Visser O, Siesling S, van Dijck JA. Incidence of cancer in The Netherlands 1999/2000. *Utrecht: Association of Comprehensive Cancer Centers*, 2003

2. Armstrong JG, Burman C, Fontenla D, et al. Three-dimensional conformal radiation therapy may improve the therapeutic ratio of high dose radiation therapy for lung cancer. *Int J Radiat Oncol Biol Phys* 1993;26:685-6892

3. Graham M, Purdy J, Emami B, et al. Preliminary results of a prospective trial using three dimensional radiotherapy for lung cancer. *Int J Radiat Oncol Biol Phys* 1995;33:993-1000

4. McGibney C, Holmberg O, McClean B, et al. Dose escalation of CHART in non-small cell lung cancer: is three-dimensional conformal radiation therapy really necessary? *Int J Radiat Oncol Biol Phys* 1999;45:339-350

5. de Boer H, van Sörnsen de Koste J, Senan S, et al. Analysis and reduction of 3D systematic and random setup errors during the simulation and treatment of lung cancer patients with CT-based external beam radiotherapy dose planning. *Int J Radiat Oncol Biol Phys* 2001;49:8578-68

6. International Commission on Radiation Units and Measurements. *ICRU report 50: Prescribing, recording, and reporting photon beam therapy.* Bethesda, MD: ICRU 1993

7. van Sörnsen de Koste JR, de Boer HC, Schuchhart-Schipper RH, et al. Procedures for high precision setup verification and correction of lung cancer patients using CT-simulation and digitally reconstructed radiographs (DRR). *Int J Radiat Oncol Biol Phys* 2003;55:804-810

8. Stroom JC, de Boer HC, Huizenga H, et al. Inclusion of geometrical uncertainties in radiotherapy treatment planning by means of coverage probability. *Int J Radiat Oncol Biol Phys* 1999;43:905-919

9. International Commission on Radiation Units and Measurements. *ICRU report 62: Prescribing, recording, and reporting photon beam therapy* (Supplement to ICRU report 50). Bethesda, MD: ICRU 1999

10. Leong J. Implementation of random positioning error in computerised radiation treatment planning systems as a result of fractionation. *Phys Med Biol* 1987;32:327-334

11. van Sörnsen de Koste JR, Lagerwaard FJ, Schuchhart-Schipper RH, et al. Dosimetric consequences of tumor mobility in radiotherapy of stage I non-small cell lung cancer--an analysis of data generated using 'slow' CT scans. *Radiother Oncol* 2001;61:93-99

12. Fiorino C, Reni M, Bolognesi A, et al. Intra- and inter-observer variability in contouring prostate and seminal vesicles: implications for conformal treatment planning. *Radiother Oncol* 1998;47:285-292

13. Senan S, van Sörnsen de Koste J, Samson M, et al. Evaluation of a target contouring protocol for 3D conformal radiotherapy in non-small cell lung cancer. *Radiother Oncol* 1999;53:247-255

14. Ketting CH, Austin Seymour M, Kalet I, et al. Automated planning target volume generation: an evaluation pitting a computer-based tool against human experts. *Int J Radiat Oncol Biol Phys* 1997;37:697-704

15. van Herk M. Errors and margins in radiotherapy. Semin Radiat Oncol 2004;14:52-64

16. Ross CS, Hussey CH, Pennington EC, et al. Analysis of movement of intrathoracic neoplasms using ultrafast computerized tomography. *Int J Radiat Oncol Biol Phys* 1990;18:671-677

17. Roeske JC, Forman JD, Mesina CF, et al. Evaluation of changes in the size and location of the prostate, seminal vesicles, bladder, and rectum during a course of external beam radiation therapy. *Int J Radiat Oncol Biol Phys* 1995;33:1321-1329

18. Seppenwoolde Y, Shirato H, Kitamura K, et al. Precise and real-time measurement of 3D tumor motion in lung due to breathing and heartbeat, measured during radiotherapy. *Int J Radiat Oncol Biol Phys* 2002;53:822-834

19. Yamada K, Soejima T, Yoden E, et al. Improvement of three-dimensional treatment planning models of small lung targets using high-speed multi-slice computed tomographic imaging. *Int J Radiat Oncol Biol Phys* 2002;54:1210-1216

20. Lagerwaard FJ, van Sörnsen de Koste JR, Nijssen-Visser MR, et al. Multiple 'slow' CT scans for incorporating lung tumor mobility in radiotherapy planning. *Int J Radiat Oncol Biol Phys* 2001;51:932-937

21. van Sörnsen de Koste JR, Lagerwaard FJ, de Boer HC, et al. Are multiple CT scans required for planning curative radiotherapy in lung tumors of the lower lobe? *Int J Radiat Oncol Biol Phys* 2003;55:1394-1399

22. van Sörnsen de Koste JR, Lagerwaard FJ, Nijssen-Visser MR, et al. Which margins are necessary for incorporating mediastinal nodal mobility in involved field radiotherapy for lung cancer? *Int J Radiat Oncol Biol Phys* 2002, 53: 115-119

23. Rosenzweig KE, Hanley J, Mah D, et al. The deep inspiration breath-hold technique in the treatment of inoperable non-small-cell lung cancer. *Int J Radiat Oncol Biol Phys* 2000;48:81-87

24. Wong JW, Sharpe MB, Jaffray DA, et al. The use of active breathing control (ABC) to reduce margin for breathing motion. *Int J Radiat Oncol Biol Phys* 1999;44:911-919

25. Wagman R, Yorke E, Ford E, et al. Respiratory gating for liver tumors: use in dose escalation. *Int J Radiat Oncol Biol Phys* 2003;55:659-668

26. Shimizu S, Shirato O, Ogura S, et al. Detection of lung tumor movement in real-time tumor-tracking radiotherapy. *Int J Radiat Oncol Biol Phys* 2001;51:304-310

27. Murphy MJ. Tracking moving organs in real time. *Semin Radiat Oncol* 2004;14:91-100

28. Keall P. 4-dimensional computed tomography imaging and treatment planning. *Semin Radiat Oncol* 2004;14:81-90

Chapter

2

Four-dimensional CT scans for treatment planning in stereotactic radiotherapy for stage I lung cancer

René WM Underberg
Frank J Lagerwaard
Johan P Cuijpers
Ben J Slotman
John R van Sörnsen de Koste
Suresh Senan

Abstract

Purpose: Hypofractionated stereotactic radiotherapy (SRT) for stage I NSCLC requires that meticulous attention be paid towards ensuring optimal target definition. Two CT scan techniques for defining internal target volumes (ITV) were evaluated.

Methods and Materials: Ten consecutive patients treated with SRT underwent six 'standard' rapid multislice CT scans to generate an $ITV_{6\,CT}$ and one 4DCT scan that generated volumetric datasets for 10 phases of the respiratory cycle, all of which were used to generate an ITV_{4DCT}. Geometric and dosimetric analyses were performed for [a] PTV_{4DCT}, derived from the ITV_{4DCT} with the addition of a 3 mm margin, [b] $PTV_{6\,CT}$, derived from the $ITV_{6\,CT}$ with the addition of a 3 mm margin, and [c] six $PTVs_{10\,mm}$, derived from each separate $GTV_{6\,CT}$, to which a 3D margin of 10 mm was added.

Results: The ITV_{4DCT} was not significantly different from the $ITV_{6\,CT}$ in 8 patients, but was considerably larger in 2 patients whose tumors exhibited the greatest mobility. On average, the $ITV_{6\,CT}$ "missed" 22% of the volume encompassing both ITVs, in contrast to a corresponding mean value of only 8.3% for ITV_{4DCT}. Plans based upon PTV_{4DCT} resulted in coverage of the $PTV_{6\,CT}$ by the 80% isodose in all patients. However, plans based on use of $PTV_{6\,CT}$ led to a mean PTV_{4DCT} coverage of only 92.5%, with a minimum of 77.7% and 77.5% for the 2 most mobile tumors. PTVs derived from a single MSCT expanded with a margin of 10 mm were on average twice the size of PTVs derived using the other methods, but still led to an underdosing in the 2 most mobile tumors.

Conclusions: Individualized ITVs can improve target definition for SRT of stage I NSCLC, and use of only a single CT scan with a 10 mm margin is inappropriate. A single 4D scan generates comparable or larger ITVs than are generated using 6 unmonitored rapid CT scans, a finding related to the ability to account for all respiration-correlated mobility.

Introduction

The local control rates after curative radiotherapy in patients with medically inoperable stage I non-small cell lung cancer (NSCLC) have been disappointing [1]. Even the use of 3-dimensional (3D) conformal radiotherapy to doses of up to 70 Gy has failed to improve upon these results, with local failure rates still as high as 40-60% at 3 years [2]. Approaches for dose-escalation using conventional, hyper- and hypofractionated schemes have been investigated as a means of improving local control. Recent studies have reported unacceptable toxicity with conventionally fractionated doses exceeding 90 Gy [3, 4]. In contrast, several phase I/II studies using hypofractionated stereotactic radiotherapy (SRT) for stage I NSCLC have shown that high local control rates of 90% or more can be obtained with only limited toxicity, although the follow-up is relatively short in some series [5-12].

The application of high-dose radiotherapy, however, requires meticulous attention towards ensuring an optimal target definition. Recent studies have shown that individualized (i.e. 'patient-based') margins, as opposed to standard 'population-based' margins, are required for radiotherapy of lung tumors [13-15]. Approaches used for determining individualized margins include 'slow' CT scans [16, 17], and the co-registration of expiratory and inspiratory target volumes [13, 18-20].

When the extracranial SRT program for stage I NSCLC commenced at our center in April 2003, the option of performing 'slow' CT scans on the CT scanner was not available. Therefore, target definition was based on the use of 6 rapid unmonitored spiral multi-slice CT (MSCT) scans in order to generate an internal target volume (ITV), a lengthy approach that requires laborious co-registration. Recently, a 16-slice CT scanner became available, and it allowed for 4-dimensional (4D) or respiration-correlated CT scans to be performed. 4DCT scans generate spatial and temporal information on mobility in a single investigation and represent a major breakthrough in imaging for radiotherapy planning [21, 22]. In this technique described as 'retrospective gating', the respiratory waveform is synchronously recorded during CT acquisition, and multiple CT slices are acquired at each table position for at least the duration of one full respiratory cycle [23]. This yields CT datasets for 10 phases of the respiratory cycle.

We evaluated the use of 4DCT scans as the sole technique for generating ITVs for peripheral lung tumors and compared this with target volumes generated using our

routine 6-scan approach. The dosimetric consequences of treatment planning using both methods of target definition were evaluated, and compared to the use of 'standard' planning target volumes (PTVs).

Materials and Methods

Ten consecutive patients with peripheral stage I NSCLC, in whom both CT scanning techniques were performed for planning hypofractionated SRT, were included in this analysis. All patients underwent staging using an FDG-PET scan and only involved-field radiotherapy was performed. Tumor characteristics are summarized in Table 1. Five patients had lesions located in the lower lobes.

Table 1. Tumor characteristics in 10 patients.

Patient	Stage	Tumor location
A	T1N0M0	Left lower lobe, central
B	T1N0M0	Left upper lobe, adjacent to mediastinum
C	T1N0M0	Right upper lobe, subpleural
D	T1N0M0	Right upper lobe, subpleural
E	T1N0M0	Left upper lobe, subpleural
F	T1N0M0	Right upper lobe, central
G	T1N0M0	Left lower lobe, central
H	T1N0M0	Right lower lobe, central
I	T1N0M0	Right lower lobe, central
J	T2N0M0	Left lower lobe, subpleural

Multiple unmonitored CT scan technique

Our routine technique for generating ITVs for SRT of stage I NSCLC involves the performance of 1 full-length rapid conventional spiral CT scan and 5 short scans limited to the tumor region. Patients were positioned supine, with the arms positioned above the head on an adjustable arm support.

The gross tumor volumes (GTVs) were contoured on all scans, and the contours were projected onto the full-length scan. The multiple CT scans are currently performed on a 16-slice GE Lightspeed with a slice thickness of 2.5 mm and an index of 2.5 (contiguous reconstruction). No intravenous contrast is used for these CT scans, and the whole procedure generally takes about 20 minutes.

4DCT scanning technique

The 6-scan procedure was followed by a single 4DCT scan using the Varian Real-Time Position Management (RPM) respiratory gating hardware for recording the breathing pattern (Varian Medical Systems, Palo Alto, CA) and 4D imaging software (Advantage 4D, GE Medical Systems, Waukesha, WI). The patient's position was maintained between the multiple scans and the 4DCT scan, in order to minimize patient movement. Briefly, the respiratory signals from the RPM were recorded using infrared-reflecting markers on the patient's thorax during uncoached free breathing, as previously described [22, 24]. The markers are illuminated by infrared-emitting diodes surrounding a camera, and the motion of these markers was captured by the camera at a frequency of 25 frames per second. A respiratory signal is recorded in synchronization with the X-ray 'ON' signal from the CT scanner. The LightSpeed MSCT scan can simultaneously generate 16 slices of 1.25 mm (16 x 1.25), 8 slices of 2.5 mm (8 x 2.5), or 4 slices of 5 mm (4 x 5) for a 2 cm total coverage per gantry rotation. Our current scanning protocol for lung tumors uses 8 slices of 2.5 mm (8 x 2.5), obtained during quiet respiration. The 4DCT scanning procedure of the thorax takes about 90 seconds. The time resolution for a single image acquisition was $1/10^{th}$ of the full respiratory cycle period. The 4D data sets were sorted out for ten phase bins within the respiratory cycle using an Advantage 4DCT application running on an Advantage Workstation 4.1 (General Electric Company, Waukesha, WI). The registration is made based on the nearest neighbor criterion, where at each slice location the image is selected so that its phase is closest to each phase bin (Figure 1). The volumetric datasets that represented 10 phases of respiration (bins) were used for further analysis.

Contouring of target volumes

All sixteen CT data sets, i.e. six MSCT scans and ten bins from the 4D scan, were imported into the BrainLab stereotactic radiotherapy planning system (Brainscan ver. 5.2, BrainLab AG, Heimstetten, Germany) and co-registered using the automated matching software of this planning system. Match results were checked visually by contouring one CT slice of a spinal vertebra adjacent to the tumor, which was then automatically projected onto each CT data set after the registration procedure. GTVs were contoured in each of the 16 CT data sets using a standardized lung window level setting (W=-500, L=1000) by the same clinician in order to minimize contouring variations.

Figure 1.   Overview of respiratory phase "bin" generation from 4DCT-data
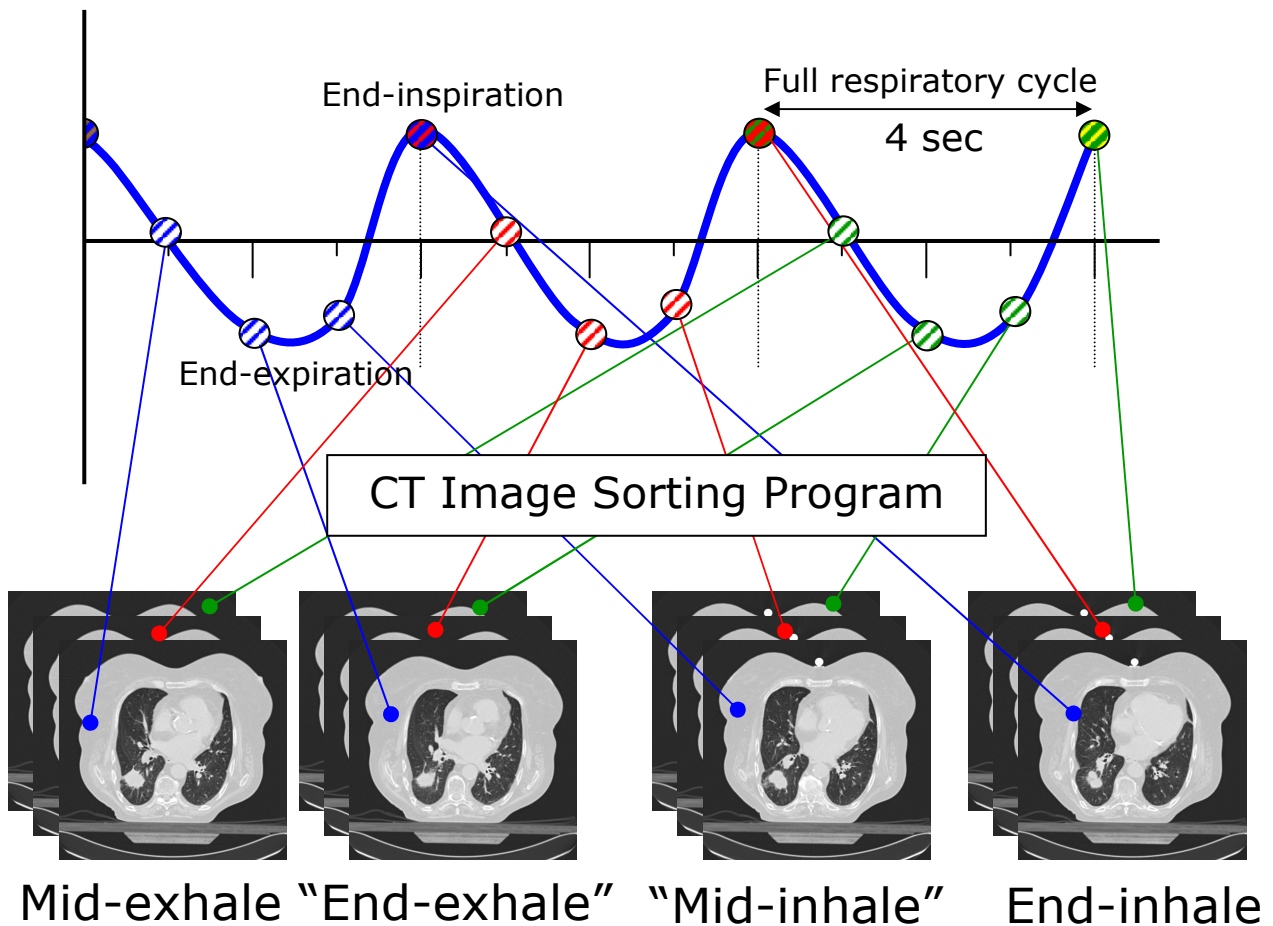
Volumetric analysis

A total of sixteen GTVs were obtained per patient, i.e. six from the multislice CT scans ($GTV_{6\ CT}$), and ten from the bins of the 4DCT scan (GTV_{4DCT}). All contours were automatically projected onto the first 'bin' of the 4DCT set, which was used for further analysis. The ITVs ($ITV_{6\ CT}$ and ITV_{4DCT}) were defined as the encompassing volumes of the $GTV_{6\ CT}$ and the GTV_{4DCT}, respectively. The agreement between both ITVs was investigated by determining the ratio of the common overlapping volume (COM), and the encompassing volume of both ITVs (SUM). The spatial positions of the ITV_{4DCT} and $ITV_{6\ CT}$ in X (medio-lateral), Y (anterior-posterior), and Z (cranio-caudal) axes were compared for all patients using the coordinate system of the Brainscan planning system.

Dosimetric analysis

Three PTVs were constructed for dosimetric analyses, namely [a] PTV_{4DCT}, which was derived from the ITV_{4DCT} with the addition of a 3D margin of 3 mm, [b] $PTV_{6\ CT}$, which was derived from the $ITV_{6\ CT}$ with the addition of a 3D margin of 3 mm, and [c] six $PTVs_{10\ mm}$, which were derived from each separate $GTV_{6\ CT}$ with the addition of a 3D margin of 10 mm. An ITV-PTV margin of 3 mm is clinically used for extracranial stereotactic radiotherapy at the VU University medical center, in order to account for residual errors in patient positioning using the online correction protocol from the Novalis ExacTrac system (BrainLab AG, Heimstetten, Germany). The GTV-PTV margin of 10 mm added to each $GTV_{6\ CT}$ was assumed to be sufficient for incorporating both target mobility and patient positioning errors for this technique. The optimal beam arrangement required for the 6-scan ITV ($ITV_{6\ CT}$) was considered as the standard treatment plan of all patients, and coverage of the different PTVs by the 80%, 70%, 60% and 50% isodoses was determined when the standard SRT plan was applied to the PTV_{4DCT}, $PTV_{6\ CT}$ and $PTVs_{10\ mm}$, respectively. The dosimetric consequences of treatment planning using the 3 different PTVs were analyzed in the Brainscan planning system using dose volume histograms.

Results

Volumetric analysis

The mean GTVs derived using both CT techniques were comparable, ranging from 1.1 to 36.8 cc for multiple MSCT scans, and 1.5 to 38.8 cc for 4DCT scans (Table 2).

In order to estimate the extent of tumor mobility, the ratio between the mean $GTV_{6\ CT}$ and $ITV_{6\ CT}$ was calculated for each patient. For completely immobile tumors, this ratio will be 1. The mean ratio $GTV_{6\ CT}/ITV_{6\ CT}$ was 0.58 ± 0.17, and was particularly low in patients A (0.36) and G (0.26), both of whom had tumors of the lower lobe.

Table 2. Target volumes obtained using multiple MSCT and 4DCT scans in 10 patients.

Patient	Mean GTV$_{6\,CT}$ (cc)	Mean GTV$_{4DCT}$ (cc)	ITV$_{6\,CT}$ (cc)	ITV$_{4DCT}$ (cc)	PTV$_{6\,CT}$ (cc)	PTV$_{4DCT}$ (cc)	Mean PTV$_{10mm}$ (cc)
A	1.1	1.5	2.9	4.5	7.0	10.7	19.2
B	6.9	7.5	12.2	13.3	23.8	25.8	58.4
C	9.1	10.5	12.0	14.0	23.3	26.6	61.6
D	22.7	23.2	32.3	36.2	53.7	58.8	107.8
E	5.6	6.2	7.9	8.7	16.5	17.4	46.1
F	2.2	2.5	3.2	3.7	7.9	9.1	27.8
G	2.1	3.7	7.9	16.1	18.3	31.2	28.5
H	3.2	3.9	6.9	6.9	14.2	14.5	32.0
I	16.2	17.3	25.6	26.6	42.1	44.4	79.6
J	36.8	38.8	53.0	51.1	81.1	79.7	149.5

The volume of the ITV$_{4DCT}$ was not different from the ITV$_{6\,CT}$, except in patients A and G, where the ITV$_{4DCT}$ was considerably larger (Table 2, Figure 2). The ratio between the ITV$_{6\,CT}$ and the ITV$_{4DCT}$ ranged from 0.49 to 1.04 (Table 3). The agreement between both scanning methods, as assessed by the ratio between the overlapping and encompassing volume (COM/SUM) of both ITVs was 0.71 (range 0.47 to 0.83). This was caused by a substantially larger surplus (i.e. the volume of each ITV outside the COM volume) of the ITV$_{4DCT}$ in all but one patient. The ITV$_{6\,CT}$ "missed" on average 22% of the encompassing volume of both ITVs, in contrast to only a mean 8.3% for the ITV$_{4DCT}$ (Table 4).

Table 3. Comparison of ITV$_{6\,CT}$ and ITV$_{4DCT}$.

Patient	COM ITVs (cc)	SUM ITVs (cc)	COM/SUM	ITV$_{6\,CT}$/ ITV$_{4DCT}$
A	2.8	4.6	0.62	0.65
B	10.3	15.1	0.68	0.91
C	11.2	15.2	0.74	0.85
D	30.5	38.7	0.79	0.89
E	7.3	9.3	0.79	0.91
F	2.9	4.2	0.69	0.86
G	7.8	16.5	0.47	0.49
H	5.6	8.1	0.69	1.00
I	23.8	28.8	0.83	0.96
J	47.1	58.9	0.80	1.04
Mean	-	-	**0.71**	**0.86**
SD	-	-	**0.11**	**0.17**

"COM" refers to the overlapping volume between both ITV$_{6\,CT}$ and ITV$_{4DCT}$.
"SUM" refers to the encompassing volume of both ITVs.

Table 4. The surplus of $ITV_{6\,CT}$ and ITV_{4DCT} (SUM_{ITVs} – ITV_{4DCT} and $ITV_{6\,CT}$, respectively)

Patient	Surplus $ITV_{6\,CT}$ (cc)	Surplus ITV_{4DCT} (cc)	Ratio Surplus $ITV_{6\,CT}$/SUM ITVs	Ratio Surplus ITV_{4DCT}/SUM ITVs
A	0.1	1.7	36.1	2.4
B	1.8	2.9	19.4	11.8
C	1.2	3.3	21.4	7.8
D	2.5	6.3	16.3	6.3
E	0.6	1.4	15.2	6.6
F	0.4	0.9	22.4	10.1
G	0.3	8.6	52.4	2.1
H	1.2	1.3	15.5	15.3
I	2.2	3.2	11.1	7.6
J	7.8	5.9	10.0	13.2
Mean	**-**	**-**	**22.0**	**8.3**
SD	**-**	**-**	**13.0**	**4.4**

The position of the center of mass of the ITV_{4DCT} and the $ITV_{6\,CT}$ was comparable, with a mean difference between both ITVs of 0.6 mm, 1.3 mm, and 0.8 mm in the X, Y, and Z-direction, respectively (Table 5), with a mean 3D displacement vector of 1.7 $\pm$ 0.6 mm.

Table 5. Positional shift (mm) between the centre of mass of $ITV_{6\,CT}$ and ITV_{4DCT}

Patient	X	Y	Z	3D
A	0.5	0.3	1.1	1.2
B	0.4	1.7	2.1	2.7
C	0.1	0.9	1.1	1.5
D	0.3	1.1	0.7	1.3
E	0.1	0.3	0.5	0.6
F	0.7	2.0	0.3	2.1
G	1.5	1.6	1.1	2.4
H	1.1	1.7	0.6	2.1
I	1.1	1.4	0.3	1.8
J	0.4	1.5	0.5	1.6
Mean	**0.6**	**1.3**	**0.8**	**1.7**
SD	**0.5**	**0.6**	**0.5**	**0.6**

Dosimetric analysis

When planning was performed using the PTV_{4DCT}, full coverage of the $PTV_{6\ CT}$ by the prescription 80% isodose was achieved in all patients (i.e. mean = 99.4%, minimum = 97.2%). When using the $PTV_{6\ CT}$, however, the mean coverage of the PTV_{4DCT} by the 80% isodose was only 92.5% of the volume, with a minimum of 77.7% and 77.5% in patients A and G, respectively (Table 6).

Table 6. Dose coverage of both $PTV_{6\ CT}$ and PTV_{4DCT} when treatment planning was performed on $PTV_{6\ CT}$ or PTV_{4DCT}, respectively

Patient	Coverage (volume %) of $PTV_{6\ CT}$ with Planning on PTV_{4DCT}				Coverage (volume %) of PTV_{4DCT} with planning on $PTV_{6\ CT}$			
	80% isodose	70% isodose	60% isodose	50% isodose	80% isodose	70% isodose	60% isodose	50% isodose
A	99.8	100	100	100	77.7	86.2	89.7	92.7
B	99.3	100	100	100	92.9	95.3	96.9	98.4
C	100	100	100	100	97.6	99.5	99.9	99.9
D	99.9	100	100	100	98.4	99.4	99.7	99.8
E	99.8	100	100	100	96.7	97.7	99.6	100
F	99.1	100	100	100	90.4	96.3	99.6	100
G	100	100	100	100	77.5	86.5	91.6	95.3
H	97.2	99.0	99.8	100	95.3	98.8	99.6	100
I	99.9	100	100	100	99.9	100	100	100
J	100	100	100	100	99.1	99.5	99.8	99.9
Mean	**99.5**	**99.9**	**100**	**100**	**92.6**	**95.9**	**97.6**	**98.6**

Additionally, an analysis was performed using the $PTVs_{10\ mm}$, derived from each single MSCT expanded with a margin of 10 mm. Although these $PTVs_{10\ mm}$ were on average twice the size of the other PTVs (Table 7), both the PTV_{4DCT} and $PTV_{6\ CT}$ were significantly underdosed, again in patients A and G (Table 8; Figure 3).

Table 7.   Volumes of three PTVs generated.

Patient	Mean PTV$_{10\,mm}$ (cc)	PTV$_{6\,CT}$ (cc)	PTV$_{4DCT}$ (cc)	PTV$_{10\,mm}$/PTV$_{6\,CT}$	PTV$_{10\,mm}$/PTV$_{4DCT}$
A	19.2 ± 1.3	7.0	10.7	2.8	1.8
B	58.4 ± 4.9	23.8	25.8	2.5	2.3
C	61.6 ± 0.8	23.3	26.6	2.7	2.3
D	107.8 ± 5.9	53.7	58.8	2.0	1.8
E	46.1 ± 2.1	16.5	17.4	2.8	2.7
F	27.8 ± 1.8	7.9	9.1	3.5	3.1
G	28.5 ± 2.9	18.3	31.2	1.6	0.9
H	32.0 ± 3.0	14.2	14.5	2.3	2.2
I	79.6 ± 10.4	42.1	44.4	1.9	1.8
J	149.5 ± 5.9	81.1	79.7	1.8	1.9
Mean	**-**	**-**	**-**	**2.4**	**2.1**

Table 8.   Mean dose coverage of PTV$_{4DCT}$ and PTV$_{6\,CT}$ with planning on PTV$_{10\,mm}$

| Patient	Mean coverage (volume%) PTV$_{4DCT}$				Mean coverage (volume%) PTV$_{6\,CT}$			
	80% isodose	70% isodose	60% isodose	50% isodose	80% isodose	70% isodose	60% isodose	50% isodose
A	78.9	82.3	84.4	86.2	87.5	90.1	92.3	94.1
B	99.9	100	100	100	100	100	100	100
C	100	100	100	100	100	100	100	100
D	100	100	100	100	100	100	100	100
E	100	100	100	100	100	100	100	100
F	100	100	100	100	100	100	100	100
G	60.9	63.3	65.5	68.0	64.6	66.7	68.7	71.2
H	96.6	97.3	98.3	99.0	96.4	97.4	97.8	98.9
I	99.5	99.8	99.9	100	99.6	99.9	100	100
J	100	100	100	100	100	100	100	100

Discussion

Far higher rates of local control have been reported in early stage NSCLC with the use of hypofractionated SRT, than achieved using other radiotherapy techniques [5-12]. Most authors used standard, population-based, margins for target definition [5, 6, 9, 11]. However, an accurate individualized 3D definition of target volumes is a more appropriate prerequisite in view of the high doses per fraction and steep dose gradients characteristic of SRT. This is particularly the case, as tumor mobility does not clearly correlate with location in the lung [13-15].

As we are unable to perform respiration-gated SRT currently, and as patients with medically inoperable stage I NSCLC poorly tolerate breath-hold techniques due to poor pulmonary function, we chose to incorporate all tumor mobility into treatment planning. Our approach for deriving ITVs had consisted of fusing GTVs from 6 rapid CT scans, as previous work had shown that ITVs derived from up to 3 rapid planning CT scans were smaller that those derived using 6 CT scans (including slow scans) [16, 25]. Although the exact number of unmonitored scans required for reliable ITV definition is uncertain, the arbitrary choice of 6 was based upon practical considerations, i.e. to limit the scanning time and the labor-intensive co-registration process. Consequently, the availability of the 4D scans led us to quickly implement a technique that permitted the incorporation of all respiration-related movement.

The present analysis compared target definitions based on the 6-scan method to that using a single 4DCT scan in a cohort of ten patients, half of whom had lower lobe lesions that exhibit greatest mobility [14]. Patients A and G had the most mobile tumors, and their ITV_{4DCT} was considerably larger than the $ITV_{6\ CT}$ (Table 2; Figure 2), indicating that 4D scans captured mobility that would have been otherwise missed.

Figure 2. Patient A: Coronal and sagittal views of the ITVs generated using both the 6-scan technique (orange - $ITV_{6\ CT}$) and 4DCT scan (green - ITV_{4DCT})
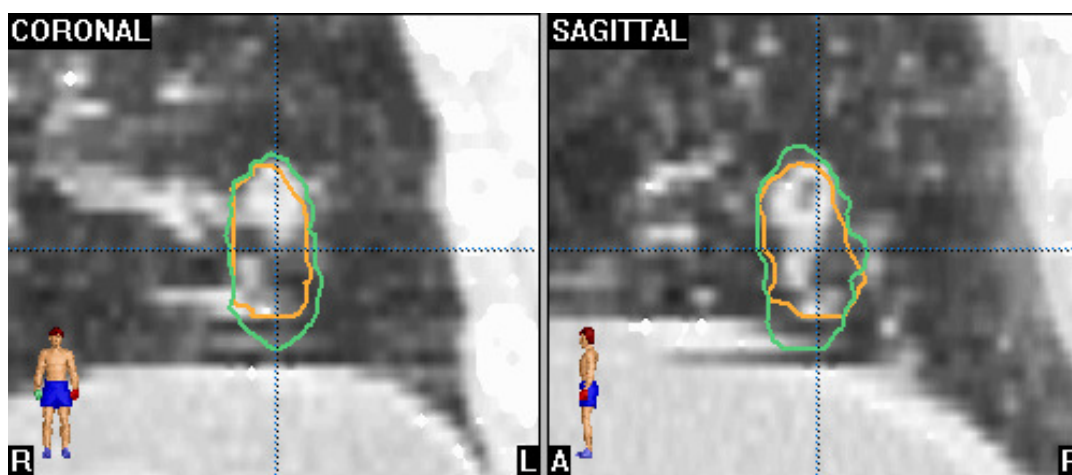
The results obtained using both the scanning techniques were comparable for the other 8 patients. Equally important was the dosimetric analysis showing the inappropriateness of using 'standard PTVs' obtained by expanding a single $GTV_{6\ CT}$ with a 3D margin of 10 mm. Not only were such PTVs on average twice as large as the $PTV_{6\ CT}$ and PTV_{4DCT}, thereby resulting in increased normal tissue irradiation, both the highly mobile tumors were underdosed cranio-caudally (Figure 3). The addition of an anisotropic margin of e.g. 15 mm cranio-caudally and 10 mm in the other directions could have ensured adequate coverage of the PTV_{4DCT}, but at the cost of an even larger irradiated volume.

Figure 3. Patient A: ITV_{4DCT} (green) versus that from a single "random" $GTV_{6\ CT}$ (pink) with added margin of 10 mm (PTV; orange) showing a failure of the latter to cover the ITV_{4DCT} caudally.
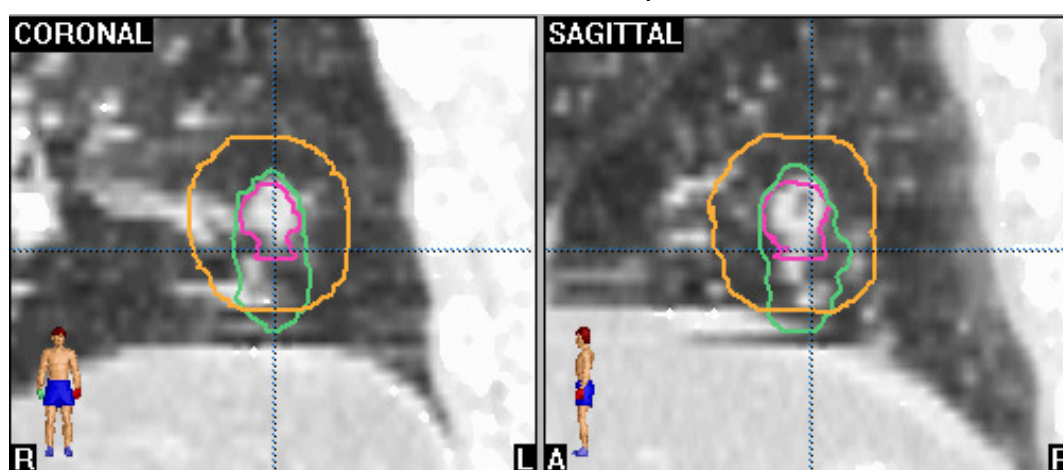
Minimizing normal tissue irradiation in SRT by using 4DCT scans can reduce the risk of late normal tissue toxicity associated with hypofractionated SRT schemes using 3 fractions of 20 Gy [5]. The reliable classification of tumors into non-mobile and mobile subgroups during treatment planning will identify patients who are candidates for more complicated techniques such as SRT using gating [26] or patient self-breath-hold [27]. Although this analysis was limited to peripheral lung tumors, these data support the use of 4D scans in generating ITVs also for locally advanced lung tumors. The generation of a single 4DCT scan during quiet respiration is a relatively simple procedure, which poses no problems to patients with compromised respiratory function. As the respiratory signal is digitally 'stamped' on each CT slice, it is possible

to reconstruct CT slices retrospectively at several phases over the respiratory cycle, yielding a 4D dataset. Although the radiation exposure to patients from 4DCT scanning is relatively large (ranging from 0.02 to 0.09 Gy) in comparison to a single conventional CT scan, the substantially smaller target volumes derived from 4DCT scans in comparison to standard PTVs that will be treated with high-dose fractions, justify this additional exposure. Furthermore, as intensity-modulated radiotherapy (IMRT) (without respiratory gating) is best reserved for non-mobile lung tumors, 4DCT scans can also identify candidates suitable for IMRT. However, data on the reproducibility of ITVs generated during a single session, as well as possible time-trends during the course of treatment are unknown, but are the subject of ongoing research in our department.

In conclusion, individualized assessment of tumor mobility can improve the accuracy of target definition in patients who are undergoing SRT for stage I NSCLC. Definition of the target volume based on a single CT scan with a margin of 10 mm is clearly inappropriate. A single 4DCT scan can replace the use of multiple unmonitored CT scans in defining individualized target volumes more accurately, in particular for highly mobile tumors. This approach can further improve tumor control and limit the likelihood of treatment-related toxicity.

References

1. Qiao X, Tullgren O, Lax I, et al. The role of radiotherapy in treatment of stage I non-small cell lung cancer. *Lung Cancer* 2003;41:1-11

2. Lagerwaard FJ, Senan S, van Meerbeeck JP, et al. Has 3D conformal radiotherapy improved the local tumor control in stage I non-small cell lung cancer? *Radiother Oncol* 2002;63:151-157

3. Bradley JD, Graham MV, Winter KW et al. Acute and late toxicity results of RTOG 9311: a dose escalation study using 3D conformal radiation therapy in patients with inoperable non-small cell lung cancer (Abstr). *Int J Radiat Oncol Biol Phys* 2003;57(Suppl):S137

4. Rosenzweig KE, Yorke E, Jackson A et al. Results of a phase I dose escalation study in the treatment of inoperable non-small cell lung cancer (Abstr). *Int J Radiat Oncol Biol Phys* 2003;57(Suppl):S417

5. Timmerman R, Papiez L, McGarry R, et al. Extracranial stereotactic radioablation: results of a phase I study in medically inoperable stage I non-small cell lung cancer. *Chest* 2003;124:1946-1955

6. Lee S, Choi EK, Park HJ, et al. Stereotactic body frame based fractionated radiosurgery on consecutive days for primary or metastatic tumors in the lung. *Lung Cancer* 2003;40:309-315

7. Whyte RI, Crownover R, Murphy MJ, et al. Stereotactic radiosurgery for lung tumors: preliminary report of a phase I trial. *Ann Thorac Surg* 2003;75:1097-1101

8. Uematsu M, Shioda A, Suda A, et al. Computed tomography-guided frameless stereotactic radiotherapy for stage I non-small cell lung cancer: a 5-year experience. *Int J Radiat Oncol Biol Phys* 2001;51:666-670

9. Fukumoto S, Shirato H, Shimizu S, et al. Small-volume image-guided radiotherapy using hypofractionated, coplanar, and noncoplanar multiple fields for patients with inoperable stage I nonsmall cell lung carcinomas. *Cancer* 2002;95:1546-1553

10. Onishi H, Nagata Y, Shirato H, et al. Stereotactic hypofractionated high-dose irradiation for patients with stage I non-small cell lung carcinoma: clinical outcomes in 241 cases of a Japanese multi-institutional study (Abstr.). *Int J Radiat Oncol Biol Phys* 2003;57(Suppl.):S142

11. Hof H, Herfarth KK, Münter M, et al. Stereotactic single-dose radiotherapy of stage I non-small-cell lung cancer (NSCLC). *Int J Radiat Oncol Biol Phys* 2003;56:335-341

12. Wulf J, Hadinger U, Oppitz U, et al. Stereotactic radiotherapy of targets in the lung and liver. *Strahlenther Onkol* 2001;177:645-655

13. Stevens CW, Munden RF, Forster KM, *et al*. Respiratory-driven lung tumor motion is independent of tumor size, tumor location, and pulmonary function. *Int J Radiat Oncol Biol Phys* 2001;51:62-68

14. van Sörnsen de Koste JR, Lagerwaard FJ, Nijssen-Visser MR, et al. Tumor location cannot predict the mobility of lung tumors: a 3D analysis of data generated from multiple CT scans. *Int J Radiat Oncol Biol Phys* 2003;56:348-354

15. Sixel KE, Ruschin M, Tirona R, et al. Digital fluoroscopy to quantify lung tumor motion: potential for patient-specific planning target volumes. *Int J Radiat Oncol Biol Phys* 2003;57:717-723

16. Lagerwaard FJ, van Sörnsen de Koste JR, Nijssen-Visser MR, et al. Multiple "slow" CT scans for incorporating lung tumor mobility in radiotherapy planning. *Int J Radiat Oncol Biol Phys* 2001;51:932-937

17. van Sörnsen de Koste JR, Lagerwaard FJ, Schuchhard-Schipper RH, et al. Dosimetric consequences of tumor mobility in radiotherapy of stage I non-small cell lung cancer– an analysis of data generated using 'slow' CT scans. *Radiother Oncol* 2001;61:93-99

18. Aruga T, Itami J, Aruga M, et al. Target volume definition for upper abdominal irradiation using CT scans obtained during inhale and exhale phases. *Int J Radiat Oncol Biol Phys* 2000;48:465-469

19. Onimaru R, Shirato H, Shimizu S, et al. Tolerance of organs at risk in small-volume, hypofractionated, image-guided radiotherapy for primary and metastatic lung cancers. *Int J Radiat Oncol Biol Phys* 2003;56:126-135

20. Yamada K, Soejima T, Yoden E, et al. Improvement of three-dimensional treatment planning models of small lung targets using high-speed multi-slice computed tomographic imaging. *Int J Radiat Oncol Biol Phys* 2002;54:1210-1216

21. Vedam SS, Keall PJ, Kini VR, et al. Acquiring a four-dimensional computed tomography dataset using an external respiratory signal. *Phys Med Biol* 2003;48:45-62

22. Ford EC, Mageras GS, Yorke E, et al. Respiration-correlated spiral CT: a method of measuring respiratory-induced anatomic motion for radiation treatment planning. *Med Phys* 2003;30:88-97

23. Pan T, Lee T, Rietzel ER, et al. 4D-CT imaging of a volume influenced by respiratory motion on multi-slice CT. *Med Phys* 2004;31:333-40

24. Wagman R, Yorke E, Ford E, et al. Respiratory gating for liver tumors: use in dose escalation. *Int J Radiat Oncol Biol Phys* 2003;55:659-668

25. van Sörnsen de Koste JR, Lagerwaard FJ, de Boer HC, et al. Are multiple CT scans required for planning curative radiotherapy in lung tumors of the lower lobe? *Int J Radiat Oncol Biol Phys* 2003;55:1394-1399

26. Hara R, Itami J, Kondo T, et al. Stereotactic single high dose irradiation of lung tumors under respiratory gating. *Radiother Oncol* 2002;63:159-163

27. Onishi H, Kuriyama K, Komiyama T, et al. A new irradiation system for lung cancer combining linear accelerator, computed tomography, patient self-breath-holding, and patient-directed beam-control without respiratory monitoring devices. *Int J Radiat Oncol Biol Phys* 2003;56:14-20

C h a p t e r

3

Use of maximum intensity projections (MIP) for target volume generation in 4DCT scans for lung cancer

René WM Underberg
Frank J Lagerwaard
Ben J Slotman
Johan P Cuijpers
Suresh Senan

Abstract

Purpose: Single 4-dimensional CT (4DCT) scans reliably capture intra-fractional tumor mobility for radiotherapy planning, but generating internal target volumes (ITVs) requires the contouring of gross tumor volumes (GTVs) in up to 10 phases of a 4DCT scan, as is routinely performed in our department. We investigated the use of maximum intensity projection (MIP) protocols for rapid generation of ITVs.

Methods and Materials: 4DCT data from a mobile phantom and from 12 patients with stage I lung cancer were analyzed. A single clinician contoured GTVs in all respiratory phases of a 4DCT, as well as in 3 consecutive phases selected for respiratory gating. MIP images were generated from both phantom and patient data, and ITVs were derived from encompassing volumes of the respective GTVs.

Results: In the phantom study, the ratio between ITVs generated from all 10 phases and those from MIP scans was 1.04. The corresponding center of mass of both ITVs differed by less than 1 mm. In scans from patients, good agreement was observed between ITVs derived from 10 and 3 (gating) phases and the corresponding MIPs, with ratios of 1.07 ± 0.05 and 0.98 ± 0.05, respectively. In addition, the center of mass of the respective ITVs differed by only 0.4 and 0.5 mm.

Conclusion: MIPs are a reliable clinical tool for generating ITVs from 4DCT datasets, thereby permitting rapid assessment of mobility for both gated and non-gated 4D radiotherapy in lung cancer.

Introduction

Recent studies have shown that individualized planning margins are required to account for the variability and unpredictability of lung tumor mobility [1-4]. 4-Dimensional (4D) radiotherapy has been defined as the explicit inclusion of temporal changes in anatomy during the imaging process, dose-planning and delivery of radiotherapy [5]. Such spatial and temporal information on tumor mobility can be derived with single CT scan procedures such as 'slow' CT scans [6-8] or respiration-correlated 4DCT scans [9-11]. Both techniques allow for the generation of individualized internal target volumes (ITVs) [12] for treatment planning, but 4D scans have the added advantage of permitting the retrospective selection of phases for gated radiotherapy [10, 13].

The need to contour tumors and/or normal organs in 10 or more phases of respiration is a major drawback to the routine clinical use of 4DCT scans. Our recent analysis revealed that significant changes in tumor volume can occur during fractionated stereotactic radiotherapy for stage I non-small cell lung cancer [14], which implies that repeat CT planning may be appropriate during 4D radiotherapy, thereby adding to the workload. Reliable auto-segmentation tools are not yet available and remain the subject of active ongoing research [15, 16]. We currently manually contour gross tumor volumes (GTVs) in all 10 phases of a 4D scan for planning stereotactic radiotherapy for stage I lung cancer and derive ITVs from the volume encompassing these GTVs [11].

To reduce the workload of contouring multiple target volumes, we evaluated the post-processing tools of maximum intensity projection (MIP) and minimum intensity projection (MinIP) for use with 4DCT datasets. Briefly, MIP projections reflect the highest data value encountered along the viewing ray for each pixel of volumetric data, giving rise to a full intensity display of the brightest object along each ray on the projection image. Conversely, MinIP projections reflect the lowest data value encountered along the viewing ray for each pixel of volumetric data. Both MIP and MinIP are standard volume rendering techniques used in diagnostic radiology [17-22], for example to extract high or low intensity structures such as blood vessels [18] from volumetric CT or MRI data. We compared ITVs derived from contouring GTVs in all respiratory phases (Figure 1a) with MIPs generated from 4DCT datasets (Figure 1b), for both a mobile phantom and patients.

Figure 1. Pixel-based intensity projection protocols from 4DCT datasets of a mobile tumor, illustrating (a) separate phases of the 4DCT, (b) maximum intensity projection, (c) minimum-intensity projection, and (d) mean intensity projection
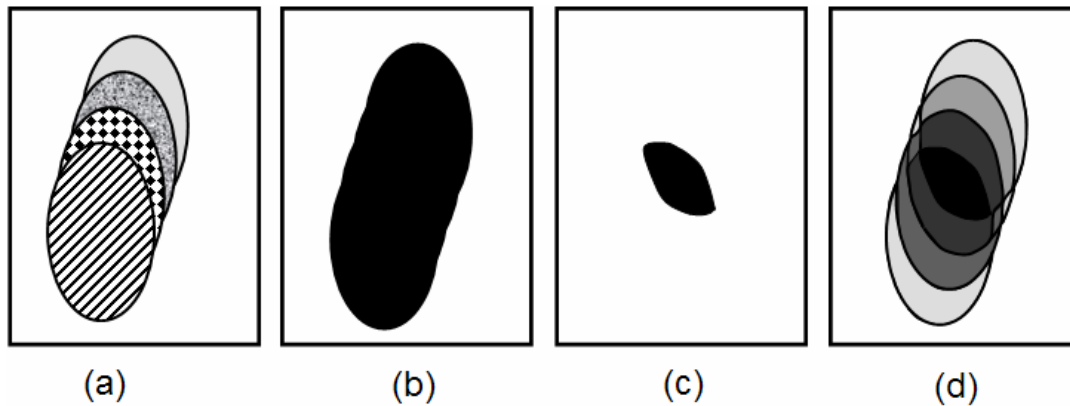
Materials and Methods

4DCT procedure

We routinely perform 4DCT scans for radiotherapy planning of lung tumors on a LightSpeed 16-slice CT scan (General Electric Company, Waukesha, WI) during quiet, uncoached respiration with an index and slice thickness of 2.5 mm. During the scanning procedure, respiratory signals are recorded using the Varian Real-Time Position Management (RPM) respiratory gating hardware (Varian Medical Systems, Palo Alto, CA). The RPM system uses infrared-reflecting markers on the upper abdomen, which are illuminated by infrared-emitting diodes surrounding a camera. The camera captures the marker motion, and a respiratory signal is recorded in synchronization with the X-ray 'ON' signal from the CT scanner. The scanner is operated in axial cine mode, with multiple scans performed at each couch position for a duration that is at least equal to the length of the patient's respiratory cycle. Each image from the acquired dataset is sorted into one of ten phase bins using the Advantage 4DCT application running on an Advantage Workstation 4.1 (General Electric Company, Waukesha, WI). The phase bins are, to a good approximation, evenly spaced in time over the respiratory cycle.

Motion phantom

As the initial step, MIP and MinIP images were generated from the raw (i.e. non phase-sorted) data of 4DCT scans performed on a motion phantom, which consisted

of a human body-like torso with lungs and a bone equivalent spine model. The phantom was filled with water to have human body equivalent properties for CT scanning and dose measurements. A 3 cm large silicon tumor substitute attached rigidly to a metal cylinder was positioned in the left side of the phantom, which could move longitudinally by approximately 1.5 cm. For detecting an external breathing signal, a vertically movable board holding infrared reflective markers was mounted above the phantom chest. Both the board and the tumor were moved under computer control by independent servo drives, and the software permitted the simulation of a simple sinusoidal breathing curve. The silicon tumor substitute was contoured on both the MIP and MinIP datasets, and these results were compared with manual contouring of all 10 phases from the 4DCT scan. These target volumes were compared also to those generated using a 'slow' CT scan performed with a CT revolution time of 4 seconds.

Patient study

A retrospective analysis was performed on 4DCT scans from 11 patients with 12 relatively mobile peripheral stage I lung tumors that were treated with stereotactic radiotherapy (Table 1). The 3D mobility vectors of tumors were determined by manual contouring of GTVs in all phases of the 4DCT scans, and these ranged from 2.5 – 29.5 mm. To evaluate the performance of the MIP software, we included tumors at different anatomic locations in the lung, including the hilus and lesions adjacent to the chest wall. GTVs were manually contoured on all 10 phases of the 4DCT scan using standard window/level settings. A window consisting of 3 consecutive phases at end-expiration was selected for respiratory-gating. Manually contoured $ITV_{10\ phases}$ and $ITV_{3\ phases}$ were derived from the encompassing volume of the respective GTVs.

Table 1.   Tumor characteristics

Tumor	T stage	Mean GTV (cc)	Location	3D mobility vector (mm)
A	T1	3.9	Left lower lobe	23.6
B	T1	1.5	Right upper lobe	11.3
C	T2	8.1	Left upper lobe	4.3
D	T1	4.9	Left lower lobe	11.6
E	T1	3.3	Right upper lobe, adjacent to hilus	5.3
F	T1	2.1	Right upper lobe	10.9
G	T1	2.0	Left lower lobe, adjacent to hilus	12.0
H	T1	2.9	Left lower lobe	29.5
I	T2	37.2	Right lower lobe, adjacent to chest wall	24.2
J	T1	0.7	Left upper lobe	2.9
K	T1	2.3	Right upper lobe, adjacent to chest wall	2.5
L	T1	1.5	Left lower lobe	16.0

MIP images were automatically generated using Advantage 4D software from the raw dataset of the 4DCT scan for both 10 phases and the same 3 respiratory-gating phases in each patient. The same clinician contoured ITVs on both the 10-phase ($ITV_{MIP\ 10\ phases}$) and 3-phase MIP scans ($ITV_{MIP\ 3\ phases}$). Similarly, MinIP images were generated and manually contoured to derive an ITV_{MinIP} that represents the space where tumor is present during the entire respiratory cycle (Figure 1c). All MIP-based ITVs were compared to the corresponding manually contoured ITVs using the BrainLab planning system (Brainscan v. 5.2, BrainLab, Heimstetten, Germany). In order to limit radiation exposure, we did not perform slow CT scans in patients. Definitions of all different ITVs generated are summarized in Table 2.

Table 2.   Summary of different internal target volumes used

Volume	Definition
$ITV_{10\ phases}$	ITV derived from manual contouring of all 10 phases of the 4DCT
$ITV_{3\ phases}$	ITV derived from manual contouring of three consecutive phases at end-expiration
$ITV_{MIP\ 10\ phases}$	ITV derived from a maximum intensity projection of all 10 phases of the 4DCT
$ITV_{MIP\ 3\ phases}$	ITV derived from a maximum intensity projection of 3 consecutive phases at end-expiration
ITV_{MinIP}	ITV derived from a minimum intensity projection of all 10 phases of the 4DCT

Results

Phantom study

Frontal reconstructions of the MIP and MinIP datasets generated from the 4DCT scans of the phantom are shown in Figure 2. A good correlation was observed between the fully contoured $ITV_{10\ phases}$ and the corresponding $ITV_{MIP\ 10\ phases}$ (Figure 3, left panel). The ratio of $ITV_{10\ phases}$ and $ITV_{MIP\ 10\ phases}$ was 1.04, and the distance between the center of mass of both ITVs was less than 1 mm (Table 3). Contouring of the volume that was common to all 10 4D phases ($ITV_{overlap\ 10\ phases}$) corresponded well with the MinIP contours (ITV_{MinIP}) (Figure 3, right panel). The ratio of $ITV_{overlap\ 10\ phases}$ and ITV_{MinIP} was 0.93, and the distance between the centers of mass was less than 1 mm (Table 3). Similarly, the ratio of the $ITV_{MIP\ 10\ phases}$ and the ITV derived with a slow CT scan was 1.08, with an absolute difference of 1.6 cc. The 3D shift between these ITVs was also less than 1 mm.

Figure 2. Maximum intensity projection (left panel) and minimum intensity projection (MinIP) of the 4DCT scan of a mobile phantom. The arrow-like shape represents the mechanism used to generate movement of the silicon tumor substitute in the phantom
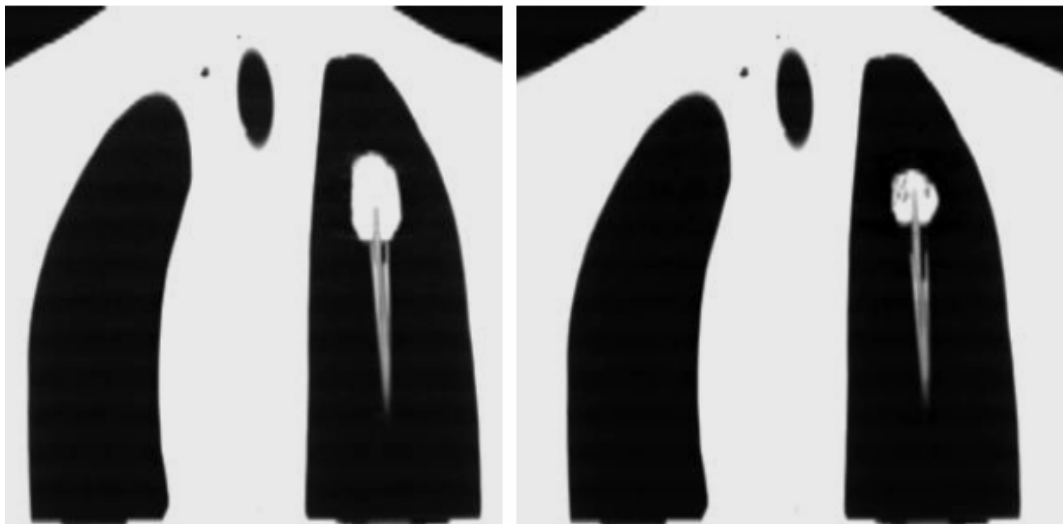
Figure 3. Projection of the $ITV_{MIP\ 10\ phases}$ (red contour) on all ten contoured phases of the 4DCT scan (yellow contours). On the right panel the contoured minimum-intensity projection dataset (purple contour) is projected on all ten contoured phases of the 4DCT scan
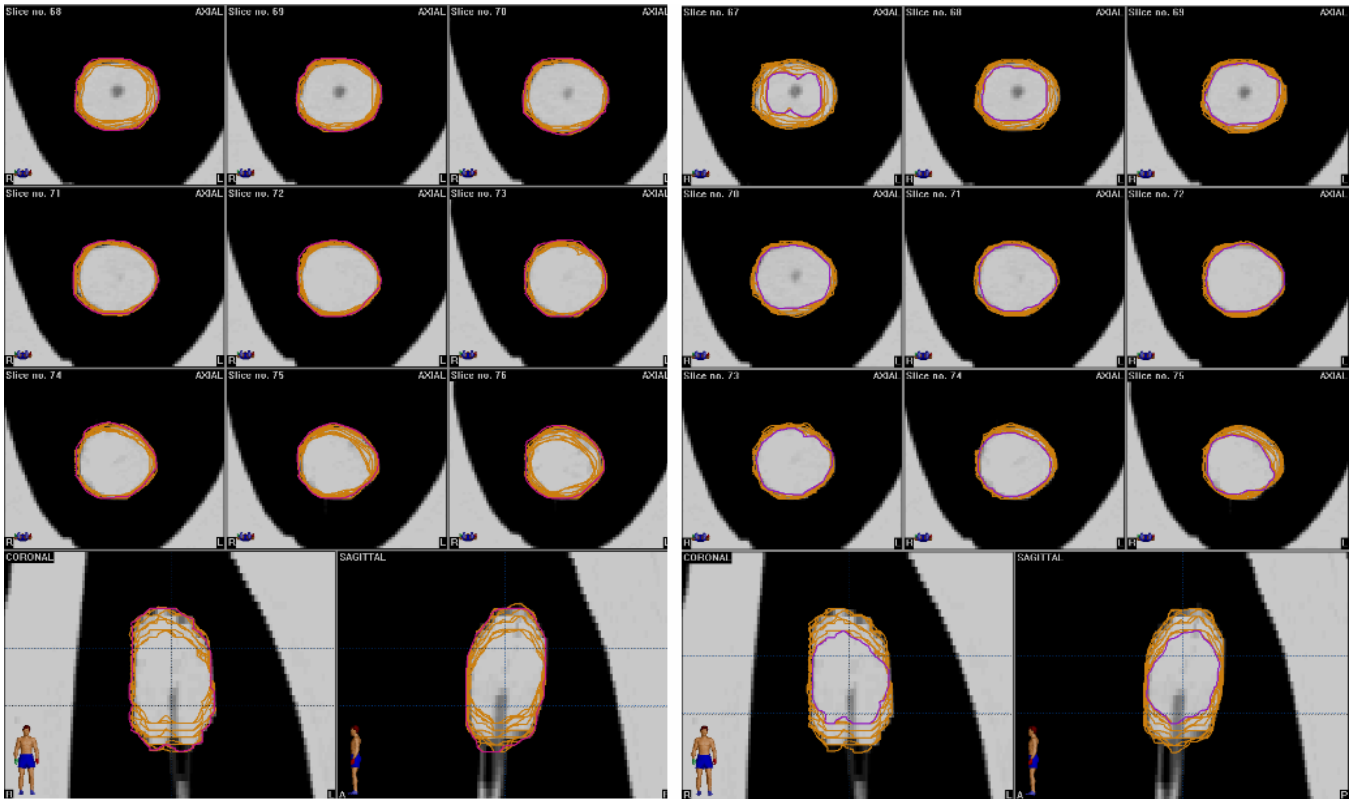

Table 3. Summary of data from the phantom study. The MIP-based ITV was compared to both $ITV_{10\ phases}$ and $ITV_{slow\ CT}$. The MinIP-ITV was compared to the common overlapping ITV of all 10 phases

$ITV_{10\ phases}$	22.8 cc
$ITV_{MIP\ 10\ phases}$	21.9 cc
Ratio $ITV_{10\ phases}/ITV_{MIP}$	0.96
Distance between the two centers of mass (mm)	0.2
$ITV_{overlap\ 10\ phases}$	10.2 cc
ITV_{MinIP}	11.0 cc
Ratio $ITV_{overlap\ 10\ phases}/ITV_{MinIP}$	0.93
Distance between the two centers of mass (mm)	0.5
$ITV_{slow\ CT}$	20.3 cc
Ratio $ITV_{MIP\ 10\ phases}/ITV_{slow\ CT}$	1.08
Distance between the two centers of mass (mm)	0.5

Patient study

Similar comparisons were performed between contours of all phases of the 4DCT and the contoured MIP images of 12 tumors. As in the phantom study, good agreement was observed for both 10-phase and 3-phase ITVs, with the ratio of $ITV_{10\ phases}/ITV_{MIP\ 10\ phases}$ being 1.07 ± 0.05, and the ratio $ITV_{3\ phases}/ITV_{MIP\ 3\ phases}$ being 0.98 ± 0.05 (Table 4). Relative differences between these ITVs in excess of 10% were observed in relatively small tumors, but the absolute differences were smaller than 1 cc in all cases. The mean distance between the center of mass of manually contoured and MIP-based ITVs was 0.4 and 0.5 mm for the 10 and 3 phases, respectively.

Table 4. Data from 12 patients comparing MIP-based ITVs with $ITV_{10\ phases}$ and $ITV_{3\ phases}$, respectively

	A	B	C	D	E	F	G	H	I	J	K	L	Mean ± SD
All 10 bins of the 4DCT													
$ITV_{10\ phases}/ITV_{MIP\ 10\ phases}$	1.08	1.14	1.03	1.02	1.12	1.17	1.02	1.04	1.06	1.00	1.05	1.12	1.07 ± 0.05
Distance between center of mass (mm)	0.5	0.5	0.3	0.3	0.5	0.6	1.0	0.4	0.1	0.2	0.4	0.2	0.4 ± 0.2
3 bins at end-expiration													
$ITV_{3\ phases}/ITV_{MIP\ 3\ phases}$	1.00	1.02	0.99	0.91	1.00	1.01	0.92	1.02	1.03	0.86	0.95	1.02	0.98 ± 0.05
Distance between center of mass (mm)	0.6	0.3	1.0	0.4	0.6	0.3	0.6	0.9	0.3	0.4	0.1	0.4	0.5 ± 0.3

Because a MIP-based ITV represents the volume where the tumor is present at any time within the respiratory cycle, and a MinIP-based ITV represents the volume where the tumor is present during the entire respiratory cycle, the ratio of these ITVs gives a measure of respiratory-induced tumor mobility. This ratio ($ITV_{MinIP}/ITV_{MIP\ 10\ phases}$) was correlated with the mobility vector derived from all 10 phases of the 4DCT scan. In two patients with highly mobile, small tumors with an intra-fractional mobility of more than 20 mm, the ITV_{MinIP}/ITV_{MIP} ratio was zero, because no tumor at all was visible on the MinIP projections (Figure 4). Analysis of all patient data revealed a correlation coefficient (R) of 0.72 for the relation between 3D mobility vector and $ITV_{MinIP}/ITV_{MIP\ 10\ phases}$ ratio. The ratio $ITV_{MinIP}/ITV_{MIP\ 10\ phases}$ is, however, determined also by the

absolute ITV volume, which is illustrated in tumors 'A' and 'I' with comparable 3D mobility vectors, but largely different ITV volumes (Table 1). In all 7 patients with an ITV$_{MinIP}$/ITV$_{MIP\ 10\ phases}$ ratio of less than 0.25, the mobility vector was more than 10 mm (Figure 5).

Figure 4. Maximum intensity projection image of a highly mobile tumor in the left lower lobe (left panel), with the corresponding minimum intensity projection image (right panel) that showed no location where tumor was present during all respiratory phases
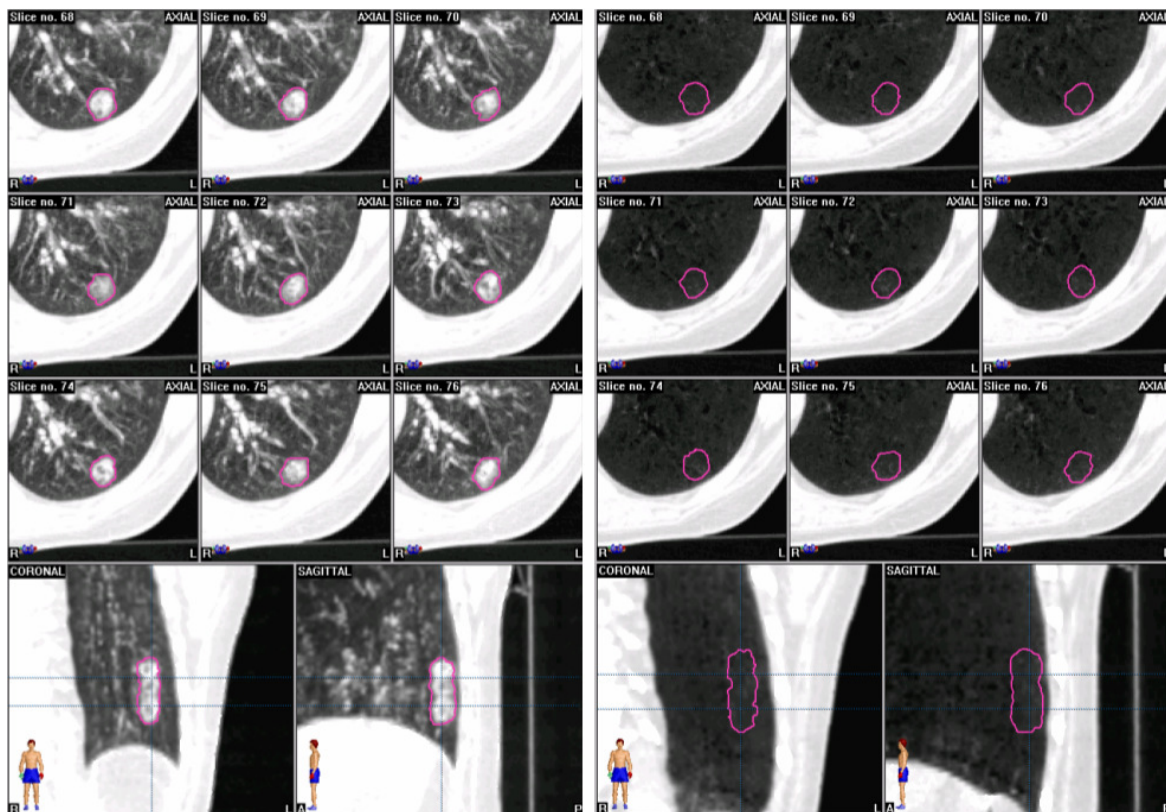
The ratio ITV$_{MinIP}$/ITV$_{MIP\ 10\ phases}$ correlated even more strongly (R=0.95) with the reduction in ITV volume that can be achieved with respiratory-gating, i.e. with the ratio ITV$_{3\ phases}$/ITV$_{10\ phases}$ (Figure 6). This indicates that the former ratio can be used clinically for rapidly identifying patients who can benefit from respiration-gated radiotherapy.

Figure 5. Relationship between the 3D mobility vector and the ratio between the ITV$_{MinIP}$ and ITV$_{MIP\ 10\ phases}$. The letters correspond to patients referred to in Table 1
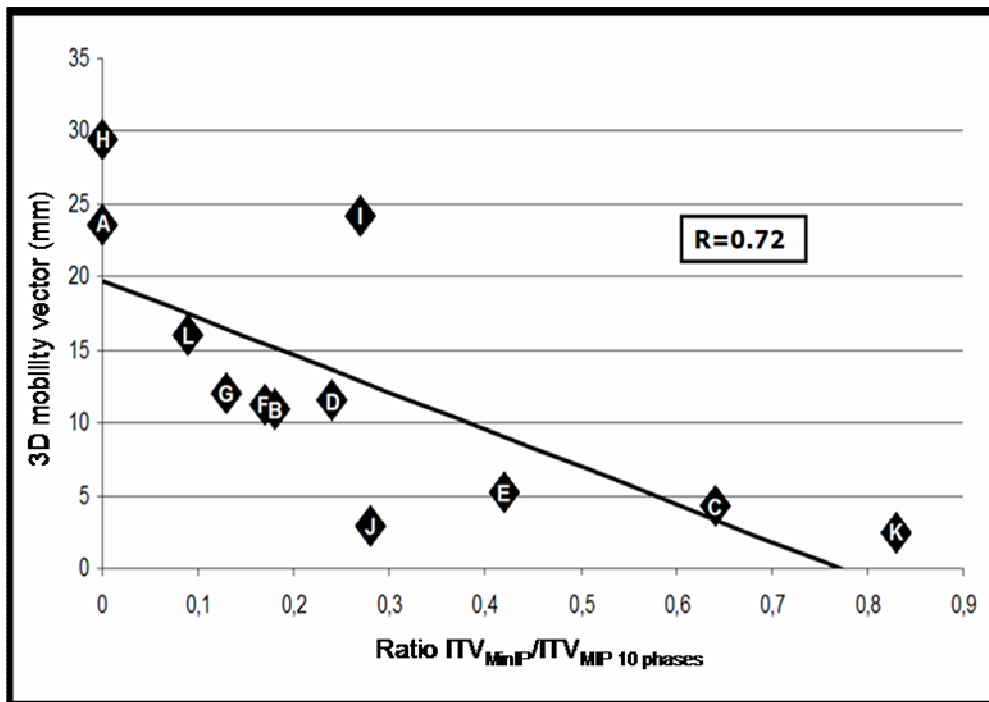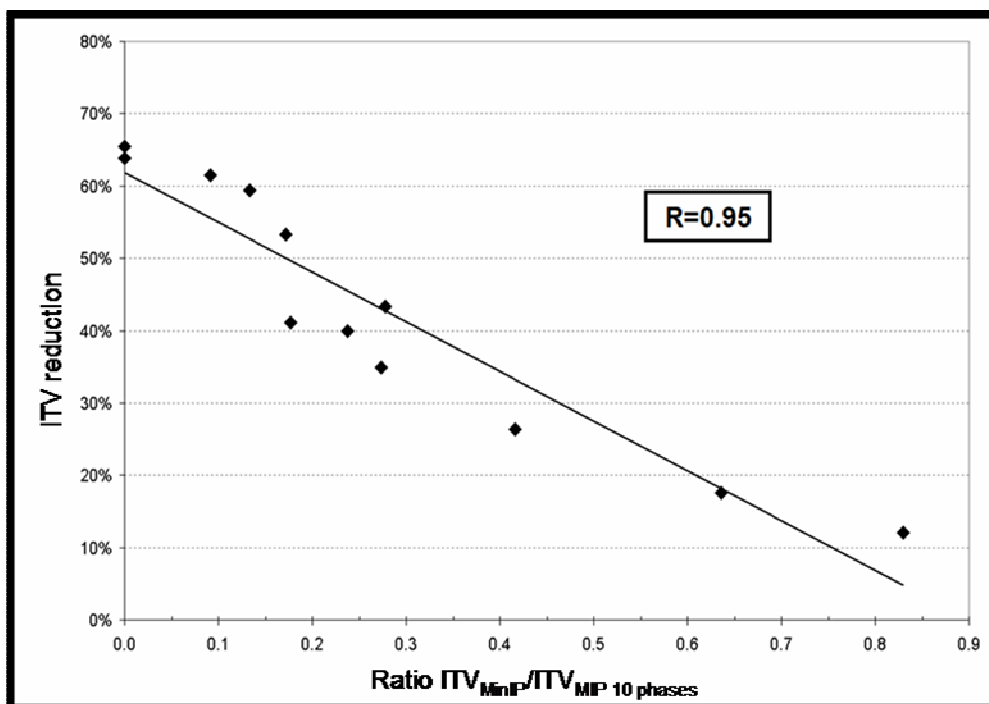

Figure 6. Relationship between the reduction in ITV (%) obtained with respiratory gating and the ratio between ITV$_{MinIP}$ and ITV$_{MIP\ 10\ phases}$

Discussion

4D radiotherapy represents an exciting development as it allows for radiotherapy to be individualized for the patient in question. However, 4DCT scans generate up to 10 times more data (and contouring work) than a single conventional planning CT scan. Our technique for 4DCT scanning involves acquiring multiple images at each couch position during quiet respiration. MIP or MinIP post-processing of the 'raw unsorted data' of these 4DCT scans results in the display of the maximum or minimum intensity of each pixel in the stack of axial CT images at each table position. As such, MIP datasets represent composite images with phase summation or compression of tumor positions during all phases of respiration, thereby allowing for direct generation of ITVs.

In both the phantom study and patient data, MIP–based ITVs showed an excellent agreement with ITVs derived from contouring GTVs on all selected phases of the 4DCT. The generation and contouring of a MIP image took less than 10 minutes per patient, and resulted in individualized ITVs. Speed was also enhanced by the fact that the technique of 4D scanning requires no co-registration of different 4D phase bins. The clinical introduction of the MIP technique has significantly reduced our clinical workload associated with treatment planning for peripheral lung tumors.

The MIP technique also facilitates the evaluation of plans for gated radiotherapy by permitting quick generation of ITVs in selected phases of respiration. Our recent analysis of 43 patients with stage I NSCLC found that only 25% of patients had mobility of sufficient magnitude (>1 cm) as to derive a benefit from gating [13]. However, determining mobility required contouring of all ten phases of the 4DCT scan. The present analysis revealed that the ratio of $ITV_{MinIP}/ITV_{MIP\ 10\ phases}$ correlates well with the reduction in ITV that resulted from selecting 3 phases in end-expiration for respiratory gating. As such, this simple two-step approach will facilitate the selection of suitable patients for gated radiotherapy in a fast and objective manner.

The minor discrepancies observed in ITVs generated using the two techniques can be accounted for by contouring variations, particularly as the displacement of the center of mass of both ITVs was less than 1 mm in all cases. Inter-clinician variability was not a confounding variable, because a single clinician performed all contouring. It can

be expected that the availability of reliable auto-segmentation tools could further simplify ITV generation [16, 23].

'Slow' CT scanning is also a single-step method for generating of ITVs in lung cancer [2, 6, 8]. This technique uses a CT revolution time of 4 seconds, which allows for the incorporation of tumor mobility into the CT images. However, slow CT scans are only suitable for peripheral lung tumors where the contrast between tumor and normal lung tissue is high. In addition, as the pixel-intensity in slow CT images is proportional to the period of time that the tumor is at its extreme positions, tumor borders tend to be smeared. In this manner, slow CT scans more resemble *mean* intensity projection images, which can also be acquired from 4DCT scans (Figure 1d). Our current software does not allow for the generation of mean intensity projection, but this will become possible in a future release. Figure 7 shows a comparison between such a slow CT scan (left panel) and a *mean* intensity projection scan (middle panel) generated for the mobile phantom. In contrast, the selection of maximum intensities in MIP scans (right panel) results in a relatively high contrast between 'tumor' boundaries and surrounding normal tissues, which allows for easier contouring. The more "blurred" ITV borders obtained with slow CT scanning may account for the 8% difference between MIP- and slow CT-based ITVs.

Figure 7. Scans of the mobile phantom showing a slow CT scan (left panel), a mean intensity projection (middle panel), and a maximum intensity projection (right panel). Note the inhomogeneous intensity in the direction of mobility with the slow CT scan and the mean intensity projection
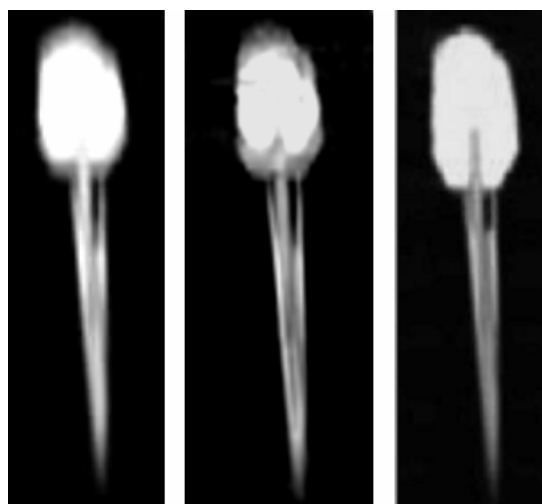
Some potential drawbacks of using MIP projections must be appreciated. Because MIP scans do not reflect the appropriate lung density for treatment planning, the latter has to be performed on a co-registered planning CT, e.g. a single phase of the 4D scans. In addition, MIP may not fully display mobile structures if an adjacent structure has equal or greater density. A number of tumors included in this study were in contact with the thoracic wall or the hilus. Although these sites did not complicate contouring on the MIP scans, it must be acknowledged that only reasonably well-demarcated T1-2 tumors were accepted for stereotactic radiotherapy. However, we recently encountered a problem with MIP scans in a patient whose tumor was located directly adjacent to the diaphragm. MIP images failed to visualize the caudal extent of the $ITV_{10\ phases}$ as a result of overlap with the high-density diaphragm (Figure 8). This important pitfall when directly generating ITVs from MIP scans can be avoided by reviewing the GTVs at extreme phases of the 4DCT in tumors that are adjacent to the thoracic wall, mediastinum, heart or diaphragm. The issue of whether MIP images also reliably allow for contouring planning volumes for organs at risk is the subject of ongoing research.

In conclusion, the generation of MIP scans is a reliable and fast clinical tool for generating ITVs from 4DCT datasets, thereby permitting rapid assessment for both gated and non-gated 4D radiotherapy for early stage lung cancer.

Figure 8. (a) Example of a tumor located adjacent to the diaphragm, which was not fully visible on repeated MIP scans as a result of the overlap with the diaphragm. (b) The extreme end-inspiration tumor position was visible on the corresponding single phase scan. (c) MIP information on this patient would underestimate the caudal extension of the ITV (orange and pink contours), compared with an $ITV_{10\ phases}$ (green contour).
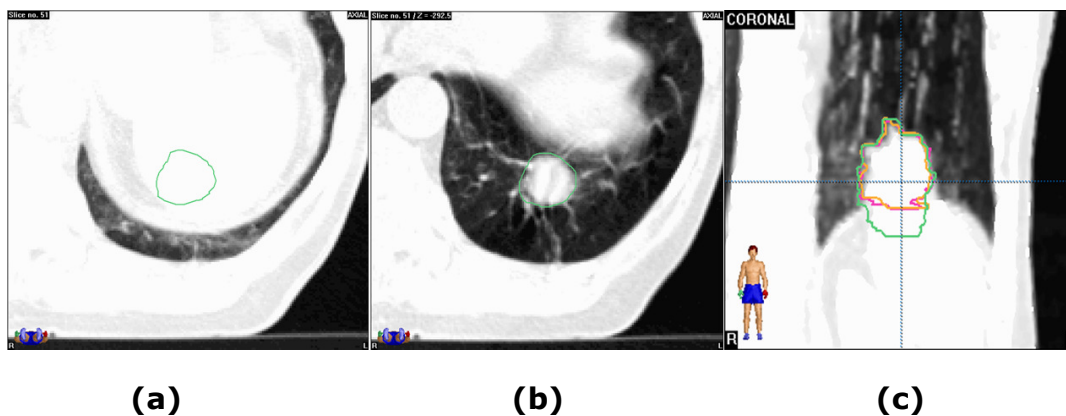
(a) **(b)** **(c)**

Acknowledgements

References

1. Stevens CW, Munden RF, Forster KM, et al. Respiratory-driven lung tumor motion is independent of tumor size, tumor location, and pulmonary function. *Int J Radiat Oncol Biol Phys* 2001;51:62-68

2. van Sörnsen de Koste JR, Lagerwaard FJ, Nijssen-Visser MR, et al. Tumor location cannot predict the mobility of lung tumors: a 3D analysis of data generated from multiple CT scans. *Int J Radiat Oncol Biol Phys* 2003;56:348-354

3. Sixel KE, Ruschin M, Tirona R, et al. Digital fluoroscopy to quantify lung tumor motion: potential for patient-specific planning target volumes. *Int J Radiat Oncol Biol Phys* 2003;57:717-23

4. Plathow C, Ley S, Fink C, et al. Analysis of intrathoracic tumor mobility during whole breathing cycle by dynamic MRI. *Int J Radiat Oncol Biol Phys* 2004;59:952-959

5. Keall P. 4-Dimensional computed tomography imaging and treatment planning. *Semin Radiat Oncol* 2004;14:81-90

6. Lagerwaard FJ, Van Sörnsen de Koste JR, Nijssen-Visser MR, et al. Multiple "slow" CT scans for incorporating lung tumor mobility in radiotherapy planning. *Int J Radiat Oncol Biol Phys* 2001;51:932-937

7. van Sörnsen de Koste JR, Lagerwaard FJ, Schuchhard-Schipper RH, et al. Dosimetric consequences of tumor mobility in radiotherapy of stage I non-small cell lung cancer--an analysis of data generated using 'slow' CT scans. *Radiother Oncol* 2001;61:93-99

8. van Sörnsen de Koste JR, Lagerwaard FJ, de Boer HC, et al. Are multiple CT scans required for planning curative radiotherapy in lung tumors of the lower lobe? *Int J Radiat Oncol Biol Phys* 2003;55:1394-1399

9. Vedam SS, Keall PJ, Kini VR, et al. Acquiring a four-dimensional computed tomography dataset using an external respiratory signal. *Phys Med Biol* 2003;48:45-62

10. Mageras GS, Pevsner A, Yorke ED, et al. Measurement of lung tumor motion using respiration-correlated CT. *Int J Radiat Oncol Biol Phys* 2004;60:933-941

11. Underberg RWM, Lagerwaard FJ, Slotman BJ, et al. 4-Dimensional CT scans for treatment planning in stereotactic radiotherapy for stage I lung cancer *Int J Radiat Oncol Biol Phys* 2004;60:1283-1290

12. International Commission on Radiation Units and Measurements. Prescribing, recording and reporting photon beam therapy (supplement to ICRU Report 50). Bethesda, MD: ICRU Report 62, 1999

13. Underberg RWM, Lagerwaard FJ, Slotman BJ, et al. Benefits of respiration-gated stereotactic radiotherapy for stage I lung cancer - An analysis of 4DCT datasets. *Int J Radiat Oncol Biol Phys* 2005;62:554-560

14. Senan S, Underberg RWM, Slotman BJ, et al. Time trends in target volumes during stereotactic radiotherapy for stage I non-small cell lung cancer (NSCLC) *Int J Radiat Oncol Biol Phys* 2004;60 Suppl:S281-S282

15. Pekar V, McNutt TR, Kaus MR. Automated model-based organ delineation for radiotherapy planning in prostatic region. *Int J Radiat Oncol Biol Phys* 2004;60:973–980

16. McInerney T, Hamarneh G, Shenton M, et al. Deformable organisms for automatic medical image analysis. *Medical Image Analysis* 2002;6:251–266

17. Cody DD. AAPM/RSNA physics tutorial for residents: topics in CT. Image processing in CT. *Radiographics* 2002;22:1255-1268

18. Gruden JF, Ouamanou S, Tigges S, et al. Incremental benefit of maximum intensity projection images on observer detection of small pulmonary nodules revealed by multidetector CT. *Am J Roentgenol* 2002;179:149-157

19. Persson A, Dahlstrom N, Engellau L, et al. Volume rendering compared with maximum intensity projection for magnetic resonance angiography measurements of the abdominal aorta. *Acta Radiol* 2004;45:453-459

20. Jeong YJ, Lee KS, Yoon YC, et al. Evaluation of small pulmonary arteries by 16-slice multidetector computed tomography: Optimum slab thickness in condensing transaxial images converted into maximum intensity projection images. *J Comput Assist Tomogr* 2004;28:195-203

21. van Straten M, Venema HW, Streekstra GJ, et al. Removal of bone in CT angiography of the cervical arteries by piecewise matched mask bone elimination. *Med Phys* 2004;31:2924-2933

22. Aziz ZA, Padley SP, Hansell DM. CT techniques for imaging the lung: recommendations for multislice and single slice computed tomography. *Eur J Radiol* 2004;52:119-136

23. Lu W, Chen ML, Olivera GH, et al. Fast free-form deformable registration via calculus of variations. *Phys Med Biol* 2004;49:3067-3087

Chapter

4

Benefit of respiration-gated stereotactic radiotherapy for stage I lung cancer: An analysis of 4DCT datasets

René WM Underberg
Frank J Lagerwaard
Ben J Slotman
Johan P Cuijpers
Suresh Senan

Abstract

Purpose: High local control rates have been reported with stereotactic radiotherapy (SRT) for stage I non-small cell lung cancer. As high dose fractions are used, reduction in treatment portals will reduce the risk of toxicity to adjacent structures. Respiratory gating can allow reduced field sizes and planning 4DCT scans were retrospectively analyzed in order to (1) study the benefits for gated SRT, and (2) identify patients who derive significant benefit from this approach.

Methods and Materials: A total of 31 consecutive patients underwent a 4DCT scan, in which 3D CT datasets for 10 phase bins of the respiratory cycle were acquired during free breathing. For a total of 34 tumors, the 3 planning target volumes (PTVs) were analyzed, namely [a] PTV_{10bins}, derived from an internal target volume (ITV) that incorporated all observed mobility (ITV_{10bins}), with the addition of a 3 mm isotropic setup margin, [b] PTV_{gating}, derived from an ITV generated from mobility observed in 3 consecutive phases ('bins') during tidal-expiration, plus addition of a 3 mm isotropic margin, and [c] PTV_{10mm}, derived from the addition of a 10 mm isotropic margin to the most central GTV in the 3 bins selected for gating.

Results: The PTV_{10bins} and PTV_{gating} were on average 48.2% and 33.3% of the PTV_{10mm}, and respective mean volumes of normal tissue (outside the PTV) receiving the prescribed doses were 57.1% and 39.1%, respectively, of that PTV_{10mm}. A significant correlation was seen between the extent of tumor mobility (i.e. a 3D mobility vector of at least 1 cm) and reduction in normal tissue irradiation achieved with gating. The ratio of the union and intersection of the tumor volumes at extreme phases of tidal respiration predicted for the benefits of gated respiration.

Conclusion: The use of 'standard population-based' margins for SRT leads to unnecessary normal tissue irradiation. The risk of toxicity is further reduced if respiration-gated radiotherapy is used to treat mobile tumors. These findings suggest that gated SRT will be of clinical relevance in selected patients with mobile tumors.

Introduction

In patients presenting with stage I non-small cell lung cancer (NSCLC), far higher local control rates have been reported using stereotactic radiotherapy (SRT) [1-8] than have been reported with conventional fractionated radiotherapy [9]. SRT generally combines high-precision irradiation with high fraction doses, and total biological doses well in excess of 100 Gy. Although the reported clinical toxicity after SRT for lung cancer is low, this may reflect both patient selection (e.g. small peripheral lung cancers) and a relatively short period of follow-up in most series. The high dose per fraction used can result in toxicity to normal lung tissue and adjacent structures such as the esophagus, spinal cord and thoracic wall [10], and it is therefore important that treatment portals for SRT should remain as small as possible. As most SRT approaches utilize online setup correction protocols, measures to reduce the margins used to account for tumor mobility offer a possible solution for minimizing toxicity.

Recent studies show that individualized, and not standard population-based margins, are necessary for high-precision radiotherapy of stage I NSCLC [11, 12]. Approaches such as breath-hold techniques and respiration-gated radiotherapy have been used to reduce target volumes for lung cancer [13, 14]. However, breath-hold techniques are often poorly tolerated by patients with lung cancer [13]. Respiratory gating permits a reduction in field sizes, as irradiation can be limited to phases in which the mobile target volume is in a predetermined position. Commercially available gating systems, e.g. the Varian Real-Time Position Monitor (RPM), are already in clinical use [15].

For SRT planning in stage I NSCLC, use of a single 4-dimensional (4D) or respiration-correlated CT scan was superior to the use of multiple conventional CT scans [16]. As our 4DCT scan technique also uses RPM gating equipment for co-registering respiratory signals, we analyzed 4D scans of 31 patients in order to (1) establish the benefit with use of respiratory gating in SRT, and (2) establish the criteria for identifying patients who could derive significant benefit from this approach.

Materials and Methods

A total of 34 tumors in 31 consecutive patients with stage I NSCLC, who were treated with fractionated SRT using 4DCT scans at the VU University medical center Amsterdam, were included in this study.

4DCT scanning procedure

Our current technique for generating internal target volumes (ITVs) for SRT of stage I NSCLC involves the use of a single 4DCT scan performed during quiet uncoached respiration. Patients are positioned supine, with the arms positioned above the head on an adjustable arm support. The RPM respiratory gating hardware (Varian Medical Systems, Palo Alto, CA) used for recording the breathing pattern entails placement of a lightweight block containing 2 reflective markers on the upper abdomen. Infrared light from an illuminator is reflected from the markers, and captured by a camera.

Our 4DCT scanning protocol for lung tumors on the Lightspeed 16 slice CT scanner simultaneously generates 8 contiguous slices of 2.5 mm for a 2 cm total longitudinal coverage per gantry rotation. The scanner is operated in axial cine mode. At each couch position, data are acquired for at least the duration of one respiratory cycle of the patient, after which the couch is advanced to the next position. Data acquisition ceases during couch movement, and a full 4DCT scanning procedure of the thorax takes about 90 seconds. Retrospective sorting of the images into spatio-temporally coherent volumes is performed using the Advantage 4D software [GE Medical Systems, Waukesha, WI]. Each reconstructed image is assigned to a specific respiratory phase (or 'bin') based on the temporal correlation between surface motion and data acquisition. Following the acquisition of a 4DCT scan, Advantage 4D software is used to resort images into 3D bins at 10 selected respiratory phases. Motion was assessed by reviewing the sorted data using 4D viewer software, which was used to identify the extremes of mobility.

The bins that represented 10 phases of respiration were imported into the BrainLab stereotactic radiotherapy planning system (Brainscan ver. 5.2, BrainLab AG, Heimstetten, Germany). As all 10 bins were derived from one single CT acquisition, image registration of the imported data sets (4D bins) on bony structures is not necessary.

Deriving target volumes

Gross tumor volumes (GTVs) were contoured in each of the 10 4D bins using standardized lung window level settings (Level=-500, Width=1000) by the same clinician in order to minimize contouring variations. All contours were automatically projected onto the first 'bin' of the 4DCT set, which was used for further analysis. As a

result of the high biological doses used with SRT, we and others apply no separate GTV to CTV margins for this indication [1, 17]. The actual internal target volumes used for SRT treatment planning were the volumes encompassing the GTVs from all 10 bins of the 4DCT scan (ITV_{10bins}).

As gating prolongs the treatment time, it is common to use a 'gate' that allows a duty cycle of between 20-40% of respiration [13]. Consequently, we selected 3 consecutive 'gating bins' during tidal-expiration by viewing the axial, frontal and sagittal reconstructions of all contoured GTVs. The encompassing volume of these 3 selected bins, labelled ITV_{gating}, was contoured separately for each patient. Planning target volumes (PTVs) were derived from ITV_{10bins} and ITV_{gating} by adding a 3-dimensional isotropic setup margin of 3 mm, which is used for extracranial SRT on the Novalis ExacTrac system (BrainLab AG, Heimstetten, Germany). A 'conventional' PTV was derived from the addition of an isotropic GTV-PTV margin of 10 mm to the most central GTV of the 3 bins used for respiratory gating (PTV_{10mm}). A volumetric comparison was made between the PTV_{10mm}, PTV_{10bins} and PTV_{gating} derived from the abovementioned definitions.

Dosimetry

The dosimetric consequences of using either PTV_{10mm}, PTV_{10bins} or PTV_{gating} were studied with the same beam configuration as was used for the actual patient treatment. This treatment plan, which was based upon PTV_{10bins} consisted of 8-12 individually optimized non-coplanar beams with 3 mm micro-multileaf collimation. The beam energy was 6 MV and the equivalent path length algorithm was used for tissue inhomogeneity correction. The clinical SRT fractionation schemes used were 3 fractions of 20 Gy, 5 fractions of 12 Gy, or 8 fractions of 7.5 Gy, prescribed to the 80% isodose and dependent on the location and size of lesion. As clinical toxicity parameters for normal tissues are not well established for such SRT schemes, the dose to normal tissues was evaluated as a percentage of the prescribed dose. Dose-volume histogram (DVH) analysis was used to determine the volume of normal tissue within the high-dose region, which was defined by 40% and 80% isodoses.

Analysis of mobility

3D mobility vectors were derived for each tumor using the X, Y, and Z coordinates of the center of mass for each bin of the 4DCT scan, as derived from the Brainscan

software. In addition, the residual mobility in the 3 bins selected for respiratory gating was determined. These mobility vectors were correlated with the reductions in PTV_{10bins} and PTV_{gating}, respectively. As generating mobility vectors requires that all ten bins of the 4DCT scan be contoured, a less time-consuming method was investigated by first identifying the extremes of mobility using Advantage 4D software. After contouring only the GTVs on these 2 bins, the ratio of the intersecting and the encompassing volumes of these extreme phases was determined. A value close to 1 indicated the relative absence of mobility.

Results

A total of 34 tumors were analyzed. Tumor characteristics are shown in Table 1. There were 24 T_1N_0 tumors (70.6%) and 10 T_2N_0 tumors (29.4%). The mean GTVs of T1 and T2 tumors were 4.8 cc and 27.3 cc, respectively. Included were 11 lower lobe tumors, 22 upper lobe tumors, and 1 middle lobe tumor, and 8 tumors were adjacent to the pleura.

Analysis of PTVs

Review of all absolute and relative PTVs revealed PTV_{10mm} to be the largest in all patients (Figure 1a-1b). Use of an individualized PTV_{10bins} led to an average volume of 48.2 $\pm$ 14.3% (SD) of the PTV_{10mm}. The PTV_{gating} was even smaller, with an average value of 33.3 $\pm$ 9.6% of the PTV_{10mm}. The mean PTV_{gating} was 70.5 $\pm$ 15.7% of the PTV_{10bins}.

Table 1.   Tumor characteristics

Tumor	Stage	Tumor location
1	T1N0M0	Left upper lobe
2	T1N0M0	Left upper lobe
3	T1N0M0	Left upper lobe
4	T1N0M0	Right upper lobe
5	T1N0M0	Right upper lobe
6	T1N0M0	Right upper lobe
7	T1N0M0	Right upper lobe
8	T1N0M0	Left upper lobe
9	T2N0M0	Right upper lobe
10	T2N0M0	Left upper lobe
11	T1N0M0	Right upper lobe
12	T1N0M0	Right upper lobe
13	T1N0M0	Left upper lobe
14	T1N0M0	Right upper lobe
15	T1N0M0	Left upper lobe
16	T1N0M0	Left upper lobe
17	T2N0M0	Left upper lobe
18	T1N0M0	Right middle lobe
19	T1N0M0	Left lower lobe
20	T1N0M0	Left lower lobe
21	T1N0M0	Left lower lobe
22	T2N0M0	Right lower lobe
23	T1N0M0	Left lower lobe
24	T2N0M0	Right lower lobe
25	T1N0M0	Right lower lobe
26	T1N0M0	Left lower lobe
27	T2N0M0	Right upper lobe; adjacent to pleura
28	T2N0M0	Right upper lobe; adjacent to pleura
29	T2N0M0	Left lower lobe; adjacent to pleura
30	T2N0M0	Right upper lobe; adjacent to pleura
31	T1N0M0	Left lower lobe; adjacent to pleura
32	T2N0M0	Right upper lobe; adjacent to pleura
33	T1N0M0	Right upper lobe; adjacent to pleura
34	T1N0M0	Right lower lobe; adjacent to pleura

Figure 1a. Absolute volumes of PTV$_{gating}$ (■), PTV$_{10bins}$ (▲) and PTV$_{10mm}$ (●)
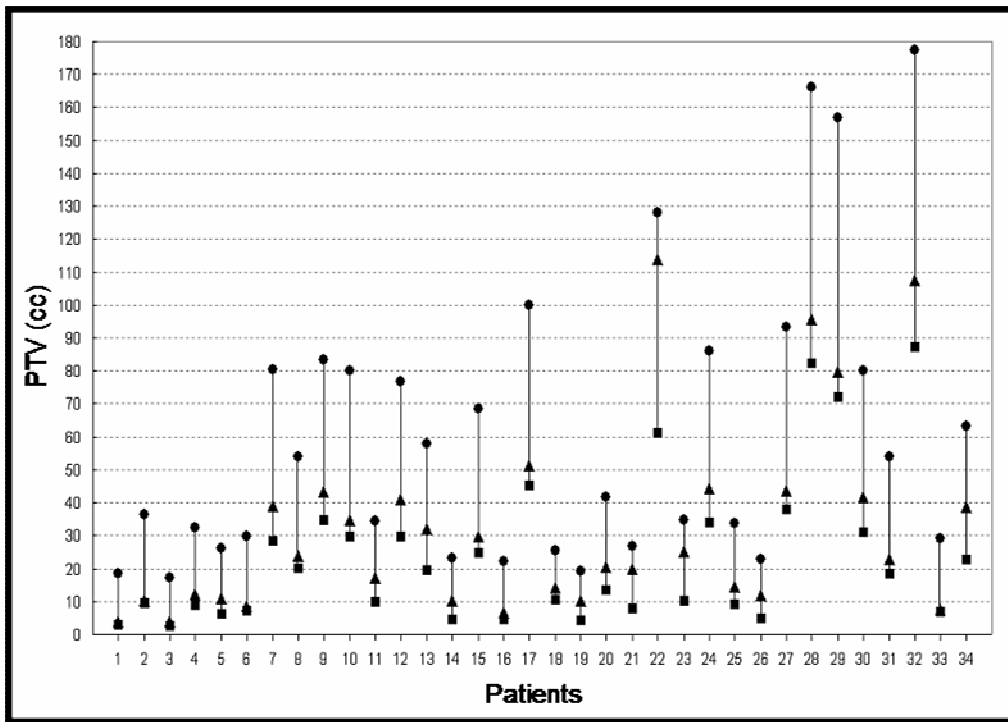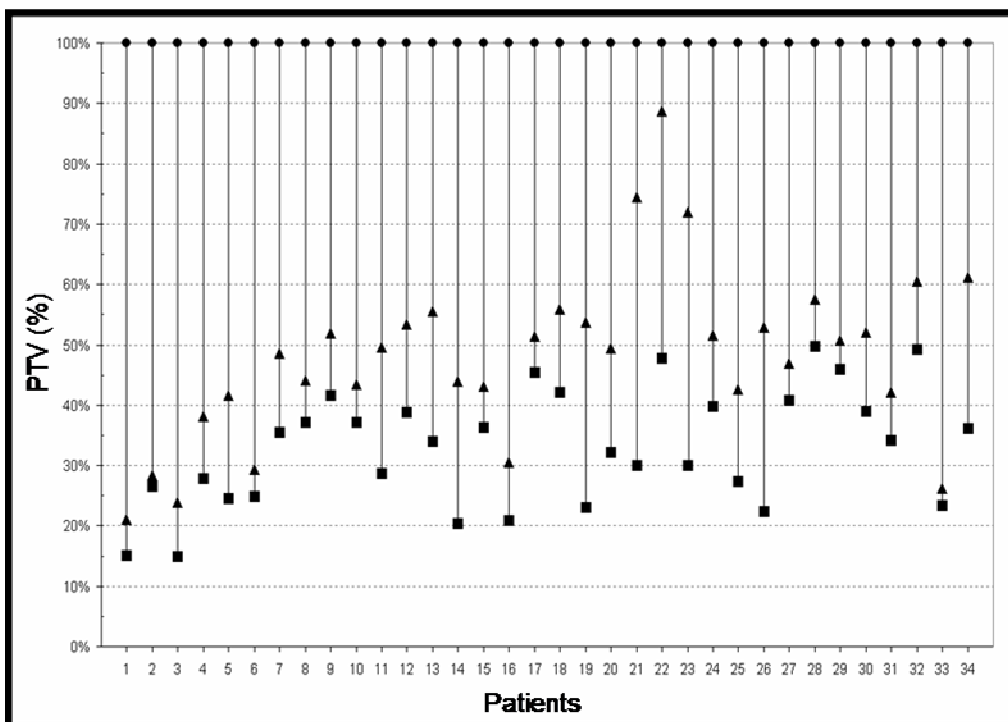

Figure 1b. Relative volumes of PTV$_{gating}$ (■), PTV$_{10bins}$ (▲) and PTV$_{10mm}$ (●)

Irradiated normal tissue volumes

The relative volumes of normal tissue encompassed by the 80% isodose were compared using treatment planning (Figure 2). The mean volumes of normal tissue, that were encompassed by the 80% isodose when PTV_{10bins} and PTV_{gating} were used, were 57.1 $\pm$ 18.0% and 39.1 $\pm$ 11.5% of the PTV_{10mm}, respectively. A similar pattern was observed for the volume of normal tissue receiving 40% of the dose (data not shown). A typical example of the dose reductions in normal tissues achieved with gated radiotherapy for a mobile tumor is illustrated in Figure 3.

Figure 2. Relative volume of normal tissue encompassed by the 80% isodose with treatment planning on PTV_{gating} (■), PTV_{10bins} (▲). All values are relative to PTV_{10mm} (●)
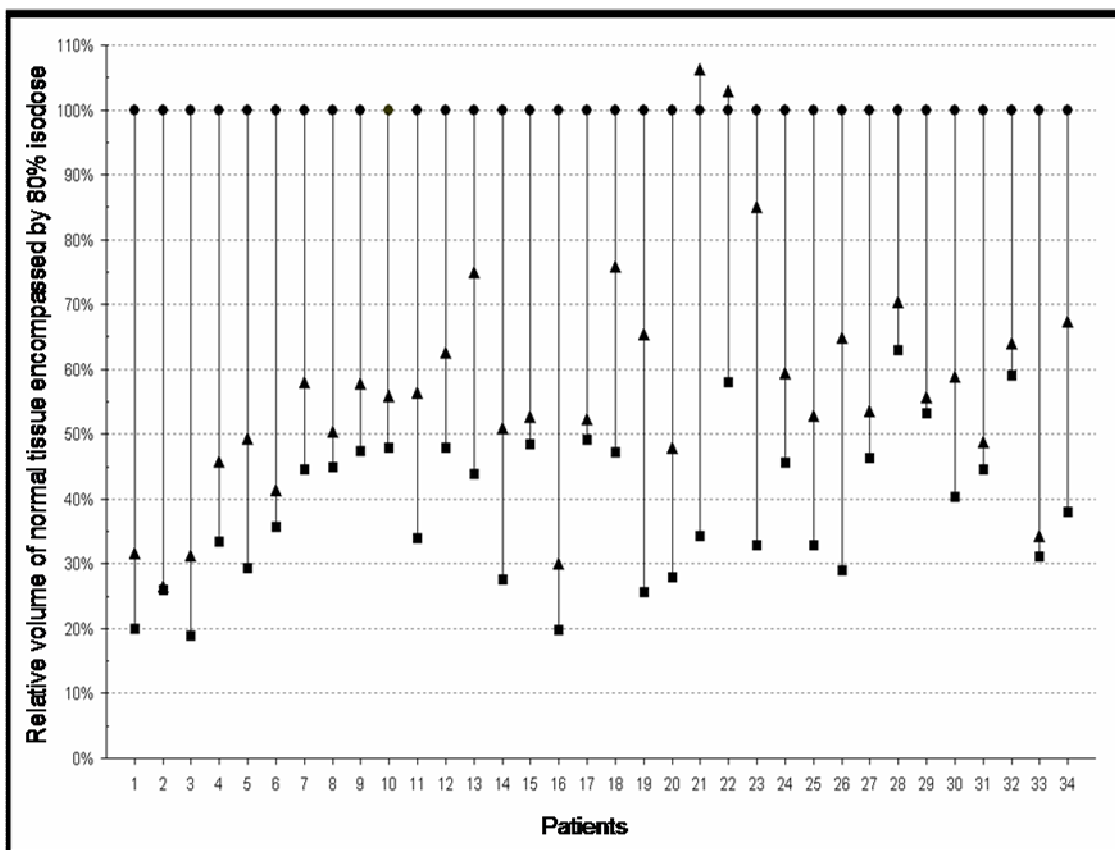
Figure 3. Example (case 21) of reduction in volume of normal tissue (in this case chest wall and lung tissue) in high-dose area (80% isodose) with treatment planning on PTV$_{10bins}$ and PTV$_{gating}$.
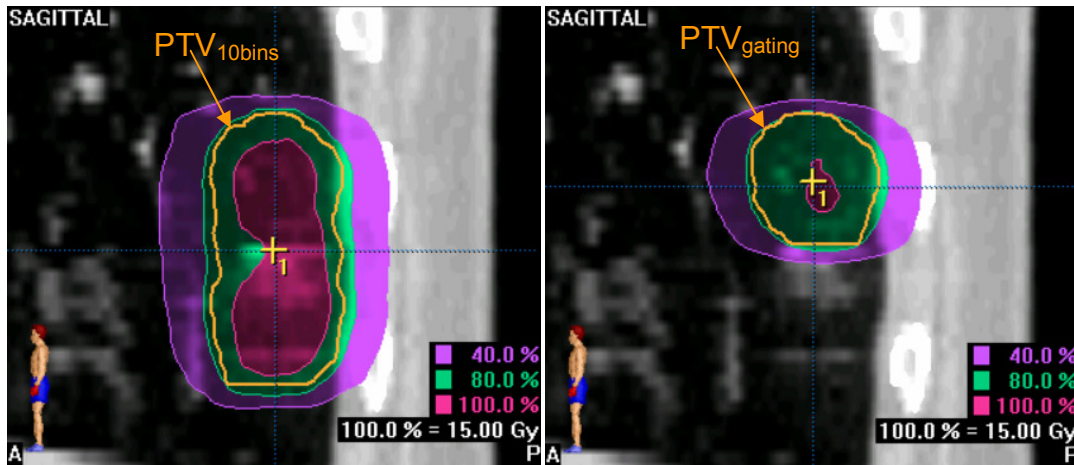
Residual mobility with gating

It is desirable that the residual motion in phases selected for gating is kept small. The mean 3D mobility vector for all 10 bins was 8.5 $\pm$ 6.5 mm, and it decreased to 1.4 $\pm$ 0.7 mm in the 3 gating bins (Figure 4). The corresponding values for tumors of the lower lobe were 13.5 $\pm$ 8.8 mm, with a decrease to 1.7 $\pm$ 0.9 mm with gating.

Figure 4. 3D mobility vectors derived from 10 bins ($\square$) versus gating window (3 bins; $\blacksquare$)
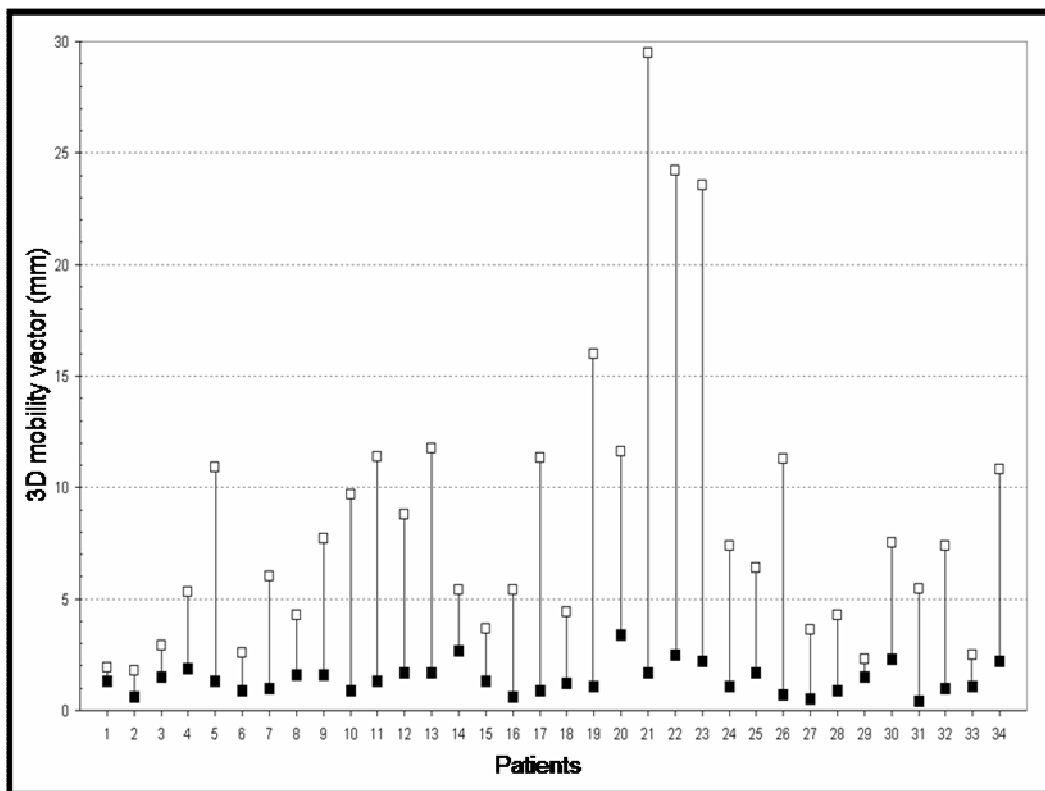
Tumor mobility versus dosimetric gain with gating

As expected, a clear correlation was seen between the size of the 3D mobility vector and reduction in target volumes obtained using 4DCT scans and gating, respectively (regression coefficient R^2 = 0.61; Figure 5). This trend was observed for both T1 and T2 tumors, although relatively few T2 patients had relatively large 3D mobility vectors.

Pre-selection of patients for gated SRT

A simplified method was investigated for identifying suitable patients for gating. The ratio of the intersecting and the encompassing volume of the GTV in extreme phases during tidal in- and expiration showed a high regression coefficient of 0.88 (Figure 6). This is a less laborious approach than using 3D mobility vectors derived from GTVs contoured on all ten bins. If a PTV reduction of at least 50% is used to select candidates for respiratory-gated SRT, only 14.7% (5 patients) of our patients would have been eligible.

Figure 5. Reduction (%) of PTV$_{gating}$ compared to PTV$_{10bins}$ versus size of 3D mobility vector
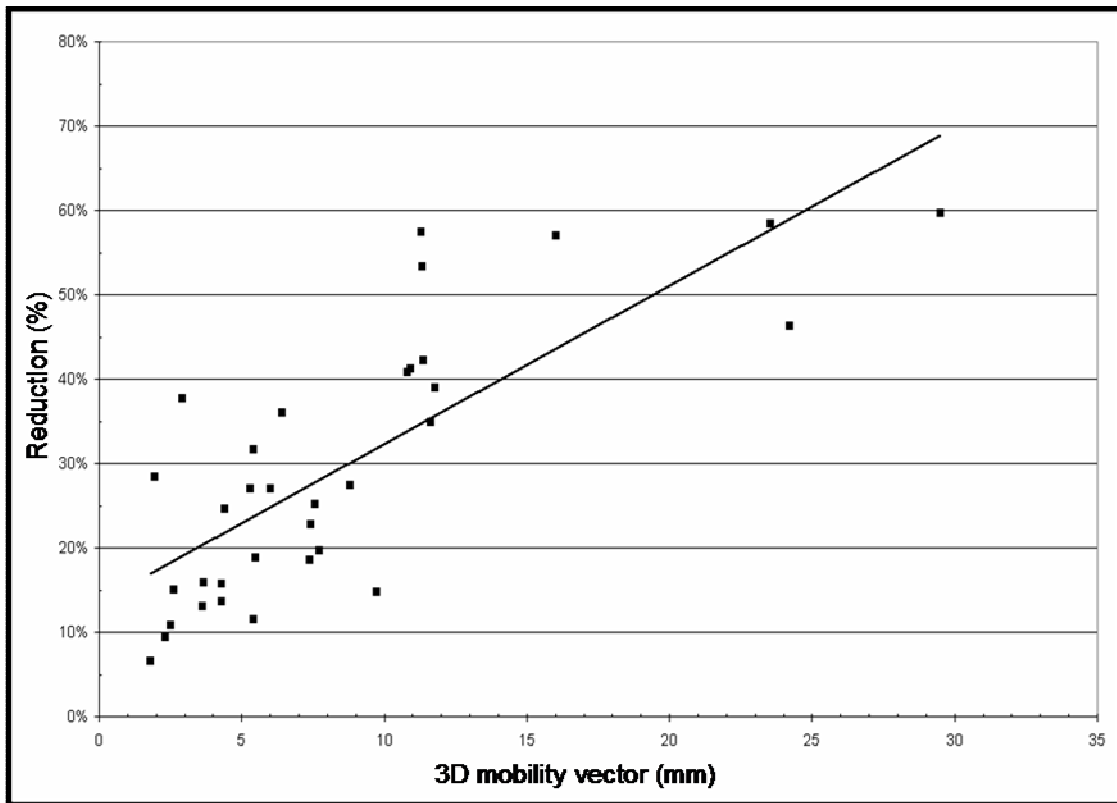
Figure 6. Relation between the ratio of the intersecting/encompassing volume of GTVs in extreme phases of respiration and PTV reduction obtained with gating
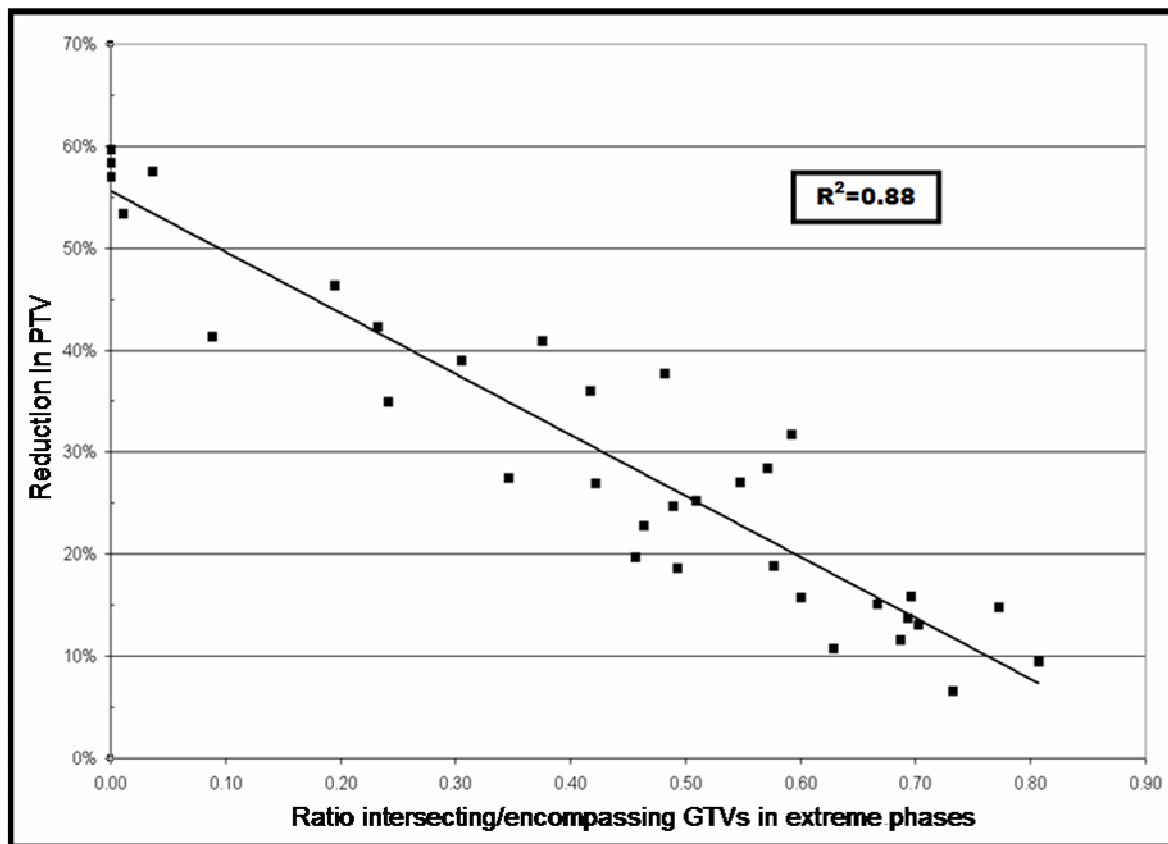
Discussion

The reduction of the planning margins required to account for tumor mobility is the subject of active, ongoing research. The majority of patients with stage I NSCLC who are referred for radiotherapy are ineligible for surgery due to poor pulmonary function [18], and this explains an inability to tolerate procedures such as DIBH in up to 50% of patients [13]. As such, passive respiration-gated radiotherapy would appear to be an ideal approach for reducing the risk of normal tissue toxicity in this patient population.

Early reports on the implementation of respiration-gated radiotherapy for lung tumors described the use of fluoroscopy for selecting phases for respiratory gating [19-21]. However, fluoroscopy does not permit accurate 3D determination of mobility for lung tumors in radiotherapy planning [22]. The use of 4DCT scans, on the other hand, enables a full characterization of tumor mobility and better detects mobility than even 6 consecutive conventional CT scans [16]. As our technique for 4DCT scanning also

uses the RPM respiratory gating system, the 4D datasets obtained permit a rapid, patient-specific analysis of tumor mobility, and of the potential gains from gating.

Recent work has shown that the use of standard margins result in inadequate target coverage for a proportion of patients with lung cancer [11, 16, 23, 24]. In comparison to PTVs generated using a 'standard' GTV to PTV margin of 10 mm, our analysis reveals that use of individualized margins (either PTV_{10bins} or PTV_{3bins}) allows for significant reductions in both PTV and mean volume of normal tissues within the 80% to 40% isodose. These findings reinforce the inappropriateness of standard mobility margins in SRT for lung cancer.

We analyzed gating using 3 consecutive phases at end-tidal expiration in order to yield a 30% treatment window, which in turn reduced the mean 3D tumor mobility vector from 8.5 mm to 1.4 mm. However, as the delivery of gated SRT can take up to 1-2 hours [17], use of larger gating windows may be more patient-friendly. When the cine-movies of 4DCT's and the GTVs on all contoured bins were reviewed, a larger gating window appeared possible for some patients without undue increases in PTV. Our planning study assumed that gated radiotherapy at the end-expiratory phase was optimal for this patient group. Gating at end-expiration permits longer duty cycles, and is facilitated by the fact that the expiratory phase is more reproducible [19, 20, 25]. The RPM system also permits gating based upon amplitude of the respiratory waveform, and the relative benefit of this approach remains to be investigated using 4DCT scans.

When compared to the PTV_{10bins}, use of gating would have reduced PTVs by more than 30% in 38% of tumors, and by more than 50% in 15% of tumors. As expected, these gains from gating were greatest in mobile tumors, which we arbitrarily defined as those with a 3D mobility vector of 1 cm or more. Such tumors comprised 32% (11 out of 34) of our tumors, and comparable figures for mobility have been reported by others. For example, analysis of data generated during tumor-tracking found that 11 of 41 measured tumor trajectory datasets showed a maximum peak-to-peak motion of 1 cm [26]. An analysis using multiple CT scans reported that 44% of all tumors showed a 3D mobility of more than 1 cm, and more than 50% of such tumors were located in the lower lobe [11].

A simplified method for identifying mobile tumors in 4DCT datasets was established by contouring only the 2 respiratory bins at the extremes of tidal respiration, after these phases were identified using 4D viewing software. The measure of tumor overlap between these two phases was shown to have a high predictive value for tumor mobility and, consequently, can be used to identify patients in whom addition treatment planning for respiration-gated radiotherapy is warranted. A reliable threshold to define which patients are suitable for respiratory-gating is difficult as this is not only dependent on the PTV reduction, but also on the absolute volume of the PTV. Furthermore, the incidence of toxicity with high-dose radiotherapy for stage I NSCLC is low. We defined a threshold of at least 50% PTV reduction as a potential indication for respiration-gated SRT. Although a volumetric reduction was observed for most cases, this threshold would indicate a clear benefit for respiratory-gating in only 5 patients (14.7%).

A number of limitations of the present study are being addressed in our ongoing work. Despite reduced normal tissue irradiation with respiratory gating, it remains to be established if reproducible target volumes can be derived from 4DCT scans generated using the RPM system. Our patients were scanned during uncoached quiet respiration after a reproducible pattern of respiration was observed. Previous work suggests that indirect tumor tracking by means of external breathing signals and/or diaphragmatic movements may fail to reflect actual 3D movements in some patients [27]. Repeat 4DCT scans performed during SRT are currently being analyzed in order to establish the reproducibility of both breathing patterns, as well as tumor position.

With interventions such as gating, direct visualization of tumor at the treatment unit offers a major advantage by permitting verification of target position, and identifies potential time-trends. Recent advances such as cone-beam CT scans and tomotherapy are ideal for this purpose [28], although gated imaging will have to be made possible for such devices. Until such time as gated imaging at the linear accelerator becomes available at our center, we will evaluate gating only in patients who have implanted fiducial markers that permit online tumor visualization.

The amplitude and frequency of the respiratory signal can be variable during free breathing, and training using visual feedback and/or audio prompting has been shown to increase the gating window [29]. We are currently investigating the use of coaching

for the delivery of gated SRT in stage I lung cancer, and this could alter the relative benefits of gating. We are aware that inaccuracies of the calculation algorithm in dealing with electron transport in lung tissue exist, and penumbra broadening in lung tissue is not adequately accounted for [30]. For our planning study multiple intersecting 6 MV photon beams were used with dose prescription to the 80% isodose, so that such inaccuracies are unlikely to influence our conclusions. Current radiotherapy planning systems are unable to perform actual time-weighted dose calculation on 4DCT scans, which would also require to take respiratory changes in total lung volume into account. Our planning study was therefore performed on the first phase of the 4DCT scan in order to allow a reliable dosimetric comparison. Other important technical aspects of gated delivery are outside the scope of our study.

In conclusion, analysis of this 4DCT database again highlights the inappropriateness of using 'standard population-based' margins for stage I NSCLC. Respiration-gated radiotherapy significantly reduces normal tissue irradiation when mobile tumors are treated. Further data on the reproducibility of respiratory waveforms (and tumor position), as well as on-line tumor visualization, will facilitate the clinical use of gated radiotherapy. As was recently pointed out, the worst intervention for mobility is one that falsely reassures and increases the chance of a geographic miss [31].

References

1. Timmerman R, Papiez L, McGarry R, et al. Extracranial stereotactic radioablation: results of a phase I study in medically inoperable stage I non-small cell lung cancer. *Chest* 2003;124:1946-1955

2. Lee S, Choi EK, Park HJ, et al. Stereotactic body frame based fractionated radiosurgery on consecutive days for primary or metastatic tumors in the lung. *Lung Cancer* 2003;40:309-315

3. Whyte RI, Crownover R, Murphy MJ, et al. Stereotactic radiosurgery for lung tumors: preliminary report of a phase I trial. *Ann Thorac Surg* 2003;75:1097-1101

4. Uematsu M, Shioda A, Suda A, et al. Computed tomography-guided frameless stereotactic radiotherapy for stage I non-small cell lung cancer: a 5-year experience. *Int J Radiat Oncol Biol Phys* 2001;51:666-670

5. Fukumoto S, Shirato H, Shimizu S, et al. Small-volume image-guided radiotherapy using hypofractionated, coplanar, and noncoplanar multiple fields for patients with inoperable stage I nonsmall cell lung carcinomas. *Cancer* 2002;95:1546-1553

6. Onishi H, Nagata Y, Shirato H, et al. Stereotactic hypofractionated high-dose irradiation for patients with stage I non-small cell lung carcinoma: clinical outcomes in 241 cases of a Japanese multi-institutional study (Abstr.). *Int J Radiat Oncol Biol Phys* 2003 ;57(Suppl.):S142

7. Hof H, Herfarth KK, Münter M, et al. Stereotactic single-dose radiotherapy of stage I non-small-cell lung cancer (NSCLC). *Int J Radiat Oncol Biol Phys* 2003;56:335-341

8. Wulf J, Hadinger U, Oppitz U, et al. Stereotactic radiotherapy of targets in the lung and liver. *Strahlenther Onkol* 2001;177:645-655

9. Qiao X, Tullgren O, Lax I, et al. The role of radiotherapy in treatment of stage I non-small cell lung cancer. *Lung Cancer* 2003;41:1-11

10. Onimaru R, Shirato H, Shimizu S, et al. Tolerance of organs at risk in small-volume, hypofractionated, image-guided radiotherapy for primary and metastatic lung cancers. *Int J Radiat Oncol Biol Phys* 2003;56:126–135

11. van Sörnsen de Koste JR, Lagerwaard FJ, Nijssen-Visser MR, et al. Tumor location cannot predict the mobility of lung tumors: a 3D analysis of data generated from multiple CT scans. *Int J Radiat Oncol Biol Phys* 2003;56:348-354

12. Plathow C, Ley S, Fink C, et al. Analysis of intrathoracic tumor mobility during whole breathing cycle by dynamic MRI. *Int J Radiat Oncol Biol Phys* 2004;59:952-959

13. Mageras GS, Yorke E. Deep inspiration breath hold and respiratory gating strategies for reducing organ motion in radiation treatment. *Semin Radiat Oncol* 2004;14:65-75

14. Keall PJ, Kini VR, Vedam SS, et al. Potential radiotherapy improvements with respiratory gating. *Australas Phys Eng Sci Med* 2002;25:1-6

15. Wagman R, Yorke E, Ford E et al. Respiratory gating for liver tumours: use in dose escalation. *Int J Radiat Oncol Biol Phys* 2003;55:659-668

16. Underberg RWM, Lagerwaard FJ, Cuijpers JP, et al. 4-dimensional CT scans for treatment planning in stereotactic radiotherapy for stage I lung cancer. *Int J Radiat Oncol Biol Phys* 2004;60:1283-1290

17. Hara R, Itami J, Kondo T, et al. Stereotactic single high dose irradiation of lung tumors under respiratory gating. *Radiother Oncol* 2002;63:159-163

18. Lagerwaard FJ, Senan S, van Meerbeeck JP, et al. Has 3D conformal radiotherapy improved the local tumor control in stage I non-small cell lung cancer? *Radiother Oncol* 2002;63:151-157

19. Minohara S, Kanai T, Endo M, et al. Respiratory gated irradiation system for heavy-ion radiotherapy. *Int J Radiat Oncol Biol Phys* 2000;47:1097–1103

20. Ford EC, Mageras GS, Yorke E, et al. Evaluation of respiratory movement during gated radiotherapy using film and electronic portal imaging. *Int J Radiat Oncol Biol Phys* 2002;52:522-531

21. Shirato H, Shimizu S, Kitamura K, et al. Four-dimensional treatment planning and fluoroscopic real-time tumor tracking radiotherapy for moving tumor. *Int J Radiat Oncol Biol Phys* 2000;48:435-442

22. Halperin R, Pobinson D, Murray B. Fluoroscopy for assessment of physiologic movement of lung tumors, a pitfall of clinical practice? (Abstr.) *Radioth Oncol* 2002;65(Suppl. 1):87

23. van Sörnsen de Koste JR, Lagerwaard FJ, Schuchhard-Schipper RH, et al. Dosimetric consequences of tumor mobility in radiotherapy of stage I non-small cell lung cancer– an analysis of data generated using 'slow' CT scans. *Radiother Oncol* 2001;61:93-99

24. Allen AM, Siracuse KM, Hayman JA, et al. Evaluation of the influence of breathing on the movement and modeling of lung tumors. *Int J Radiat Oncol Biol Phys* 2004;58:1251-1257

25. Balter JM, Lam KL, McGinn CJ, et al. Improvement of CT-based treatment-planning models of abdominal targets using static exhale imaging. *Int J Radiat Oncol Biol Phys* 1998;41:939-43

26. Neicu T, Shirato H, Seppenwoolde Y, et al. Synchronized moving aperture radiation therapy (SMART): average tumour trajectory for lung patients. *Phys Med Biol* 2003;48: 587-598

27. Murphy MJ, Martin D., Whyte R., et al. The effectiveness of breath-holding to stabilize lung and pancreas tumors during radiosurgery. *Int J Radiat Oncol Biol Phys* 2002;53:475-482

28. Mackie TR, Kapatoes J, Ruchala K, et al. Image guidance for precise conformal radiotherapy. *Int J Radiat Oncol Biol Phys* 2003;56:89-105

29. Kini VR, Vedam SS, Keall PJ, et al. Patient training in respiratory-gated radiotherapy. *Med Dosim* 2003;28:7-11

30. Engelsman M, Damen EMF, Koken PW, et al. Impact of simple tissue inhomogeneity correction algorithms on conformal radiotherapy for lung tumors. *Radioth Oncol* 2001;60:299-309

31. Dawson LA, Balter JM. Interventions to reduce organ motion effects in radiation delivery. *Semin Radiat Oncol* 2004;14:76-80

C h a p t e r

5

Time trends in target volumes for stage I non-small cell lung cancer after stereotactic radiotherapy

René WM Underberg
Frank J Lagerwaard
Harm van Tinteren
Johan P Cuijpers
Ben J Slotman
Suresh Senan

<u>Abstract</u>

<u>Purpose</u>: To identify potential time trends in target volumes and tumor mobility after stereotactic radiotherapy (SRT) for stage I non-small cell lung cancer.

<u>Patients and methods</u>: Repeat planning CT scans were performed for 40 tumors during fractionated SRT delivered in either three (n=21), five (n=14) or eight fractions (n=5). The planning CT scans used to define internal target volumes (ITVs) consisted of either 6 multi-slice CT scans or a single 4DCT scan. All repeat CT scans were co-registered with the initial (D_0) scan to determine volumetric or spatial changes in target volume, and tumor mobility vectors were determined from each scan.

<u>Results:</u> A significant decrease in target volumes (ITVs and GTVs) relative to baseline values was observed starting at the fourth week of SRT (p=0.015). No trends in tumor mobility were detected during SRT. Significant positional shifts in the ITV, of more than 5 mm, were seen in 26-43% of patients at different times during SRT.

<u>Conclusion</u>: Significant changes in target volumes can occur during SRT for stage I NSCLC. A failure to account for such changes, e.g. by repeat CT-planning or verification using on-board volumetric imaging, can lead to inadequate target coverage.

Introduction

The optimal approach for defining internal target volumes (ITVs) for mobile tumors such as lung cancer is the subject of active research [1]. Individualized assessment of tumor mobility has been shown to be necessary for lung tumors [2-4], and such individualized ITVs can be derived using slow scans [5], multiple computed tomography (CT) scans [6] or four-dimensional CT (4DCT) scans [7]. Despite a potentially major impact on local control, the reproducibility of ITVs for lung cancer during the entire course of treatment has not been well studied. An analysis of electronic portal images obtained during conventional radiotherapy reported 'tumor shrinkage' of 20% or more, in 40% of patients [8]. However, portal images are unsuitable for accurate volumetric or spatial assessment, and an evaluation using CT scans found the response to conventional radiotherapy or chemo-radiotherapy to be a slow process, with tumor volumes reaching their nadir 11 months after treatment completion [9].

The issue of target reproducibility is of critical importance for high-dose hypofractionated treatment regimens such as stereotactic radiotherapy (SRT). Local control rates of approximately 85-90% have been reported after SRT for lung cancer [10-15], which are in marked contrast to those achieved with conventional 3-dimensional conformal (3D) radiotherapy [16,17].
Repeat planning CT scans performed before each fraction of pulmonary SRT revealed that the target coverage was below 95% of the prescribed dose in 9% of patients [18]. In view of this, as well as potential time trends in target volumes and changes in respiratory patterns, we elected to perform repeat treatment planning during SRT in all patients with stage I non-small cell lung cancer (NSCLC). The aim of the present study was to investigate inter-fractional changes in target volumes and tumor mobility during this 3- to 5-week period of SRT.

Materials and Methods

A retrospective analysis was performed on all treatment planning CT scans performed for SRT in 37 patients, who had a total of 40 stage I NSCLC. Tumor and treatment characteristics, including the overall treatment time, are summarized in Table 1. Before SRT, all patients underwent a setup procedure at the Novalis linear accelerator (BrainLab AG, Heimstetten, Germany). Adjustable arm support, as well as knee and ankle supports were used. The Novalis ExacTrac system of online setup correction

using both external reference markers and kilovolt images was used for stereotactic treatment. In the first 15 patients, the routine CT scanning procedure for deriving ITVs consisted of a single uncoached multislice CT scan (MSCT) of the entire thorax during quiet respiration, followed by five similar scans that were limited to the tumor region. All subsequent patients underwent a single respiration-correlated or 4DCT scan [7]. In view of the number and size of fractions delivered, and reports of the inadequacy of an initially defined PTV [18], CT planning was generally repeated before each weekly fraction in patients undergoing a three- or five-fraction scheme, and in the second week when the 8-fraction scheme was used. The indications for use of the different fractionation schemes are summarized in Table 2. Each subsequent fraction was planned and delivered using the most recent planning CT scan.

Multiple MSCT technique

The multiple spiral MSCT scans were performed during quiet uncoached respiration on a 16-slice GE Lightspeed CT scanner (GE Medical Systems, Waukesha, WI) with a slice thickness of 2.5 mm and an index of 2.5 with contiguous reconstruction. Co-registration of all CT scans (one full range scan and five limited to the tumor region) from any given time during treatment was performed using the image-fusion software from the stereotactic planning system (Brainscan version 5.2, BrainLab, Heimstetten, Germany).

4DCT scanning technique

4DCT scanning was performed during quiet uncoached respiration on the 16-slice GE Lightspeed CT scanner using the Varian Real-Time Position Management (RPM) respiratory gating hardware for recording of the breathing pattern (Varian Medical Systems, Palo Alto, CA) and 4D imaging software (Advantage 4D, GE Medical Systems, Waukesha, WI). Briefly, the respiratory signals from the RPM hardware are recorded using infrared-reflecting markers on the patient's thorax during quiet, uncoached respiration. The markers are illuminated by infrared-emitting diodes surrounding a camera, and the motion of these markers is captured by the camera at a frequency of 25 frames per second. A respiratory signal is recorded in synchronization with the X-ray 'ON' signal from the CT scanner. Our current 4D protocol for lung tumors uses the 8-slice mode of the CT scanner with a slice thickness of 2.5 mm, obtained during quiet respiration. The 4D data sets are sorted out for ten phase bins within the respiratory cycle using an Advantage 4DCT

application running on an Advantage Workstation 4.1. The volumetric datasets that represent 10 different phases of respiration (bins) were used for further analysis.

Table 1. Tumor and treatment characteristics

Tumor	TNM-stage	Fraction size (Gy)	Total dose (Gy)	OTT (weeks)
1	T2N0M0	7.5	60	2
2	T2N0M0	7.5	60	2
3	T1N0M0	7.5	60	2
4	T2N0M0	7.5	60	2
5	T2N0M0	7.5	60	2
6	T2N0M0	20	60	3
7	T1N0M0	20	60	3
8	T1N0M0	20	60	3
9	T2N0M0	20	60	3
10	T1N0M0	20	60	3
11	T1N0M0	20	60	3
12	T1N0M0	20	60	3
13	T2N0M0	20	60	3
14	T1N0M0	20	60	3
15	T1N0M0	20	60	3
16	T1N0M0	20	60	3
17	T1N0M0	20	60	3
18	T1N0M0	20	60	3
19	T1N0M0	20	60	3
20	T1N0M0	20	60	3
21	T1N0M0	20	60	3
22	T1N0M0	20	60	3
23	T1N0M0	20	60	3
24	T2N0M0	20	60	3
25	T1N0M0	20	60	3
26	T2N0M0	20	60	3
27	T2N0M0	12	60	5
28	T2N0M0	12	60	5
29	T1N0M0	12	60	5
30	T1N0M0	12	60	5
31	T2N0M0	12	60	5
32	T1N0M0	12	60	5
33	T1N0M0	12	60	5
34	T2N0M0	12	60	5
35	T1N0M0	12	60	5
36	T2N0M0	12	60	5
37	T1N0M0	12	60	5
38	T1N0M0	12	60	5
39	T2N0M0	12	60	5
40	T2N0M0	12	60	5

OTT = overall treatment time

Table 2. Fractionation schemes used at the VU University medical center

Scheme	Indication
3 x 20 Gy	T1N0 tumours, no or minimal contact with chest wall/mediastinum
5 x 12 Gy	T1N0 and T2N0 tumours with extensive contact with chest wall or mediastinum
8 x 7.5 Gy	"High risk" patients (e.g. proximity to spinal cord or pulmonary artery)

Generating target volumes

All CT data sets (i.e. six MSCT scans or ten bins from the 4DCT scan) were imported into the BrainLab stereotactic radiotherapy planning system (Brainscan ver. 5.2). Co-registration of CT scans was performed using the automated matching software of this planning system, and the results were checked visually by contouring spinal vertebra adjacent to the tumor, which was then automatically projected onto each co-registered CT scan. Gross tumor volumes (GTVs) were contoured in each of the scans using a standardized lung window level setting, and the same clinician contoured all scans of a particular patient to minimize contouring variations. Up to ten GTVs were obtained per patient, i.e. either six from MSCT scans ($GTV_{6\ scans}$) or ten from the bins of a 4DCT scan (GTV_{4DCT}). All contours were automatically projected onto either the full range MSCT scan or the first 'bin' of the 4DCT set, which were used for the subsequent analysis. In accordance with recent American Society of Therapeutic Radiology and Oncology guidelines [19], no separate margins for deriving clinical target volumes (CTVs) were used. For clinical delivery of SRT, the data from the multiple MSCT and 4DCT were used to derive individualized mobility margins for treatment planning. ITVs for treatment were defined as the encompassing volumes of all $GTV_{6\ scans}$ or all GTV_{4DCT}, respectively.

Analysis of time trends

To study volumetric time trends in GTVs during the course of SRT, the mean GTV (derived from 10 GTV_{4DCT} or 6 $GTV_{6\ scans}$) for each fraction of SRT was compared to the D_0 value. For 25 tumors for which complete 4DCT data were available, an analysis for trends in tumor mobility was performed. 3D mobility vectors were derived for each stereotactic treatment fraction as follows. Using the Brainscan software, the X, Y and Z coordinates of the center of mass of the GTVs derived from each 4DCT bin were

established. The maximal 2-dimensional displacement in all three directions was determined, and a 3D vector was calculated using the Pythagoras's algorithm.

Because changes in both GTVs and tumor mobility can influence ITVs, the latter were also analyzed for each new scan. A spatial analysis of time trends in ITVs was possible in only 36 tumors as a result of patient-setup variations in the remaining 4 patients. Interfractional shifts in ITV were studied by projecting the center of mass of each ITV onto the co-registered D_0 planning scan. This co-registration was performed using image-registration software from the BrainLab planning system and a contoured vertebra at the level of the tumor. Registrations were visually adjusted when needed in the sagittal plane to minimize anterior-posterior rotations. The shifts in ITV were derived from the X, Y and Z coordinates of the subsequent ITVs, and 3D shift vectors compared with the D_0 ITV were calculated for each fraction.

Finally, in tumors in which post-treatment follow-up CT scans at three months or six months were available, and evaluable for tumor size (36 and 25 tumors, respectively), the residual mass was contoured and compared with the mean GTVs during SRT.

Statistical analysis

The differences in time in mean GTVs and ITVs were evaluated using a mixed model for repeated measures data (PROC MIXED, SAS V8.2, SAS Institute Inc., Cary, NC) [20]. The existence of potential time trends was correlated with T-classification (T1 versus T2 tumors), CT scanning technique (multiple MSCT scans versus 4DCT), and number of SRT fractions (three versus five versus eight). For within-subject correlations, a spatial (spatial power law) covariance structure was defined. This structure assumes that correlations of repeated measures are smaller for observations that are further apart in time. There was a small difference in variance between the "multiple MSCT" and "4DCT" group. Therefore different variance structures were allowed. Time, number of fractions, CT scanning technique and T-classification of the tumor were considered fixed parameters.

Results

Time trends in GTVs

The successive mean GTV of 40 tumors during the course of SRT is shown in Figure 1. There was a time-trend towards decreasing GTVs, but this was only statistically significant when D_0 values were compared to GTVs at 4 weeks after the start of treatment (p=0.015). As can be seen in Figure 2a, 11 of 40 tumors showed substantial regression during treatment. The observed time trend in GTVs was irrespective of T-stage, CT scanning technique, or fraction dose. Although overall the GTVs decreased over time, a transient increase in the mean GTV of >10 cc was observed in 2 tumors during the first two weeks of SRT.

Follow-up CT scans at 3 and 6 months after SRT were assessable for volumetric measurement in 36 and 25 tumors, respectively. In all other cases, the follow up was either too short or the residual mass could not be distinguished from radiation-induced fibrosis. Analysis of these follow-up CT scans revealed that regression of stage I NSCLC after SRT is a process that proceeds at least until 6 months after treatment (Figure 2b).

Figure 1.   Absolute volumetric changes in mean GTVs during stereotactic radiotherapy (N=40)
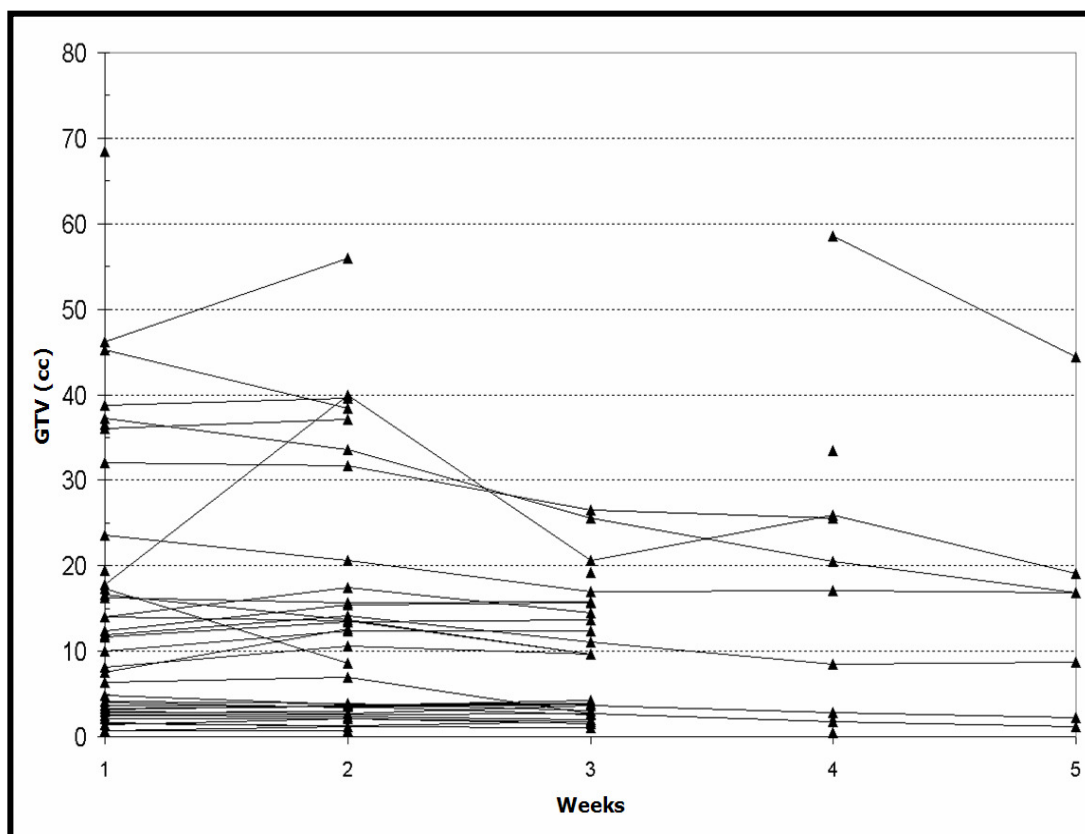
Figure 2a. Absolute volumes of GTVs at pre-treatment (■; N=40), end of SRT SRT (▲; N=40), and at 3 months (○; N=36), 6 months (□; N=25) follow-up and 1 year follow-up (△; N=6)
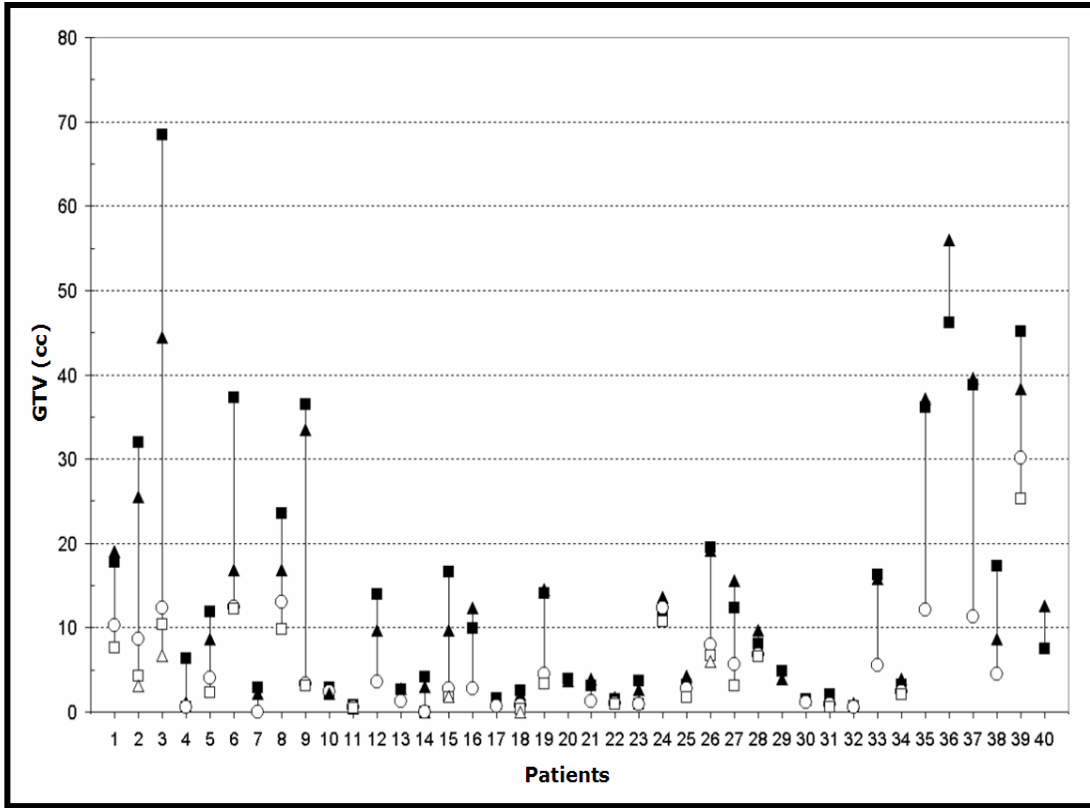
Figure 2b. Relative changes in mean GTV during and after stereotactic radiotherapy
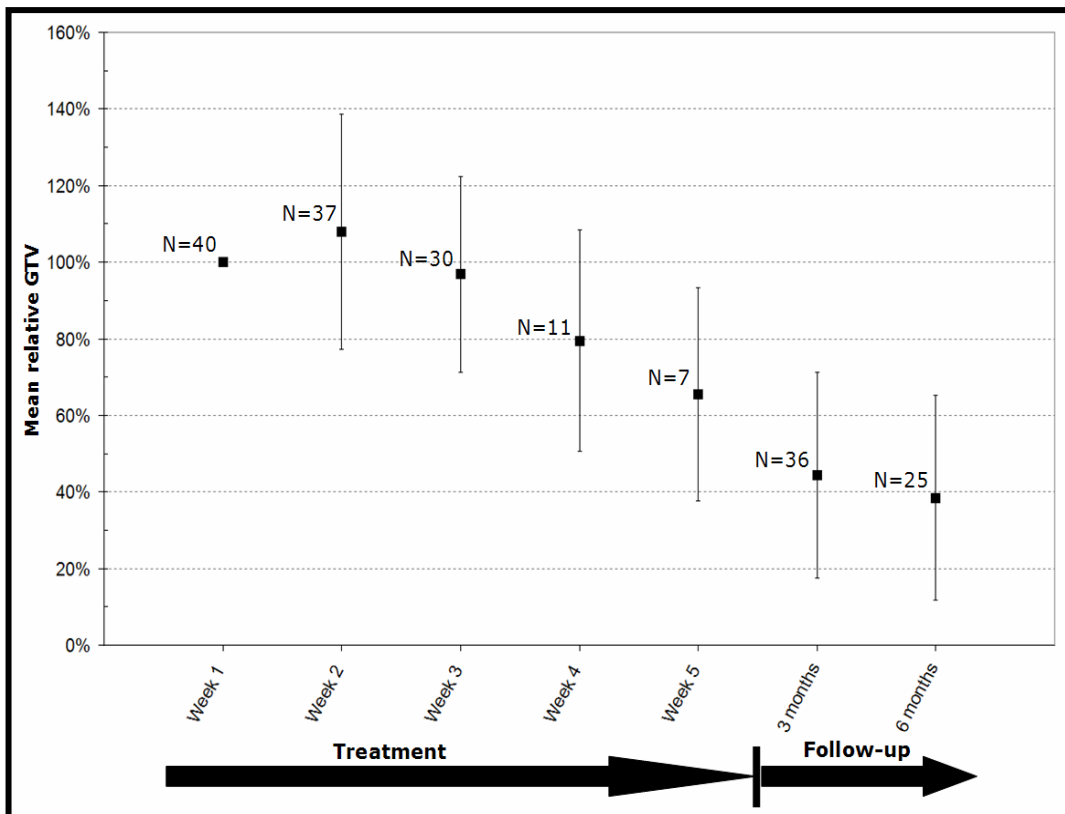
Time trends in ITVs

A similar time trend as for the GTVs was observed for the ITVs (Figure 3) with an overall decrease during SRT. However, just as for the GTVs, this decrease became significant only after 4 weeks (p=0.03). The same two cases that showed an increase in GTVs during the first two weeks of treatment also showed an increase in ITVs compared with baseline values (Figure 3).

Time trends in tumor mobility

No significant time trend in 3D mobility vectors could be detected in the 25 tumors investigated with 4DCT scans (p-value = 0.29-0.94 for the comparison of week 1-4 with D_0 values). However, as can be seen from Figure 4, there was a substantial intra-patient variability in 3D mobility vectors between fractions, particularly for tumors showing a 3D mobility of more than 10 mm.

Figure 3.   Absolute volumetric changes of ITVs during stereotactic treatment (N=40)
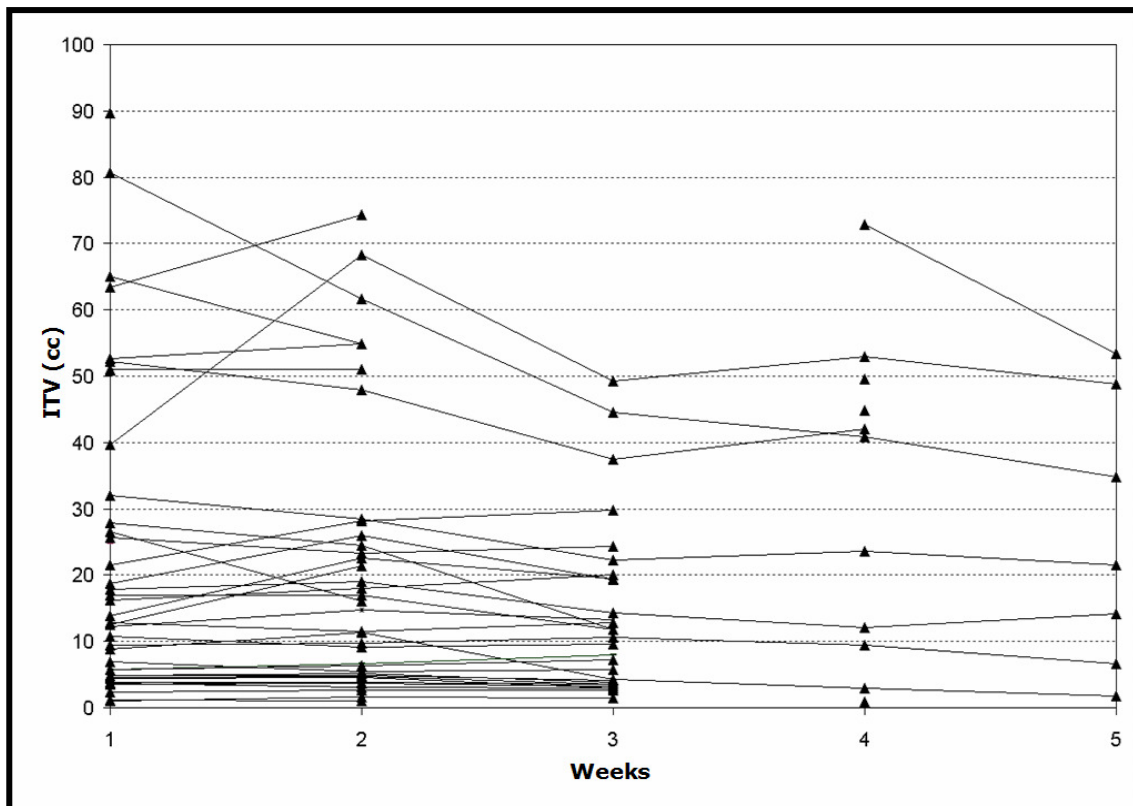
Figure 4.   Tumor mobility vectors during stereotactic treatment (N=25)
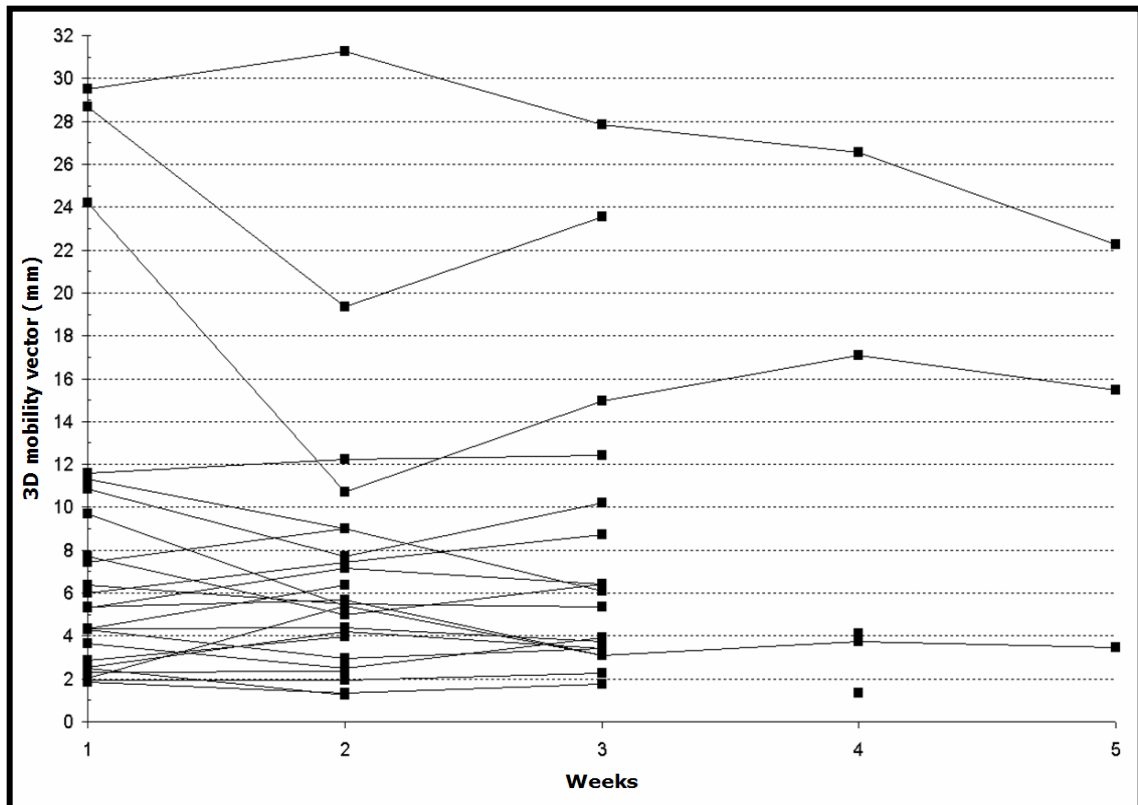
Time trends in spatial position of the ITV

With reference to position of the center of mass of the D_0 ITV, the mean ITV-shifts in week 1 to 4 were 4.0 ± 2.5 mm, 3.8 ± 2.2 mm, 4.0 ± 1.4 mm and 4.6 ± 1.5 mm, respectively (Table 3). Of the 36 tumors in which repeat CT scans were available for treatment planning, 9/33 (27.3%), 7/27 (25.9%), 4/11 (36.4%) and 3/7 (42.9%) showed a 3D ITV shift of >5 mm in weeks 1, 2, 3 and 4 respectively. As can be observed from Table 3, this ITV-shift exceeded 10 mm in two cases.

Shifts in the center of mass of ITVs can be caused either by changes in tumor mobility or by positional translations of the tumor due to, for example, edema or retractions. Therefore, the ITV shifts of week 1 and 2 were correlated with changes in tumor mobility vectors during SRT. Changes in tumor mobility did not account for the observed ITV shifts during SRT, because the correlation coefficient was 0.19 and -0.07 for week 2 and 3 compared to D_0, respectively.

Table 3. Inter-fractional 3D shift in ITV position during a course of stereotactic radiotherapy

Tumor	3D shift (mm) of isocenter			
	week 2 vs. week 1	week 3 vs. week 1	week 4 vs. week 1	week 5 vs. week 1
1	1.2	3.7	-	-
2	1.0	0.8	-	-
3	4.5	1.7	-	-
4	7.8	11.0	-	-
5	2.2	2.7	-	-
6	7.7	6.9	-	-
7	3.5	-	-	-
8	3.5	-	-	-
9	4.8	3.8	-	-
10	3.0	4.9	-	-
11	5.1	-	1.7	-
12	1.8	3.0	-	-
13	2.4	1.1	5.2	1.5
14	3.1	5.6	-	-
15	4.0	5.1	-	-
16	-	2.5	-	-
17	2.5	5.4	4.2	5.7
18	6.1	4.3	6.0	5.0
19	8.5	4.0	-	-
20	3.4	3.4	-	-
21	1.1	-	-	-
22	4.1	-	-	-
23	10.9	6.5	-	-
24	4.1	2.5	-	-
25	7.2	4.7	-	-
26	5.6	1.9	-	-
27	7.3	-	5.3	-
28	1.4	-	4.3	-
29	-	-	2.7	-
30	3.7	3.7	2.7	4.6
31	-	-	3.0	4.5
32	1.6	1.4	-	-
33	2.0	5.3	5.2	6.2
34	3.1	2.2	-	-
35	0.6	1.5	-	-
36	4.3	3.3	3.8	4.5
Mean 3D shift	**4.0**	**3.8**	**4.0**	**4.6**
Standard Deviation	**2.5**	**2.2**	**1.4**	**1.5**

Discussion

The accurate definition of a target volume is crucial for the delivery of high-precision radiotherapy in lung cancer. For patients with peripheral stage I NSCLC, a single 4DCT scan appears to be superior to other approaches [7]. However, changes in tumor

volume or mobility arising during the course of treatment may make it necessary to adjust a treatment plan to maintain target coverage, while ensuring that critical normal organs continue to be spared.

SRT is characterized by both steep dose gradients and a limited number of fractions, thereby increasing the impact of any intra- or inter-fractional changes in anatomy. Most reports on SRT for lung cancer have used an overall treatment time of 1-2 weeks, with treatment planning performed only once before the first fraction [10-15]. The overall treatment time of our patients extended to a maximum of 5 weeks. Because patient-specific margins were used to account for tumor mobility, we opted to redefine the ITV prior to each fraction of the common 3 and 5 fraction scheme.

Tumor regression during the course of conventional radiotherapy has been reported for NSCLC [8], cervical carcinoma [21, 22], and head-and-neck cancer [23]. The latter study reported changes in external contour, shape, and location of the target volume and critical structures during radiotherapy for head and neck cancer, indicating that periodic adjustment of treatment plans is needed to account for such time trends when techniques such as IMRT are delivered. In contrast, no time trends were observed for the prostate or seminal vesicles when 3 additional CT scans were performed during conventional radiotherapy in 50 patients [24]. An analysis of electronic portal images in lung cancer patients reported that it took on average 4.5 weeks from the start of conventional radiotherapy before 'tumor size' decreased to below 80% of the original size [8]. A slow regression rate was also observed in 22 patients with NSCLC who were treated with either radiotherapy alone or chemo-radiotherapy. In the latter study, the time required for maximum tumor regression ranged from 5-11 months [9]. Our study confirmed the finding of a slow regression of lung tumors, because significant decreases in target volumes were only observed after the fourth week of SRT, with most regression evident in the first three months after completion of SRT.

An initial increase in tumor volumes after stereotactic radiotherapy or radiosurgery has been reported for intracranial lesions such as brain metastases [25, 26], vestibular schwannomas [27, 28], craniopharyngiomas [29], gliomas [30], and pituitary adenomas [31]. The present analysis of planning CT scans performed during SRT with similar fraction sizes revealed an increase in GTVs and ITVs of 10 cc or more

in the second week of treatment in only 5% of stage I tumors. It can be concluded from these data that volumetric changes do not play an important role in inter-fractional variations in target volumes during SRT for lung cancer.

A study on spirometry assisted breath-hold CT scans at the end of high-dose conventionally fractionated radiotherapy reported significant changes in both tumor position at end-expiration and mobility [32]. In our study, a change in 3D mobility vectors with respect to baseline values of at least 3 mm was observed in 20% of tumors. This finding was observed in tumors that were more mobile, and may be related to the variations in respiratory amplitude during quiet uncoached respiration. The latter is the subject of ongoing analysis and may underscore the importance of performing respiratory coaching during both 4DCT scanning and treatment delivery.

An important finding of this study was the occurrence of substantial inter-fractional shifts of ITVs during the 3- to 5-week course of SRT. These shifts could be demonstrated as early as one week from the start of SRT and did not correlate with the observed alterations of tumor mobility. These shifts, which may be caused by radiation-induced changes in the surrounding normal tissues [33, 34], illustrate the importance of repeat imaging during SRT for lung cancer.

In conclusion, clinically significant positional time trends in target volumes can occur during a course of SRT for stage I NSCLC. A failure to account for such changes, e.g. by repeat CT-planning or verification using on-board volumetric imaging, can lead to inadequate target coverage.

References

1. Senan S, Chapet O, Lagerwaard FJ, et al. Defining target volumes for non-small cell lung carcinoma. *Semin Radiat Oncol* 2004;14:308-314

2. van Sörnsen de Koste JR, Lagerwaard FJ, Nijssen-Visser MR, et al. Tumor location cannot predict the mobility of lung tumors: a 3D analysis of data generated from multiple CT scans. *Int J Radiat Oncol Biol Phys* 2003;56:348-354

3. Sixel KE, Ruschin M, Tirona R, et al. Digital fluoroscopy to quantify lung tumor motion: potential for patient-specific planning target volumes. *Int J Radiat Oncol Biol Phys* 2003;57:717-723

4. Plathow C, Ley S, Fink C, et al. Analysis of intrathoracic tumor mobility during whole breathing cycle by dynamic MRI. *Int J Radiat Oncol Biol Phys* 2004;59:952-959

5. van Sörnsen de Koste JR, Lagerwaard FJ, Schuchhard-Schipper RH, *et al.* Dosimetric consequences of tumor mobility in radiotherapy of stage I non-small cell lung cancer – an analysis of data generated using 'slow' CT scans *Int J Radiat Oncol Biol Phys* 2001;61:93-99

6. Lagerwaard FJ, van Sörnsen de Koste JR, Nijssen-Visser MR, et al. Multiple "slow" CT scans for incorporating lung tumor mobility in radiotherapy planning. *Int J Radiat Oncol Biol Phys* 2001;51:932-937

7. Underberg RW, Lagerwaard FJ, Cuijpers JP, et al. Four-dimensional CT scans for treatment planning in stereotactic radiotherapy for stage I lung cancer. *Int J Radiat Oncol Biol Phys* 2004;60:1283-1290

8. Erridge SC, Seppenwoolde Y, Muller SH, et al. Portal imaging to assess set-up errors, tumor motion and tumor shrinkage during conformal radiotherapy of non-small cell lung cancer. *Radiother Oncol* 2003;66:75-85

9. Werner-Wasik M, Xiao Y, Pequignot E, et al. Assessment of lung cancer response after nonoperative therapy: tumor diameter, bidimensional product, and volume. A serial CT scan-based study. *Int J Radiat Oncol Biol Phys* 2001;51:56-61

10. Timmerman R, Papiez L, McGarry R, et al. Extracranial stereotactic radioablation: results of a phase I study in medically inoperable stage I non-small cell lung cancer. *Chest* 2003;124:1946-1955

11. Whyte RI, Crownover R, Murphy MJ, et al. Stereotactic radiosurgery for lung tumors: preliminary report of a phase I trial. *Ann Thorac Surg* 2003;75:1097-1101

12. Uematsu M, Shioda A, Suda A, et al. Computed tomography-guided frameless stereotactic radiotherapy for stage I non-small cell lung cancer: a 5-year experience. *Int J Radiat Oncol Biol Phys* 2001;51:666-670

13. Fukumoto S, Shirato H, Shimizu S, et al. Small-volume image-guided radiotherapy using hypofractionated, coplanar, and noncoplanar multiple fields for patients with inoperable stage I nonsmall cell lung carcinomas. *Cancer* 2002;95:1546-1553

14. Onishi H, Araki T, Shirato H, et al. Stereotactic hypofractionated high-dose irradiation for stage I nonsmall cell lung carcinoma: clinical outcomes in 245 subjects in a Japanese multiinstitutional study. *Cancer* 2004;101:1623-1631

15. Hof H, Herfarth KK, Münter M, et al. Stereotactic single-dose radiotherapy of stage I non-small-cell lung cancer (NSCLC). *Int J Radiat Oncol Biol Phys* 2003;56:335-341

16. Lagerwaard FJ, Senan S, van Meerbeeck JP, et al. Has 3-D conformal radiotherapy (3D CRT) improved the local tumour control for stage I non-small cell lung cancer? *Radiother Oncol* 2002;63:151-157

17. Qiao X, Tullgren O, Lax I, et al. The role of radiotherapy in treatment of stage I non-small cell lung cancer. *Lung Cancer* 2003;41:1-11

18. Wulf J, Hadinger U, Oppitz U, et al. Stereotactic radiotherapy of targets in the lung and liver. *Strahlenther Onkol* 2001;177:645-655

19. Potters L, Steinberg M, Rose C, *et al.* American Society for Therapeutic Radiology and Oncology and American College of Radiology Practice Guideline for the Performance of Stereotactic Body Radiation Therapy. *Int J Radiat Oncol Biol Phys* 2004;60:1026-1032

20. Littell RC, Milleken GA, Stroup WW, et al. SAS System for Mixed Models. 1996, SAS Institute Inc., Cary, NC, United States

21. Mayr NA, Taoka T, Yuh WT, et al. Method and timing of tumor volume measurement for outcome prediction in cervical cancer using magnetic resonance imaging. *Int J Radiat Oncol Biol Phys* 2002;52:14-22

22. Lee CM, Shrieve DC, Gaffney DK. Rapid involution and mobility of carcinoma of the cervix. *Int J Radiat Oncol Biol Phys* 2004;58:625-630

23. Barker JL Jr, Garden AS, Ang KK, et al. Quantification of volumetric and geometric changes occurring during fractionated radiotherapy for head-and-neck cancer using an integrated CT/linear accelerator system. *Int J Radiat Oncol Biol Phys* 2004;59:960-970

24. Mechalakos JG, Mageras GS, Zelefsky MJ, et al. Time trends in organ position and volume in patients receiving prostate three-dimensional conformal radiotherapy. *Radiother Oncol* 2002;62:261-265

25. Peterson AM, Meltzer CC, Evanson EJ, et al. MR imaging response of brain metastases after gamma knife stereotactic radiosurgery. *Radiology* 1999;21:807-814

26. Huber PE, Hawighorst H, Fuss M, et al. Transient enlargement of contrast uptake on MRI after linear accelerator (linac) stereotactic radiosurgery for brain metastases. *Int J Radiat Oncol Biol Phys* 2001;49:1339-1349

27. Szeifert GT, Massager N, DeVriendt D, et al. Observations of intracranial neoplasms treated with gamma knife radiosurgery. *J Neurosurg* 2002;97 (Suppl 5):623-626

28. Nakamura H, Jokura H, Takahashi K, et al. Serial follow-up MR imaging after gamma knife radiosurgery for vestibular schwannoma. *Am J Neuroradiol* 2000;21:1540-1546

29. Chung WY, Pan DH, Shiau CY, et al. Gamma knife radiosurgery for craniopharyngiomas. *J Neurosurg* 2000;93(Suppl 3):47-56

30. Bakardjiev AI, Barnes PD, Goumnerova LC, et al. Magnetic resonance imaging changes after stereotactic radiation therapy for childhood low grade astrocytoma. *Cancer* 1996;78:864-873

31. Tung GA, Noren G, Rogg JM, et al. MR imaging of pituitary adenomas after gamma knife stereotactic radiosurgery. *Am J Roentgenol* 2001;177:919-924.

32. Forster KM, Stevens CW, Kitamura K, et al. Changes of tumor motion patterns during a course of radiation therapy for lung cancer. *Int J Radiat Oncol Biol Phys* 2003;57 (Suppl 1):S234

33. Takeda T, Takeda A, Kunieda E, et al. Radiation injury after hypofractionated stereotactic radiotherapy for peripheral small lung tumors: serial changes on CT. *AJR Am J Roentgenol* 2004;182:1123-1128

34. Aoki T, Nagata Y, Negoro Y, et al. Evaluation of lung injury after three-dimensional conformal stereotactic radiation therapy for solitary lung tumors: CT appearance. *Radiology* 2004;230:101-108

Chapter 6

A dosimetric analysis of respiration-gated radiotherapy in patients with stage III lung cancer

René WM Underberg
John R van Sörnsen de Koste
Frank J Lagerwaard
Andrew Vincent
Ben J Slotman
Suresh Senan

Abstract

Background: Respiration-gated radiotherapy can permit the irradiation of smaller target volumes. 4DCT scans performed for routine treatment were retrospectively analyzed to establish the benefits of gating in stage III non-small cell lung cancer (NSCLC).

Methods and Materials: Gross tumor volumes (GTVs) were contoured in all 10 respiratory phases of a 4DCT scan in 15 patients with stage III NSCLC. Treatment planning was performed using different planning target volumes (PTVs), namely: (i) $PTV_{routine}$, derived from a single GTV plus 'conventional' margins; (ii) $PTV_{all\ phases}$ incorporating all 3D mobility captured by the 4DCT; (iii) PTV_{gating}, incorporating residual 3D mobility in 3-4 phases at end-expiration. Mixed effect models were constructed in order to estimate the reductions in risk of lung toxicity for the different PTVs.

Results: Individual GTVs ranged from 41.5 - 235.0 cm^3. With patient-specific mobility data ($PTV_{all\ phases}$), smaller PTVs were derived than when 'standard' conventional margins were used ($p<0.001$). The average residual 3D tumor mobility within the gating window was 4.0 ± 3.5 mm, which was 5.5 mm less than non-gated tumor mobility ($p<0.001$). The reductions in mean lung dose were 9.7% and 4.9%, respectively, for $PTV_{all\ phases}$ versus $PTV_{routine}$, and PTV_{gating} versus $PTV_{all\ phases}$. The corresponding reductions in V_{20} were 9.8% and 7.0%, respectively. Dosimetric gains were smaller for primary tumors of the upper lobe versus other locations ($p=0.02$). Respiratory gating also reduced the risks of radiation-induced esophagitis.

Conclusion: Respiration-gated radiotherapy can reduce the risk of pulmonary toxicity but the benefits are particularly evident for tumors of the middle and lower lobes.

Background

As lung tumors can show significant respiration-induced motion [1, 2], sufficient margins have to be added to account for target mobility in radiotherapy planning [3]. For stage I non-small cell lung cancer (NSCLC), commonly used 'population-based' margins result in unnecessary irradiation of significant amounts of normal tissue [2, 4], thereby increasing the risk of toxicity. For stage III NSCLC, local control after radiotherapy is poor [5, 6], and both radiation dose-escalation and concurrent chemo-radiotherapy schemes have been used in an attempt to improve local control. However, such approaches can increase late radiation-induced toxicity [7-11], and reductions in treated volumes may help in reducing toxicity.

Respiration-correlated (or 4D) CT scans permit an individualized assessment of tumor mobility [12]. Respiratory gating enables smaller target volumes to be used as treatment delivery is restricted to predetermined phases of respiration, during which tumor mobility is relatively limited. However, planning and delivery of gated radiotherapy requires reliable data on intra- and inter-fractional tumor mobility. In stage I NSCLC, individualized planning target volumes (PTVs) that incorporated all tumor mobility or the residual mobility in three end-expiratory phases allowed for mean PTV reductions of 48.2% and 33.3%, respectively, relative to standard margins [2]. The magnitude of benefit that can be achieved with gating in stage I tumors was found to correlate with the extent of mobility.

A recent study in patients with stage III NSCLC reported that limited decreases in lung doses could be achieved with gating, but only if GTVs did not exceed 100-150 cm^3 [13]. However, tumor mobility in this study was derived from breath-hold CT scans at full inspiration and tidal end-expiration. A more realistic analysis requires knowledge of mobility in all phases of quiet respiration, i.e. 4DCT data. We retrospectively analyzed 4D datasets in order to determine the geometric and dosimetric benefits of respiration-gated radiotherapy in stage III NSCLC.

Methods

The 4DCT scans of 15 consecutive patients with stage III NSCLC, who were treated with conventionally fractionated involved-field radiotherapy at the VU University medical center, were retrospectively analyzed. The primary tumors were located in the upper (n=9), middle (n=2) and lower lobe (n=4), respectively. Patient

characteristics are summarized in Table 1. All patients had at least one metastatic N2-3 lymph node, and nodal locations were described according to Mountain et al. [14].

Table 1.   Patient characteristics

Patient	TNM-stage	Primary tumor location	Lymph node locations	GTV (cm^3)
1	T2N2M0	Right upper lobe	2R, 4R	101.4
2	T3N2M0	Left upper lobe	4L	231.6
3	T2N3M0	Right upper lobe	4R, 4L	63.6
4	T2N2M0	Right lower lobe	7	77.9
5	T3N3M0	Right upper lobe	4R, 4L	174.7
6	T2N2M0	Right lower lobe	4R	99.1
7	T3N2M0	Right lower lobe	4R, 7	61.7
8	T2N2M0	Right upper lobe	4R	74.8
9	T1N3M0	Right middle lobe	4R, 4L	71.8
10	T2N2M0	Left lower lobe	4L, 7	180.9
11	T4N3M0	Right upper lobe	4L	154.6
12	T2N2M0	Left upper lobe	2L, 4L	41.5
13	T2N3M0	Right upper lobe	2R, 4R, 4L	84.2
14	T3N2M0	Left upper lobe	4L	235.0
15	T3N2M0	Right middle lobe	2R, 4R, 7	164.3

Lymph node locations are according to Mountain et al. [14]

4DCT scanning procedure

Patients were immobilized in the supine position, with the arms positioned above the head on an adjustable arm support and a knee rest device was used (Posirest-2 and Kneefix cushion device, Sinmed, Reeuwijk, The Netherlands). A 4DCT thoracic scan was performed during uncoached quiet respiration on a 16 slice CT scanner. The Respiratory Position Management gating hardware (Varian Medical Systems, Palo Alto, CA) was used for recording the breathing pattern. A lightweight block containing two reflective markers is placed on the upper abdomen, typically halfway between the xiphoid and umbilicus, and infrared light from an illuminator is reflected from the markers, and captured by a camera.

Our 4DCT protocol for scanning lung tumors has been reported in detail previously [12]. Briefly, 8 contiguous slices of 2.5 mm are generated for a 2 cm total longitudinal coverage per gantry rotation with the scanner operated in axial cine mode. Other

scanning parameters include 140 KV, 95 mA and tube rotation set closest to 1/10 of the average breathing cycle time to allow high temporal and spatial resolution. With the scanner couch in static mode, data is acquired for at least the duration of one full respiratory cycle, after which the couch advances to the next position. Data acquisition ceases during the couch movement, and a full 4DCT scanning procedure of the thorax generally takes about 90 seconds. The radiation exposure from the 4DCT acquisition is about 52.7 mGy in $CTDI_{vol}$ when the patients' breathing cycle is 4 sec, which is about 6 times the dose of our single conventional helical CT scan procedure. Retrospective sorting of the images into spatio-temporally coherent volumes is performed using the Advantage 4D software (GE Medical Systems, Waukesha, WI). Each reconstructed image is assigned to a specific respiratory phase (or 'bin') based on the temporal correlation between surface motion and data acquisition, and 10 respiratory phases are generated. The actual clinical treatment of these patients was based upon non-gated treatment delivery to a PTV that incorporated mobility seen in all phases of respiration ($PTV_{all\ phases}$).

In this retrospective analysis, the bins representing all 10 phases of respiration were imported into the Eclipse radiotherapy planning system (Eclipse version 6.5, Varian Medical Systems, Palo Alto, CA). All ten 3D data sets derived from a 4DCT scan shared DICOM coordinates, which simplified image registration of the data sets using the "shared DICOM coordinates" option. After image registration, the position of a vertebra at the level of the primary tumor was checked to ensure that no patient movement had occurred during the 4DCT acquisition procedure.

Defining the 'gating- window'

As gating will prolong treatment delivery, it is common to use a 'gate' that allows a duty cycle of at least between 20-40% of respiration [15]. In order to identify the gate, all ten 4DCT bins were imported into the '4D Review' application in the Advantage workstation where 3 or 4 consecutive 'gating bins' in expiration were simultaneously viewed in axial, frontal and sagittal reconstructions. A 'gating window' was identified at end-expiration in which mobility of the primary tumor and/or hilus was minimal. The use of larger gating windows improve the efficiency of treatment delivery, and a total of 4 phases were selected in 4 patients as review of the 4DCT movies suggested limited mobility of the primary tumor within in these 'gates'.

Deriving target volumes and contouring critical structures

Gross tumor volumes (GTVs) were contoured in each of the 10 phases of a 4DCT using standardized lung and mediastinal window level settings by one clinician in order to minimize contouring variations. The use of involved-field radiotherapy is standard practice at our center for the treatment of stage III NSCLC [16], and the GTV included the primary tumor, ipsilateral hilus, lymph nodes with a short axis diameter of 1.0 cm or greater and/or FDG-PET positive lymph nodes. All contours were automatically projected onto the second 'bin' in the middle of the gating window. Similarly, the spinal cord and esophagus were also contoured in this specific 'gating bin'. In six patients, the primary tumor and the hilus were contoured as a single entity as the two structures were adjacent to each other. For all 15 patients, three PTVs were generated:

(i) $PTV_{routine}$, derived from a phase at the center of the 'gating window', i.e. from a single component CT scan. An isotropic margin of 1.5 cm (but 2.0 cm for cranial and caudal margins in lower lobe tumors) was added to the GTV in order to account for microscopic extension, mobility and set-up inaccuracies;

(ii) $PTV_{all\ phases}$, which consisted of the volume encompassing all ten GTVs (i.e. all respiration-induced mobility), plus an isotropic margin of 1.0 cm for microscopic extension and set-up inaccuracies;

(iii) PTV_{gating}, consisting of the volume encompassing 3-4 GTVs in the gating window, plus an isotropic margin of 1.0 cm for microscopic extension and set-up inaccuracies.

Analysis of target mobility

A 'bounding box' technique was used to assess the mobility of GTVs, as was previously reported [17]. Briefly, the approach involves fitting a rectangular box to each target volume, and changes in the position of a moving target in the X-, Y- and Z-axes are derived from the corresponding sides of the box. The overall 3D displacement of each GTV was derived using Pythagoras's algorithm. The following analyses were performed: (i) mobility of individual GTVs, derived from displacement of a single GTV ($GTV_{single\ phase}$) within GTV all phases, (ii) the reduction in mobility achieved with the use of respiratory gating, derived from calculating the displacement of the GTV_{gating} within $GTV_{all\ phases}$, and (iii) residual GTV mobility within gating windows, derived from displacement of the $GTV_{single\ phase}$ within GTV_{gating}.

Treatment planning and dosimetric analysis

Treatment planning was performed on each PTV$_{routine}$, PTV$_{all\ phases}$ and PTV$_{gating}$, all of which were projected onto a single end-expiratory CT set. The study patients were treated using two different fractionation schemes, namely 60 Gy in 30 fractions and 46 Gy in 23 fractions. The latter was a dose used for pre-operative concurrent chemo-radiotherapy. For both schemes, the PTVs received at least 95% of the prescribed dose, and a dose maximum of 107% of the prescribed dose was accepted unless a higher dose maximum was located within the PTV. The V$_{20}$ values had to be 35% or less, with a dose to the spinal cord of 50 Gy or less. An initial treatment plan was derived for PTV$_{routine}$, and treatment plans for PTV$_{all\ phases}$ and PTV$_{gating}$ were then derived by shrinking the fields of the initial plan, without other changes to the beam setup. The target conformity indices (CI), i.e. ratio of the target volume to volume treated to the 95% dose, of all three plans for each patient were derived to ensure that plan coverage was comparable. Dose–volume histograms (DVH) were computed for the total lung minus the volume of PTV$_{gating}$ in order to generate a reference lung volume that was copied to each treatment plan. The maximum spinal cord dose and predictors of lung toxicity, the V$_{20}$ and mean lung dose (MLD) [18], were evaluated for each plan. The length of the esophageal circumference encompassed by the 40 Gy and 50 Gy isodose was obtained by visually scrolling through axial CT slices.

Statistical analysis

The differences between the three PTVs and the reduction in GTV mobility achieved with gating were evaluated using the Hodges-Lehman non-parametric test. The existence of a correlation between the reduction in GTV mobility with respiratory gating and the dosimetric gains achieved, were evaluated using the Spearman's nonparametric correlation test. In addition, the dosimetric data were analyzed for differences according to tumor stage and tumor location (upper vs. non-upper lobe). All statistical analyses were conducted using the Cytel Studio's StatXact-6 software (Version 6.2.0). Finally, mixed effect models were constructed (SAS version 8.02 and S-plus version 6.2) in order to estimate the general dosimetric gains that can be achieved (PTV$_{routine}$ vs. PTV$_{all\ phases}$; PTV$_{routine}$ vs. PTV$_{gating}$; PTV$_{all\ phases}$ vs. PTV$_{gating}$) on the V$_{20}$ and MLD, as well as on critical structures (esophagus and spinal cord).

Results

Volumetric comparison of PTVs

The individual GTVs ranged from 41.52 cm^3 to 235.04 cm^3, and six GTVs were larger than 150 cm^3 (Table 1). The PTV$_{routine}$ was the largest volume for all patients (Figure 1). Use of individualized margins led to significantly smaller volumes (PTV$_{all\ phases}$) than with the use of standard margins (p<0.001). The same was observed for PTV$_{gating}$ versus PTV$_{all\ phases}$ (p<0.001).

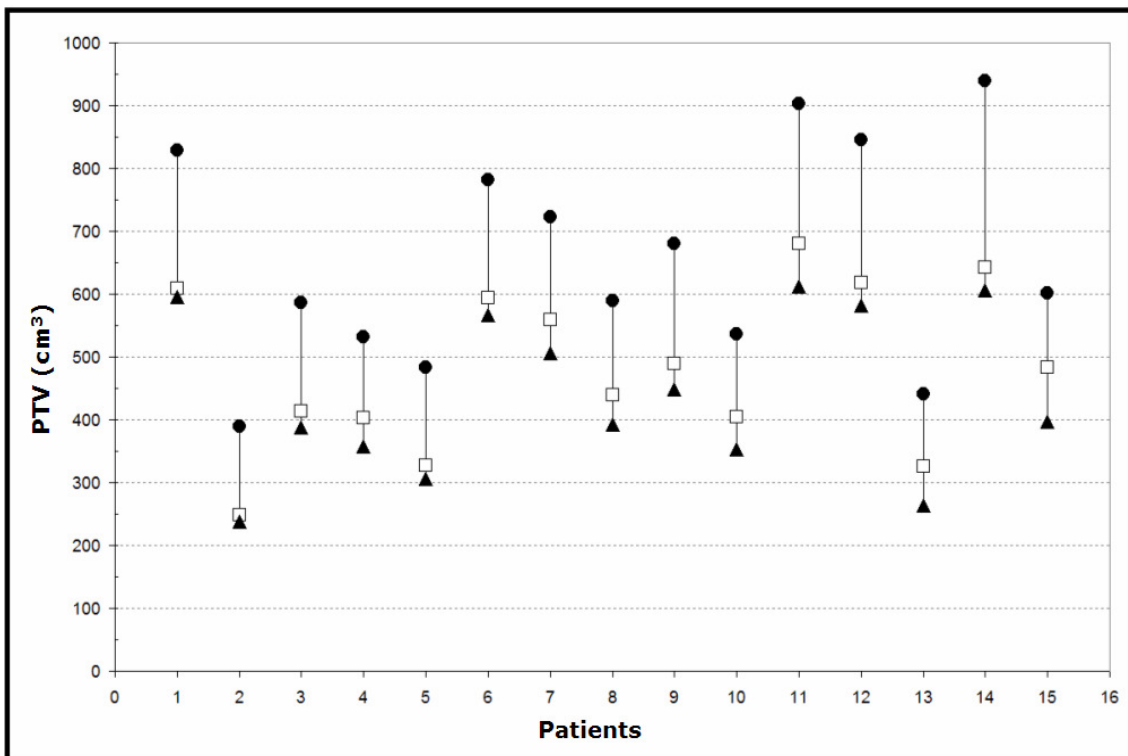**Figure 1.** Absolute volumes of PTV$_{routine}$ (●), PTV$_{all\ phases}$ (□) and PTV$_{gating}$ (▲)

Table 2.   GTVs and GTV mobility

Patient	GTV$_{all\ phases}$ (cm^3)	GTV$_{gating}$ (cm^3)	Ungated GTV mobility (mm)	Residual GTV mobility (mm)
1	126.9	104.1	5.6	2.2
2	247.4	239.0	1.0	0.0#
3	76.3	68.1	11.2	5.8
4	132.3	90.6	17.3	6.4
5	201.0	183.4	8.2	3.2#
6	128.6	112.5	22.6	14.0#*
7	98.4	66.8	18.2	5.9
8	112.7	81.9	10.9	2.0
9	109.8	79.8	8.4	1.4
10	216.3	193.2	3.0	2.0
11	199.8	162.5	8.7	4.6
12	49.7	44.0	1.0	1.0#
13	97.7	89.0	8.4	6.4
14	254.0	239.3	4.6	1.0
15	240.7	193.3	12.6	3.6
Mean	**152.8**	**129.8**	**9.4**	**4.0**
SD	**67.1**	**65.5**	**6.3**	**3.5**

gating-window incorporated four successive phase bins

 * mainly due to residual nodal mobility in the mediastinum

Treatment planning

Treatment was planned to a dose of 60 Gy for 11 of the 15 patients. The other four had lesions of the upper lobe that extended to the contralateral mediastinum, and all these patients underwent pre-operative chemo-radiotherapy to 46 Gy. A similar target conformity index (CI) was achieved for plans based on the 3 specified PTV definitions (data not shown).

Reduction in the risk of pulmonary toxicity with gating was assessed using dedicated statistical models for all patients (n=15) on mean lung dose (MLD) and in 14 patients with respect to the volume of lungs receiving at least 20 Gy (V_{20}). One patient was excluded from the V_{20} model as the V_{20} values of the plans did not meet the V_{20} inclusion criteria, i.e. V_{20} (routine) > V_{20} (all phases) > V_{20} (gating). In this patient with a right lower lobe tumor, the V_{20} (all phases) was larger than the V_{20} (routine), which was the result of substantial lateral mobility of the mediastinal lymph nodes. Nevertheless, the PTV$_{all\ phases}$ plan did meet the inclusion criteria used in the MLD model, i.e. MLD (routine) > MLD (all phases) > MLD (gating). The mixed effect model showed that the MLD was reduced by 9.7%, 4.9% and 14.2%, respectively, for

$PTV_{\text{all phases}}$ versus PTV_{routine}, PTV_{gating} versus $PTV_{\text{all phases}}$ and PTV_{gating} versus PTV_{routine}. The corresponding figures for the V_{20} were 9.8%, 7.0% and 16.2% (Tables 3-4). Upper lobe tumors showed a significantly lower dosimetric gain than tumors located in other lobes (p=0.02). When the analysis was restricted to lower and middle lobe tumors, the corresponding figures for V_{20} reduction were 7.2%, 10.1% and 16.5%, and for reduction in MLD 9.9%, 6.4% and 15.7%, respectively. Tumor stage had no significant influence on the dosimetric improvements achieved with respiratory gating.

As could be expected, a strong correlation was observed between the reduction in PTV observed with respiratory gating and the reduction in GTV mobility (Spearman's Non-parametric correlation test S=0.78, linear regression coefficient=4.3 (p<0.001)). In addition, a correlation could be demonstrated between the reduction in PTV with gating and reductions in both in V_{20} and MLD values (Figure 2a-b).

Table 3. Reduction in mean lung dose (Gy) using different PTV definitions

Patient	Mean lung dose (Gy) PTV_{routine}	Absolute (Gy) and relative (%) reduction in mean lung dose		
		$PTV_{\text{all phases}}$ vs. PTV_{routine}	PTV_{gating} vs. PTV_{routine}	PTV_{gating} vs. $PTV_{\text{all phases}}$
1	25.2	2.7 (10.7%)	3.6 (14.3%)	0.9 (4.0%)
2	20.6	1.6 (7.8%)	2.4 (11.7%)	0.8 (4.2%)
3	18.9	1.6 (8.5%)	2.2 (11.6%)	0.6 (3.5%)
4	23.0	1.3 (5.7%)	3.0 (13.0%)	1.7 (7.8%)
5	12.8	1.1 (8.6%)	1.5 (11.7%)	0.3 (2.6%)
6	18.7	1.7 (9.1%)	2.5 (13.4%)	0.8 (4.7%)
7	23.1	3.1 (13.4%)	4.2 (18.2%)	1.1 (5.5%)
8	10.4	0.7 (6.7%)	0.7 (6.7%)	0.0 (0.0%)
9	19.3	1.1 (5.7%)	2.7 (14.0%)	1.6 (8.8%)
10	20.2	3.0 (14.9%)	3.8 (18.8%)	0.8 (4.7%)
11	17.2	1.0 (5.8%)	2.1 (12.2%)	1.1 (6.8%)
12	19.5	3.2 (16.4%)	3.3 (16.9%)	0.1 (0.6%)
13	14.2	1.2 (8.5%)	2.4 (16.9%)	1.2 (9.3%)
14	15.7	2.1 (13.4%)	2.6 (16.6%)	0.5 (3.7%)
15	27.8	3.0 (10.8%)	4.7 (16.9%)	1.7 (6.9%)
Mean	**19.1**	**1.9 (9.7%)**	**2.8 (14.2%)**	**0.9 (4.9%)**
SD	**4.6**	**0.9 (3.4%)**	**1.0 (3.2%)**	**0.5 (2.7%)**

Table 4.   Reduction in V_{20} (%) using different PTV definitions

Patient	V_{20} (%) PTV$_{routine}$	Absolute V_{20} (%) and relative (%) reduction in V_{20}		
		PTV$_{all\ phases}$ vs. PTV$_{routine}$	PTV$_{gating}$ vs. PTV$_{routine}$	PTV$_{gating}$ vs. PTV$_{all\ phases}$
1	38.0	4.1 (10.8%)	5.1 (13.4%)	1.0 (2.9%)
2	27.1	2.2 (8.1%)	3.5 (12.9%)	1.3 (5.2%)
3	29.0	2.0 (6.9%)	2.8 (9.7%)	0.8 (3.0%)
4	31.0	3.8 (12.3%)	6.7 (21.6%)	2.9 (10.7%)
5	26.1	2.2 (8.4%)	2.9 (11.1%)	0.7 (2.9%)
6	28.9	-1.5 (-5.2%)	0.1 (0.3%)	1.6 (5.3%)
7	26.2	0.9 (3.4%)	4.3 (16.4%)	3.4 (13.4%)
8	20.5	3.7 (18.0%)	4.4 (21.5%)	0.7 (4.2%)
9	28.2	1.7 (6.0%)	4.8 (17.0%)	3.1 (11.7%)
10	27.5	4.2 (15.3%)	6.5 (23.6%)	2.3 (9.9%)
11	27.6	2.4 (8.7%)	4.9 (17.8%)	2.5 (9.9%)
12	25.5	4.4 (17.3%)	4.9 (19.2%)	0.5 (2.4%)
13	28.8	2.9 (10.1%)	6.0 (20.8%)	3.1 (12.0%)
14	23.9	3.7 (15.5%)	4.2 (17.6%)	0.5 (2.5%)
15	42.8	5.0 (11.7%)	8.6 (20.1%)	3.6 (9.5%)
Mean	**28.7**	**2.8 (9.8%)**	**4.6 (16.2%)**	**1.9 (7.0%)**
SD	**5.4**	**1.7 (5.9%)**	**2.0 (6.0%)**	**1.2 (4.1)**

Esophageal and spinal dose parameters

With the use of involved-field radiotherapy, only 11 patients received an esophageal circumference dose of at least 40 Gy. The mean circumferential length receiving a dose of 40 Gy was 6.8 ± 2.3 cm for PTV$_{routine}$. Use of PTV$_{all\ phases}$ reduced this value by a mean of 0.8 cm, and the reduction with PTV$_{gating}$ was 1.2 cm, both proven significant (Satterthwaite approximation for the denominator degrees of freedom used to give accurate F approximations). A circumferential dose of 50 Gy was seen in 8 patients, and the mean esophageal circumference receiving 50 Gy was 5.3 ± 2.0 for PTV$_{routine}$. Use of PTV$_{all\ phases}$ and PTV$_{gating}$ reduced this value by a mean of 1.8 and and 2.3 cm, respectively ($p < 0.001$, Page T: k-tuple non-parametric exact test for grouped data).

The maximum spinal cord dose was 44.7 ± 7.4 Gy for involved-field treatment plans generated for PTV$_{routine}$, and non-significant reductions to 43.7 ± 7.7 Gy and 42.8 ± 8.8 Gy were seen for plans based on PTV$_{all\ phases}$ and PTV$_{gating}$.

Figure 2a-b. Dosimetric correlation between (a) PTV reduction and V_{20} reduction, and (b) PTV reduction and MLD reduction
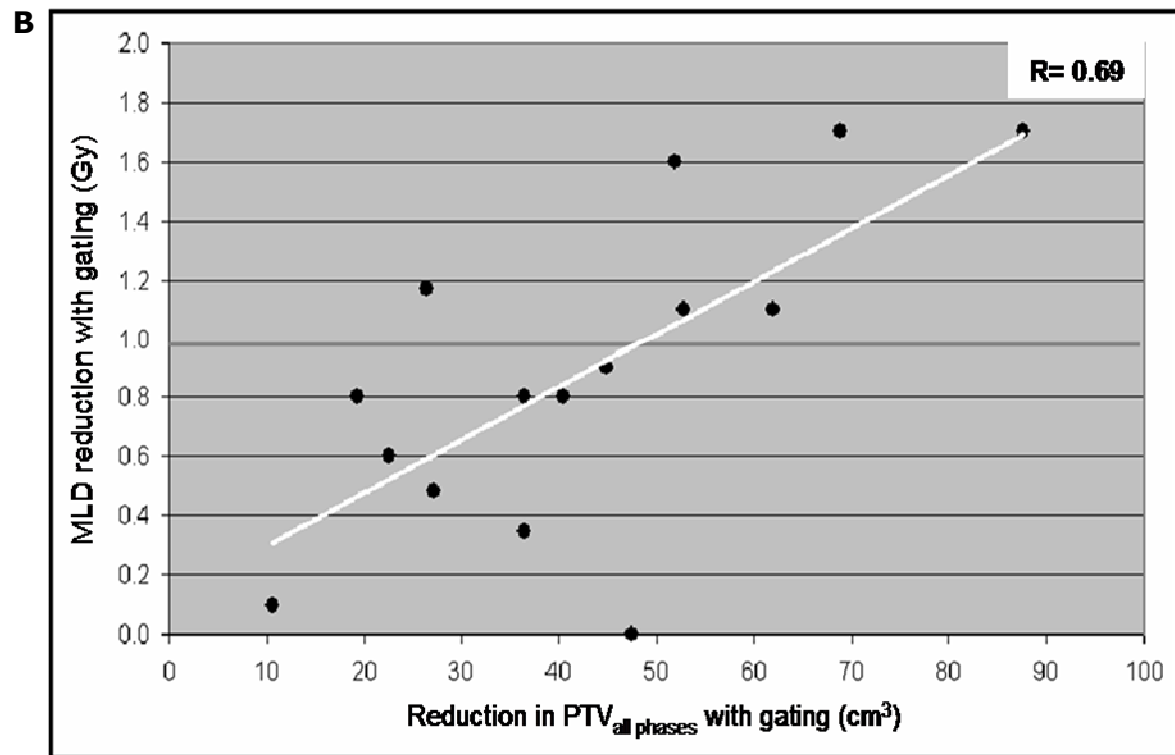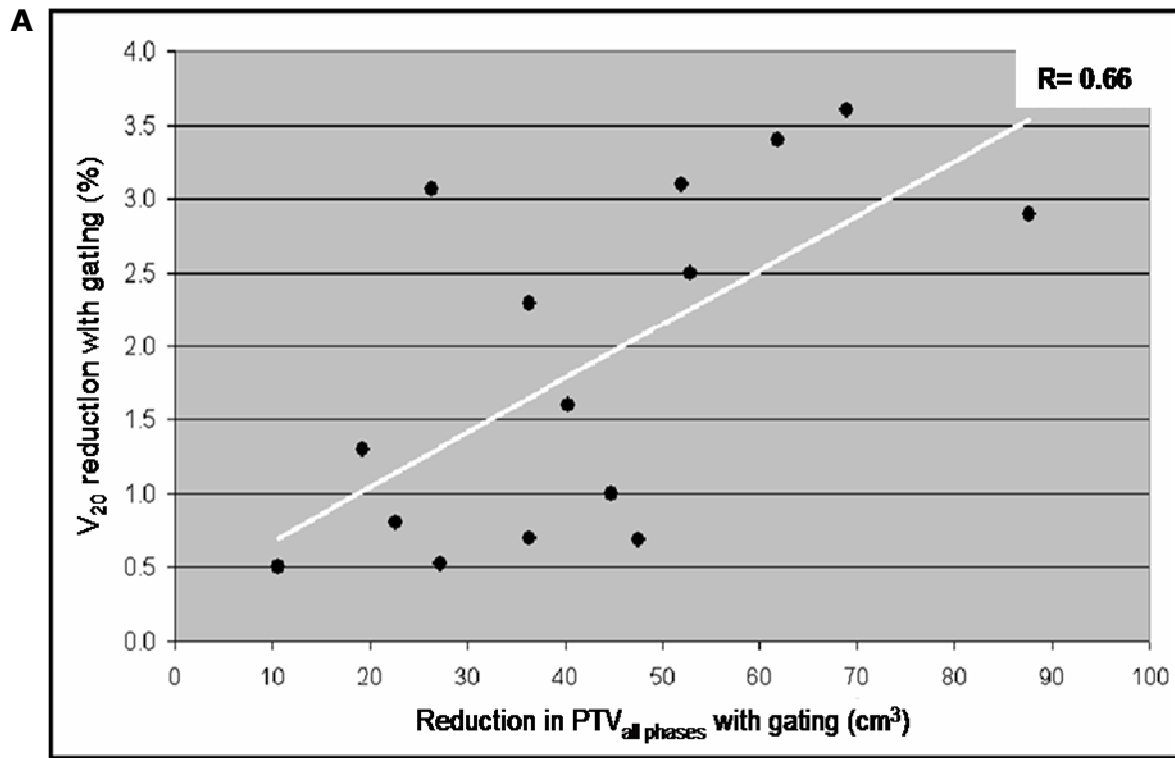
Discussion

Attempts to improve local control in stage III NSCLC have been confounded by an increased incidence of treatment-related toxicity, including unexpected late toxicities such as symptomatic bronchial stenosis, mediastinal fibrosis and stenosis of the pulmonary artery [9, 11]. The reporting of significant lung tumor motion has led to large margins being added to the clinical target volume to ensure adequate dose coverage. As such, respiration-gated radiotherapy is an approach that can reduce the volume of irradiated normal tissue.

This study in 15 consecutive patients with stage III NSCLC highlights the volumetric and dosimetric gains that can be achieved using individualized PTVs that incorporate all tumor motion and also respiration-gated PTVs in expiratory phases. Of note is the finding that significant gains are attained simply by using individualized 4D mobility margins (i.e. $PTV_{all\ phases}$) instead of PTVs based upon standard margins of 1.5 cm. The additional reductions in lung toxicity parameters achieved with respiratory gating were generally modest, but strongly correlated with the reduction in tumor mobility achieved with gating. Careful patient selection appears required to establish the optimal benefit.

Just as for stage I NSCLC [2], the larger $PTV_{routine}$ did not achieve coverage of all mobility in 7 of the 15 patients with tumors in upper- (n=2), middle- (n=2), and lower lobes (n=3). For the upper lobe tumors, the mobility of mediastinal lymph nodes appeared to be inadequately incorporated using standard margins; for the middle and lower lobe tumors this was the case for either the subcarinal nodes (n=2), mediastinal lymph nodes (n=3) or the primary tumor (n=2).

This analysis of 4DCT data revealed that reductions in both V_{20} and MLD can be achieved even when GTVs exceed 150 cm^3, but that this was restricted to tumors located in middle and lower lobes. For the latter, the mean reduction in V_{20} was 10.1 ± 2.7% for PTV_{gating} relative to $PTV_{all\ phases}$. In contrast, recent reports suggested that dosimetric benefits for gated radiotherapy were restricted to patients whose GTVs were 150 cm^3 or less, and which also exhibited significant mobility [13]. The mean mobility in our 15 patients (9.4 ± 6.3 mm) was similar to that of the 20 patients in the abovementioned report (9.4 ± 4.1 mm).

The potential benefits of respiratory gating must be viewed in the light of the residual uncertainties during gated delivery, for example the correlation between the PTV and external respiratory surrogates [19]. As changes in target volumes for lung cancer have been observed during both stereotactic radiotherapy [20] and conventionally fractionated radiotherapy [21], the relationship between external markers and the PTV may have to be re-established during treatment. Ongoing developments in volumetric imaging at the treatment unit may increase the accuracy of respiration-gated radiotherapy.

Another approach explored for reducing toxicity is intensity-modulated radiotherapy (IMRT). A planning study comparing IMRT and 3D conformal radiotherapy in 41 patients with locally-advanced stage NSCLC reported a median reduction in V_{20} of 10% and a reduction in MLD of ≥ 2 Gy [22]. However, 4D treatment planning for conformal radiotherapy and IMRT is in its infancy [23].

A limitation of our study is the fact that the esophagus was contoured in only one phase of respiration position. Recent data suggests that respiration-induced mobility of the lower esophagus can occur [24], which can confound our conclusions about the dosimetric impact of gated delivery.

Conclusions
Our analysis of 4DCT data indicates that individualized 4DCT-based PTVs ensure optimal target coverage with minimal irradiation of normal tissues in patients with stage III NSCLC. Respiration-gated radiotherapy can further reduce the risk of pulmonary toxicity, particularly for tumors located in the middle and lower lobes.

Author's contributions
S.S. and J.VSDK designed the study, analyzed all study data and prepared the final version of the manuscript. R.U. generated patient contours, performed treatment planning and initial analysis and generated the first drafts of the manuscript. F.L. analysed all study data and prepared the final manuscript. B.S. was involved in study design and drafting of the manuscript. A.V. performed statistical analysis of the study data and drafting of the manuscript.

References

1. Plathow C, Fink C, Ley S, et al. Measurement of tumor diameter-dependent mobility of lung tumors by dynamic MRI. *Radiother Oncol* 2004;73:349-354

2. Underberg RW, Lagerwaard FJ, Slotman BJ, et al. Benefit of respiration-gated stereotactic radiotherapy for stage I lung cancer: an analysis of 4DCT datasets. *Int J Radiat Oncol Biol Phys* 2005;62:554-600

3. International Commission on Radiation Units and Measurements. Prescribing, recording and reporting photon beam therapy (supplement to ICRU Report 50). Bethesda, MD: ICRU Report 62, 1999

4. van Sörnsen de Koste JR, Lagerwaard FJ, Nijssen-Visser MR, et al. Tumor location cannot predict the mobility of lung tumors: a 3D analysis of data generated from multiple CT scans. *Int J Radiat Oncol Biol Phys* 2003;56:348-354

5. Furuse K, Fukuoka M, Kawahara M, et al. Phase III study of concurrent versus sequential thoracic radiotherapy in combination with mitomycin, vindesine, and cisplatin in unresectable stage III non-small-cell lung cancer. *J Clin Oncol* 1999;17:2692-2699

6. Fournel P, Robinet G, Thomas P, et al. Randomized phase III trial of sequential chemoradiotherapy compared with concurrent chemoradiotherapy in locally advanced non-small-cell lung cancer: Groupe Lyon-Saint-Etienne d'Oncologie Thoracique-Groupe Francais de Pneumo-Cancerologie NPC 95-01 Study. *J Clin Oncol* 2005;23:5910-5917

7. Albain KS, Crowley JJ, Turrisi AT 3rd, et al. Concurrent cisplatin, etoposide, and chest radiotherapy in pathologic stage IIIB non-small-cell lung cancer: a Southwest Oncology Group phase II study, SWOG 9019. *J Clin Oncol* 2002;20:3454-3460

8. Tsujino K, Hirota S, Endo M, et al. Predictive value of dose-volume histogram parameters for predicting radiation pneumonitis after concurrent chemoradiation for lung cancer. *Int J Radiat Oncol Biol Phys* 2003;55:110-115

9. Marks LB, Garst J, Socinski MA, et al. Carboplatin/paclitaxel or carboplatin/vinorelbine followed by accelerated hyperfractionated conformal radiation therapy: report of a prospective phase I dose escalation trial from the Carolina Conformal Therapy Consortium. *J Clin Oncol* 2004;22:4329-4340

10. Socinski MA, Morris DE, Halle JS, et al. Induction and concurrent chemotherapy with high-dose thoracic conformal radiation therapy in unresectable stage IIIA and IIIB non-small-cell lung cancer: a dose-escalation phase I trial. *J Clin Oncol* 2004;22:4341-4350

11. Miller KL, Shafman TD, Anscher MS, et al. Bronchial stenosis: an underreported complication of high-dose external beam radiotherapy for lung cancer? *Int J Radiat Oncol Biol Phys* 2005;61:64-69

12. Underberg RW, Lagerwaard FJ, Cuijpers JP, et al. Four-dimensional CT scans for treatment planning in stereotactic radiotherapy for stage I lung cancer. *Int J Radiat Oncol Biol Phys* 2004;60:1283-1290

13. Starkschall G, Forster KM, Kitamura K, et al. Correlation of gross tumor volume excursion with potential benefits of respiratory gating. *Int J Radiat Oncol Biol Phys* 2004;60:1291-1297

14. Mountain CF, Dresler CM. Regional lymph node classification for lung cancer staging. *Chest* 1997;111:1718-1723

15. Mageras GS, Yorke E. Deep inspiration breath hold and respiratory gating strategies for reducing organ motion in radiation treatment. *Semin Radiat Oncol* 2004;14:65-75

16. Senan S, De Ruysscher D, Giraud P, et al. Literature-based recommendations for treatment planning and execution in high-dose radiotherapy for lung cancer. *Radiother Oncol* 2004;71:139-146

17. van Sörnsen de Koste JR, Lagerwaard FJ, Schuchhard-Schipper RH, et al. Dosimetric consequences of tumor mobility in radiotherapy of stage I non-small cell lung cancer--an analysis of data generated using 'slow' CT scans. *Radiother Oncol* 2001;61:93-99

18. Rodrigues G, Lock M, D'Souza D, et al. Prediction of radiation pneumonitis by dose - volume histogram parameters in lung cancer--a systematic review. *Radiother Oncol* 2004;71:127-138

19. Ozhasoglu C, Murphy MJ. Issues in respiratory motion compensation during external-beam radiotherapy. *Int J Radiat Oncol Biol Phys* 2002;52:1389-1399

20. Underberg RW, Lagerwaard FJ, Tinteren H, et al. Time trends in target volumes for stage I non-small cell lung cancer after stereotactic radiotherapy. *Int J Radiat Oncol Biol Phys* 2006;64:1221-1228

21. Kupelian PA, Ramsey C, Meeks SL, et al. Serial megavoltage CT imaging during external beam radiotherapy for non-small-cell lung cancer: observations on tumor regression during treatment. *Int J Radiat Oncol Biol Phys* 2005;63:1024-1028

22. Murshed H, Liu HH, Liao Z, et al. Dose and volume reduction for normal lung using intensity-modulated radiotherapy for advanced-stage non-small-cell lung cancer. *Int J Radiat Oncol Biol Phys* 2004;58:1258-1267

23. Keall P. 4-dimensional computed tomography imaging and treatment planning. *Semin Radiat Oncol* 2004;14:81-90

24. Dieleman EMT, Underberg RW, van Sörnsen de Koste JR, et al. Intrafractional esophageal mobility: Analysis of data generated using 4-D CT-scans. *Radiother Oncol* 2004;73:216 (Abstr.)

Chapter

7

General discussion and future directions

Respiration-induced tumor mobility is an important source of geometric uncertainty in both radiotherapy planning and delivery for lung cancer. Furthermore, it has been reported that mobility of lung tumors is unpredictable, as no clear correlation exists between the anatomical location of the lung tumor and the amount of mobility [1].

Radiotherapy planning is commonly based on a single rapid planning CT scan that is acquired during free breathing. It has, however, been demonstrated that such a scan of a moving tumor can lead to distortions in shape and deviations in spatial position of the target volume [2]. A single conventional CT scan represents a random position of the tumor during the respiratory cycle. As a mobile tumor or organ may not be at its mean position at the time of imaging, the dose calculated in such a static patient model is unlikely to represent the actual dose delivery during treatment. This can result in systematic errors in target definition, which are important as they influence all treatment fractions, thereby causing a 'change' in the dose distribution with respect to the target volume. Therefore, the use of a single rapid CT scan for target definition is questionable.

In order to improve target definition, the International Commission on Radiation Units and Measurements has recommended the use of an internal target volume (ITV) that includes all internal motion of the clinical target volume (CTV) [3]. In order to generate a planning target volume (PTV) most departments use population-based CTV-PTV margins for 3-dimensional conformal radiotherapy (3DCRT), and also even for stereotactic radiotherapy (SRT) in stage I non-small cell lung cancer (NSCLC). Several approaches have been developed to incorporate individualized ITVs into treatment planning, including multiple planning CT scans [4], fusion of target volumes generated from 'two-phase' CT scans [5] and slow CT scanning [6].

Recently, a more sophisticated approach, respiration-correlated (or 4D) CT scanning, has become available, which enables changes in position and shape of a patient's internal anatomy to be quantified as a function of the respiratory cycle. 4DCT requires multiple CT slices to be performed for at least the duration of one respiratory cycle ('oversampling') at each predefined table position, while the respiratory signal is recorded simultaneously using a respiratory monitoring system. Usually, all images from a 4DCT scan are evenly distributed over 10 bins, each corresponding to the phase of the respiratory cycle in which the image was acquired. The complete set of

bins accumulated over a respiratory cycle constitutes a 4D dataset. Motion artefacts are significantly reduced in the 4D datasets, compared to conventional CT scans.

Optimal target definition is a key requirement for radiotherapy. However, this is especially important for high-precision radiotherapy techniques, such as hypofractionated SRT, respiratory gating, and intensity modulated radiotherapy (IMRT). Several phase I/II studies recently reported local control rates of 80-90% with hypofractionated SRT for patients with inoperable stage I NSCLC [7-11]. In view of the high radiation doses (>100 Gy) and the steep dose gradient characteristic of SRT, this requires optimal target definition to ensure accurate dose delivery. As previously mentioned, most reports on SRT [7-9] and 3DCRT [12] in stage I lung cancer use population-based CTV-PTV margins to deal with internal tumor mobility. Our analysis demonstrates that the use of a single 4DCT scan captures more respiration-induced motion in highly mobile tumors, compared to population-based margins [Chapter 2, this thesis]. The latter leads to a diminished dose delivery to the target volume in these cases, while more healthy tissue is irradiated, indicating that population-based margins are inappropriate for ITV generation in stage I NSCLC. Furthermore, we showed that a single 4DCT scan is equal to, or better than, using 6 rapid CT scans for ITV generation, especially in highly mobile tumors [Chapter 2, this thesis].

The clinical implementation of 4DCT scanning leads to a huge increase of patient data that has to be used for target definition. Usually, ten respiration-correlated 3D datasets are derived from a single 4D dataset, each representing the patient's anatomy during a single respiratory phase. Without practical solutions this requires contouring of the gross tumor volume (GTV) in 10 respiratory phases, which is a major drawback to the routine clinical use of 4DCT scans in lung cancer. This underscores the need for solutions that result in a more efficient clinical use of 4DCT scans. One method is the use of 'maximum intensity projections' (MIP). Our analysis regarding the use of this post-processing tool reveals that it enables reliable generation of individualized ITVs from 4D datasets, thereby establishing a significant decrease in contouring time [Chapter 3, this thesis]. However, this tool is unable to visualize the movement of mediastinal lymph nodes that are present in stage III lung tumors. Furthermore, caution is needed with tumors that are located adjacent to high-intensity thoracic structures such as the heart, the diaphragm and the thoracic wall,

as we showed that MIP images may fail to visualize the entire ITV, due to the overlap with these high-density organs. The use of MIPs has the 'disadvantage' that it represents all spatial positions of a lung tumor during the respiratory cycle, and not the time spent at each position. This can be seen as suboptimal use of 4DCT information. The use of another post-processing tool, 'average intensity projection', represents the 'time-weighted' location of a tumor. To date, however, no data has been published about the use of average intensity projections in target definition and treatment planning. Therefore its role remains to be established.

In the same analysis we describe the use of contouring GTVs on the 'minimum intensity projection' (MinIP) in 4D datasets. The MinIP volume represents the volume where tumor tissue is present during the entire breathing cycle. Engelsman et al. reported that the probability of tumor control could be increased by the combination of field-size reduction and dose-escalation (i.e. an inward shift of the 95% isodose), thus increasing the target dose inhomogeneity [13]. This was performed while maintaining an equal mean lung dose (MLD), while respiratory motion was also taken into account. A possible explanation for the increased probability of tumor control is that an inwards shift of the 95% isodose enables delivery of a higher total dose to the volume in which tumor tissue was present during most of the breathing cycle time, resulting in a higher percentage of cell kill. However, in order to test this hypothesis, tools for efficient 4D data visualization are required. Recently, 'color intensity projections' were reported to rapidly visualize the percentage of time tumor tissue was present in a certain part of the ITV during the breathing cycle [14].

The clinical toxicity of SRT for inoperable stage I NSCLC is limited due to the application of involved-field radiotherapy in relatively small tumors and the use of small margins. However, recent publications have reported unexpected toxicities such as main bronchus stenosis, tracheal necrosis, oesophageal ulceration and pericardial effusion [15, 16]. Other potential organs at risk are the spinal cord and the thoracic wall. In order to limit the risk of treatment-related toxicity to these organs, respiratory gating can be performed. Our analysis of respiration-gated SRT for stage I NSCLC indicates that this technique enables reduction of normal tissue irradiation in all analyzed patients. However, we also found that the largest volumetric gains are obtained with the incorporation of all respiration-induced tumor mobility into the PTV. As PTVs in stage I NSCLC are generally small, a considerable volumetric reduction has

to be achieved in order to attain a benefit in clinical toxicity. We arbitrarily defined a threshold of at least a 50% PTV reduction and found that less than 15% of the patients fulfilled these criteria. This indicates that careful selection of patients is required. We proposed two simple approaches for this purpose. The first method is the use of the ratio between the ITV that is contoured on the MinIP projection to that delineated on the MIP image. Our analysis shows that this ratio correlates very well with the reduction in ITV that could be achieved with respiratory gating (Chapter 3, this thesis). The second approach requires the use of the two extreme GTV positions during the respiratory cycle. The ratio of the intersecting and the encompassing volume of these GTVs proved to be an excellent predictor for the reduction of the PTV with respiration-gated treatment (Chapter 4, this thesis). These two measures both were less time-consuming than contouring all ten respiratory bins. In clinical practise, however, we do not yet apply respiratory gating in this patient group, mainly because gating would result in unacceptable prolongation of the duration of each SRT fraction.

The use of tumor-tracking systems that continuously monitor the tumor position would, in theory, yield the largest benefits with respect to patient comfort and treatment time, since radiation is delivered throughout the patient's entire respiratory cycle. However, this approach requires the insertion of fiducial markers, which can be performed through invasive techniques, such as endobrochial or transthoracic placement. With endobrochial placement often only one marker can be placed *near* the tumor [17], while it has been reported that at least 3 markers are needed to detect rotational tumor movement [18]. Furthermore, it is questionable whether movements of implanted markers reliably track hysteresis, and if their movement changes synchronously with the inter-fractional changes in mobility, that we observed throughout the treatment [Chapter 5, this thesis]. In addition, the reported risk of marker-drop is as high as 14% [19], while other authors suggested that as much as 25% of the inserted markers could not be detected throughout the treatment [20]. Transthoracic marker placement is comparable to a CT-guided biopsy and complications such as pneumothorax may occur in up to 46% [21]. This complication is potentially fatal for these patients due to their compromised respiratory function.

In our analyses on respiration-gated treatment, all patients were scanned during uncoached quiet respiration after a reproducible pattern of respiration was observed. However, one should be aware that the amplitude and frequency of the respiratory

signal can vary during free breathing, especially in patients with limited pulmonary function. It has been reported that respiratory coaching using visual feedback and/or audio prompting can increase the gating window [22]. The issue whether respiratory coaching can be used in stage III NSCLC patients is topic of ongoing research. If this seems applicable, the gating window can be prolonged, which would shorten the treatment time for each fraction.

In stage III NSCLC, the current standard treatment consists of concurrent chemo-radiotherapy, a combination that has shown superior local control and survival rates when compared to sequential chemotherapy and radiotherapy [23, 24]. However, an important limiting factor in the management of stage III NSCLC is treatment-related toxicity, such as radiation-induced pneumonitis. In addition, unexpected late toxicities have been reported in trials with radiation dose escalation after platinum based induction chemotherapy [25, 26]. One of the main causes of these toxicities is the relatively large volume that has to be treated in locally advanced lung cancer. Thus, in order to decrease the risk of radiation-induced toxicity, treatment volumes have to be reduced. Our analysis reveals that considerable volumetric and dosimetric gains can be achieved in most stage III lung cancer patients with the use of individualized PTVs. The additional gains that can be established with respiratory gating are generally modest, but correlate strongly with the reduction in mobility of the target volume. Since stage III lung tumors consist of a primary tumor and mediastinal lymph nodes, a reduction in mobility can be attributed to both these 'individual' structures. We also demonstrated that modest, but significant, dosimetric benefits can be obtained in tumors located in the middle and lower lobes. These two issues once again underscore the need for careful patient selection. Furthermore, our analysis shows a correlation between the reduction of toxicity parameters (V_{20} and MLD) and the PTV reduction achieved with respiratory gating, which can be used to identify benefits of gating in individual patients with stage III lung cancer. This correlation seems very obvious. However, we found this correlation to be valid for all GTV sizes which contradicts an earlier report that found dosimetric benefits for only GTVs smaller than 100-150 cm^3 [27].

SRT for stage I NSCLC requires careful monitoring of inter-fractional geometric changes of the target volume. These time-trends can arise due to changes in tumor volume, spatial position, or mobility during the course of radiotherapy. The former has

been described for several tumor sites, including locally advanced stage NSCLC [28] and head and neck cancer [29]. We observed an initial increase in GTVs and ITVs of >10 cm^3 in only 5% of the stage I tumors treated with SRT, indicating that changes in tumor volume are not a very important reason for inter-fractional variations in target volumes during SRT for lung cancer. However, an important finding of our analysis is the incidence of inter-fractional positional shifts of ITVs during the 3-5 weeks course of SRT in a substantial portion of tumors. These shifts occur as early as one week after the start of SRT and may be caused by radiation-induced changes in the surrounding normal tissues, such as edema or retraction. Furthermore, we observed a change in 3D tumor mobility of >3 mm in 20% of tumors. It is of key importance that the interfraction changes in tumor position were not solely caused by changes in tumor mobility. This may be explained by the fact that 4DCT scanning was performed during uncoached quiet respiration in patients with generally poor pulmonary function, e.g. due to chronic obstructive pulmonary disease, which can cause variations in the respiratory signal at different 4DCT scans. These findings illustrate the importance of adequate treatment verification, e.g. by repeated imaging and adjustment of treatment plans during SRT for lung cancer in order to maintain adequate target coverage. This is performed for all patients treated with SRT in the VU University medical center for stage I NSCLC. Instead of repeated treatment planning, the geometric accuracy of the treatment can be verified prior to each fraction, which enables adjustment of the treatment portals. However, inter-fractional changes of the target consist of a spatial and a volumetric component, both of which have to be accounted for. For this purpose, measures have to be implemented for adequate imaging of the target volume, such as use of a cone beam CT scan that is installed at the treatment unit. For hypofractionated SRT an online verification protocol should be used in order to reduce both random and systematic errors and adjust treatment portals to the actual tumor position prior to each fraction. However, the clinical use of online verification requires additional treatment time. Furthermore, cone beam CT images should be reconstructed rapidly and should be of high quality. The main restrictions of cone beam CT imaging are the image acquisition time (usually 1 minute), the reconstruction time and the image quality. Data collection is relatively slow due to the relatively slow gantry rotation. For lung tumors, this can result in respiration-induced artifacts, such as blurring and distortion, which can be compared to the images acquired from a slow CT scan. However, a recent report stated that image quality was sufficient for accurate discrimination of soft-tissue structures, and

that lung tumors were clearly visualized [30]. Two recent publications report on the reduction of respiration-induced artifacts in cone beam CT images by simultaneous recording of the patient's respiratory cycle to obtain time-resolved images [31], and through incorporation of a patient's motion model into the image reconstruction process [32].

Finally, our analysis confirms the finding of earlier reports that regression of lung tumors is a slow process, as significant decreases in target volumes have been observed after the fourth week of SRT [Chapter 5, this thesis]. Most tumor regression was, however, observed in the first three months after completion of SRT, which underscores the need for adequate follow-up. Another important reason for adequate follow-up is that this patient group is at risk for developing second primary lung tumors or regional recurrences, for which they can still undergo radical treatment with curative intent.

Future directions to optimize 4D radiotherapy

Several issues have to be established to optimize the clinical benefit of 4D radiotherapy. First, the reproducibility of respiratory motion during the patient's breathing cycles has to be guaranteed. The amplitude and frequency of the respiratory signal can vary during free breathing. This may lead to systematic and/or random errors in the entire chain of treatment planning and execution. Therefore, further research on the reproducibility of respiratory waveforms and tumor position is necessary to facilitate the clinical use of gated radiotherapy. One method for improving reproducibility is respiratory coaching. However, it remains to be tested whether respiratory coaching is generally applicable in lung cancer patients, as many of these patients have cardio-pulmonary co-morbidity. Theoretically, respiratory coaching offers a potential clinical application for radiotherapy in lung cancer, particularly for SRT. Since this treatment is administered in a limited amount of fractions, one has to make sure that a change in the respiratory signal, compared to that during 4D image acquisition, does not lead to unnecessary tumor miss. For this purpose predictive software is required at the treatment unit that adequately compares the respiratory signal during each fraction with that recorded during 4D image acquisition in an effort to obtain a more reproducible target volume.

It has been reported that respiration-induced motion can lead to significant changes in the dose distribution in normal organs, due to the fact that the doses to normal tissues are incorrectly displayed without including patient-related geometric uncertainties. [33]. However, it is presently not possible to fully explore the dosimetric benefits of 4DCT data, as current commercial treatment planning systems are not capable to incorporate 4DCT data in dose-calculation (time-weighted dosimetry), which is essential to adequately assess the risk of normal tissue toxicity. In addition, an adequate dosimetric analysis of a 4D treatment plan includes the total mobility of the target volume, as well as that of adjacent uninvolved organs. For this purpose, the ICRU Report 62 [3] recommends the use of planning organ at risk volumes (PRVs) in order to account for geometric uncertainty. However, generation of PRVs requires knowledge on organ mobility, which is not generally available. Furthermore, deformable registration, a software tool that relates 4DCT volumes of different respiratory phases to each other, is also not commercially available. This compromises the clinical use of 4DCT information, both for large tumors (e.g. stage III NSCLC) and normal organs at risk.

Conclusions

This thesis deals with the clinical implementation of 4DCT scanning in radiotherapy practice for lung cancer. Several chapters highlight the fact that determination of individual margins should replace the use of 'population based' margins. Radiotherapy planning based on individual 4DCT data greatly reduces the risk of geometric errors in treatment delivery for both stage I and stage III NSCLC. In addition, it enables respiration-gated treatment delivery in order to achieve further PTV reduction. The incorporation of 4DCT data into lung cancer treatment planning has paved the way for the routine clinical use of image-guided radiotherapy. It ensures that complex radiation treatment can be delivered precisely. This may ultimately lead to improved tumor control and reduced treatment-related toxicity.

References

1. van Sörnsen de Koste JR, Lagerwaard FJ, Nijssen-Visser MR, et al. Tumor location cannot predict the mobility of lung tumors: a 3D analysis of data generated from multiple CT scans. *Int J Radiat Oncol Biol Phys* 2003;56:348-354

2. Rietzel E, Chen GT, Choi NC, et al. Four-dimensional image-based treatment planning: Target volume segmentation and dose calculation in the presence of respiratory motion. *Int J Radiat Oncol Biol Phys* 2005;61:1535-1550

3. International Commission on Radiation Units and Measurements. *ICRU report 62: Prescribing, recording, and reporting photon beam therapy* (Supplement to ICRU report 50). Bethesda, MD: ICRU 1999

4. van Sörnsen de Koste JR, Lagerwaard FJ, de Boer H, et al. Are multiple CT scans required for planning curative radiotherapy in lung tumors of the lower lobe? *Int J Radiat Oncol Biol Phys* 2003;55:1394-1399

5. Yamada K, Soejima T, Yoden E, et al. Improvement of three-dimensional treatment planning models of small lung targets using high-speed multi-slice computed tomographic imaging. *Int J Radiat Oncol Biol Phys* 2002;54:1210-1216

6. Lagerwaard FJ, van Sörnsen de Koste JR, Nijssen-Visser MR, et al. Multiple "slow" CT scans for incorporating lung tumor mobility in radiotherapy planning. *Int J Radiat Oncol Biol Phys* 2001;51:932-937

7. Timmerman R, Papiez L, McGarry R, et al. Extracranial stereotactic radioablation: results of a phase I study in medically inoperable stage I non-small cell lung cancer. *Chest* 2003;124:1946-1955

8. Lee SW, Choi EK, Park HJ, et al. Stereotactic body frame based fractionated radiosurgery on consecutive days for primary or metastatic tumors in the lung. *Lung Cancer* 2003;40:309-315

9. Hof H, Herfarth KK, Munter M, et al. Stereotactic single-dose radiotherapy of stage I non-small-cell lung cancer (NSCLC). *Int J Radiat Oncol Biol Phys* 2003;56:335-341

10. Onishi H, Araki T, Shirato H, et al. Stereotactic hypofractionated high-dose irradiation for stage I nonsmall cell lung carcinoma: clinical outcomes in 245 subjects in a Japanese multiinstitutional study. *Cancer* 2004;101:1623-1631

11. Uematsu M, Shioda A, Suda A, et al. Computed tomography-guided frameless stereotactic radiotherapy for stage I non-small cell lung cancer: a 5-year experience. *Int J Radiat Oncol Biol Phys* 2001;51:666-670

12. Lagerwaard FJ, Senan S, van Meerbeeck JP, et al. Has 3-D conformal radiotherapy (3D CRT) improved the local tumour control for stage I non-small cell lung cancer? *Radiother Oncol* 2002;63:151-157

13. Engelsman E, Remeijer P, van Herk M, et al. Field size reduction enables iso-NTCP escalation of tumor control probability for irradiation of lung tumors. *Int J Radiat Oncol Biol Phys* 2001;51:1290-1298

14. Cover KS, Lagerwaard FJ, Senan S. Color intensity projections: a rapid approach for evaluating four-dimensional CT scans in treatment planning. *Int J Radiat Oncol Biol Phys* 2006;64:954-961

15. Onimaru R, Shirato H, Kitamura K, et al. Tolerance of organs at risk in small-volume, hypofractionated, image-guided radiotherapy for primary and metastatic lung cancers. *Int J Radiat Oncol Biol Phys* 2003;56:126-135

16. McGarry RC, Papiez L, Williams M, et al. Stereotactic body radiation therapy of early-stage non-small-cell lung carcinoma: phase I study. *Int J Radiat Oncol Biol Phys* 2005;63:1010-1015

17. Seppenwoolde Y, Shirato H, Kitamura K, et al. Precise and real-time measurement of 3D tumor motion in lung due to breathing and heartbeat, measured during radiotherapy. *Int J Radiat Oncol Biol Phys* 2002;53:822-834

18. Murphy MJ. Fiducial-based targeting accuracy for external-beam radiotherapy. *Med Phys* 2002;29:334-344

19. Shirato H, Harada T, Harabayashi T, et al. Feasibility of insertion/implantation of 2.0-mm-diameter gold internal fiducial markers for precise setup and real-time tumor tracking in radiotherapy. *Int J Radiat Oncol Biol Phys* 2003;56:240-247

20. Imura M, Yamazaki K, Shirato H, et al. Insertion and fixation of fiducial markers for setup and tracking of lung tumors in radiotherapy. *Int J Radiat Oncol Biol Phys* 2005;63:1442-1447

21. Haramati LB, Austin JH. Complications after CT-guided needle biopsy through aerated versus nonaerated lung. *Radiology* 1991;181:778

22. Kini VR, Vedam SS, Keall PJ, et al. Patient training in respiratory-gated radiotherapy. *Med Dosim* 2003;28:7-11

23. Furuse K, Fukuoka M, Kawahara M, et al. Phase III study of concurrent versus sequential thoracic radiotherapy in combination with mitomycin, vindesine, and cisplatin in unresectable stage III non-small-cell lung cancer. *J Clin Oncol* 1999;17:2692-2699

24. Fournel P, Robinet G, Thomas P, et al. Randomized phase III trial of sequential chemoradiotherapy compared with concurrent chemoradiotherapy in locally advanced non-small-cell lung cancer: Groupe Lyon-Saint-Etienne d'Oncologie Thoracique-Groupe Francais de Pneumo-Cancerologie NPC 95-01 Study. *J Clin Oncol* 2005;23:5910-5917

25. Marks LB, Garst J, Socinski MA, et al. Carboplatin/paclitaxel or carboplatin/vinorelbine followed by accelerated hyperfractionated conformal radiation therapy: report of a prospective phase I dose escalation trial from the Carolina Conformal Therapy Consortium. *J Clin Oncol* 2004;22:4329-4340

26. Miller KL, Shafman TD, Anscher MS, et al. Bronchial stenosis: an underreported complication of high-dose external beam radiotherapy for lung cancer? *Int J Radiat Oncol Biol Phys* 2005;61:64-69

27. Starkschall G, Forster KM, Kitamura K, et al. Correlation of gross tumor volume excursion with potential benefits of respiratory gating. *Int J Radiat Oncol Biol Phys* 2004;60:1291-1297

28. Erridge SC, Seppenwoolde Y, Muller SH, et al. Portal imaging to assess set-up errors, tumor motion and tumor shrinkage during conformal radiotherapy of non-small cell lung cancer. *Radiother Oncol* 2003;66:75-85

29. Barker JL Jr, Garden AS, Ang KK, et al. Quantification of volumetric and geometric changes occurring during fractionated radiotherapy for head-and-neck cancer using an integrated CT/linear accelerator system. *Int J Radiat Oncol Biol Phys* 2004;59:960-970

30. McBain CA, Henry AM, SykesJ, et al. X-ray volumetric imaging in image-guided radiotherapy: the new standard in on-treatment imaging. *Int J Radiat Oncol Biol Phys* 2006;64:625-634

31. Sonke JJ, Zijp L, Remeijer P, et al. Respiratory correlated cone beam CT. *Med Phys* 2005;32:1176-1186

32. Li T, Schreibmann E, Yang Y, et al. Motion correction for improved target localization with on-board cone-beam computed tomography. *Phys Med Biol* 2006;51:253-267

33. Rosu M, Dawson LA, Balter JM, et al. Alterations in normal liver doses due to organ motion. *Int J Radiat Oncol Biol Phys* 2003;57:1472-1479

Summary

In the **Introduction** to this thesis, an overview is provided about the current standard of external beam radiotherapy treatment planning and the use of population-based margins for target definition. Although 3-dimensional conformal radiotherapy has been a major step forward in treatment planning for lung cancer, geometric errors can be introduced if tumor mobility is not taken into account. Several approached are discussed to deal with this problem. Furthermore, respiration-correlated (4D) CT scanning is introduced as a measure to incorporate respiration-induced tumor motion into target definition. This enables the use of individualized margins for mobility and, in addition, makes it possible to apply respiration-gated radiotherapy.

The implementation of 4DCT scanning into clinical practice requires validation of this approach. This is provided in **Chapter 2**, in which the generation of an internal target volume (ITV) in stage I lung cancer patients using a single 4DCT scan was compared to that of six consecutive rapid 'multislice' CT scans and a single conventional CT scan to which standard margins were added. The results show that a single 4DCT scan generates comparable or larger ITVs than six rapid CT scans, thus improving target definition. Furthermore, the use of a single CT scan with a standard margin of 10 mm margin seemed inappropriate in some cases.

The use of 4DCT scans in stage I lung cancer leads to an increased workload, as gross tumor volumes (GTVs) and/or normal organs have to be contoured in at least ten respiratory phases. To reduce the workload, measures have to be implemented for quick ITV generation. **Chapter 3** illustrates that maximum intensity projections (MIPs) are a reliable post-processing tool for generating ITVs from 4DCT datasets. In addition, MIPs can be used for a rapid assessment of tumor mobility.

The clinical toxicity of hypofractionated stereotactic radiotherapy (SRT) for stage I non-small cell lung cancer (NSCLC) is limited. However, as dose fractions of up to 20 Gy are used, a reduction in size of treatment portals reduces the risk of toxicity to adjacent structures. In **Chapter 4** a retrospective analysis is presented, which shows that respiration gated SRT enables a significant reduction to be achieved in normal tissue volume receiving the prescribed dose. In addition, a rapid assessment for

identification of patients that derive significant benefit from this approach is reported. Although planning target volumes can be reduced by over 50% with respiratory gating, compared to the use of standard margins, only 15% of the patients in this analysis qualify for this criterion.

Chapter 5 highlights the inter-fractional changes of the target volume that can occur during a course of SRT for stage I NSCLC. These have both a volumetric and a positional component. A significant decrease of the target volume was observed at the fourth week of treatment. On the contrary, inter-fractional positional shifts in the ITV of more than 5 mm were seen in up to 43% of patients, stressing the need to account for these possible time trends during the treatment course, e.g. by repeat CT planning or adequate on-board verification of the target volume.

Patients with lung cancer who present with stage I disease are in a minority, and most patients who are treated with high-dose radiotherapy have locally advanced, stage III disease. Concurrent chemo-radiotherapy has shown superior local control and survival rates for stage III NSCLC compared to sequential chemo-radiotherapy or radiation alone. However, concurrent chemo-radiotherapy has also substantially increased the incidence of treatment-related toxicity. As respiration-gated radiotherapy allows for a reduction in target volumes, the benefits of this approach were explored in **Chapter 6**, as well as incorporation of all respiration-induced motion into treatment planning. This analysis once again highlights the inappropriateness of population-based margins that are added to a GTV based on a single planning CT scan. Furthermore, it was observed that modest, but significant, dosimetric benefits (in V_{20} and mean lung dose) could be achieved, particularly for tumors located in the middle and lower lobes.

Samenvatting

In de **Introductie** van dit proefschrift wordt een overzicht gegeven betreffende de huidige klinische standaard van het planningsproces voor uitwendige bestralingen en het toevoegen van standaard marges om tot een uiteindelijk doelvolume te komen. Hoewel het uitvoeren van 3-dimensionale bestralingstechnieken een enorme stap voorwaarts is geweest voor bestralingsplanningen bij longkanker, kunnen geometrische onnauwkeurigheden worden geïntroduceerd wanneer geen rekening gehouden wordt met tumorbeweeglijkheid. Om dit klinische probleem op te lossen worden verschillende methoden belicht. Hiernaast wordt een korte beschrijving gegeven over ademhalings-gecorreleerde (4D) CT scans, welke het mogelijk maken om ademhalings-gerelateerde tumorbeweeglijkheid te incorporeren in de bepaling van het uiteindelijke doelvolume van de bestraling. Tevens verschaffen 4DCT scans de mogelijkheid om tijdens de behandeling de bestraling alleen toe te dienen tijdens een bepaald deel van de ademhalingscyclus ('gate'), welke vooraf bepaald wordt. Deze bestralingstoepassing wordt 'respiratory gating' genoemd.

De klinische implementatie van 4DCT scans vereist validatie van deze methode ten opzichte van de tot dan toe gebruikte klinische standaard. Dit wordt uiteen gezet in **Hoofdstuk 2**, waarin het 'internal target volume' (ITV; het volume dat alle posities van een tumor met zijn microscopische uitbreiding omvat), dat is gebaseerd op een enkele 4DCT scan, wordt vergeleken met dat zes conventionele, multislice CT scans en dat gebaseerd op een enkele conventionele CT scan na toevoeging van een standaard marge. De resultaten tonen dat een enkele 4DCT scan vergelijkbare of grotere ITVs oplevert in vergelijking met zes conventionele plannings-CT scans, waardoor het doelvolume nauwkeuriger kan worden gedefinieerd. Hiernaast blijkt dat zelfs het toevoegen van een standaard marge van 10 mm aan een ingetekend tumorvolume op basis van een enkele conventionele CT scan tot veel grotere doelvolumes leidt, die in sommige gevallen echter nog onvoldoende zijn.

De toepassing van 4DCT bij het stadium I niet-kleincellig longcarcinoom heeft geleid tot een aanzienlijke toename van de klinische werkdruk, daar het 'gross tumor volume' (al het aantoonbare tumorweefsel) en/of de normale omliggende organen ingetekend moet worden op tenminste tien fasen van de ademhalingscyclus. Hiertoe

moeten maatregelen worden getroffen om op een zo efficiënt mogelijke wijze een ITV te verkrijgen. In **Hoofdstuk 3** wordt geïllustreerd dat het gebruik van 'maximum intensity projections' (MIPs; een reconstructietechniek gebaseerd op CT informatie waarbij van elke pixel alleen de hoogste dichtheid wordt weergegeven) een betrouwbare methode vormen voor het genereren van ITVs uit alle 4DCT informatie. Ook wordt beschreven dat MIPs kunnen worden toegepast om op een snelle manier tumorbeweeglijkheid in kaart te brengen.

De klinische toxiciteit van gehypofractioneerde stereotactische radiotherapie voor het stadium I niet-kleincellig longcarcinoom is beperkt. Echter, omdat er per fractie doses tot 20 Gray worden toegediend, wordt de kans op toxiciteit verder verlaagd door de bestralingsvelden te verkleinen. In **Hoofdstuk 4** wordt een retrospectieve analyse beschreven, welke laat zien dat het toedienen van stereotactische bestraling tijdens een vooraf gedefinieerd deel van de ademhaling het mogelijk maakt om het volume aan normaal weefsel dat de totale dosis ontvangt, significant te reduceren. Tevens wordt een methode gepresenteerd waarmee op snelle wijze patiënten kunnen worden geselecteerd die het meeste voordeel zullen hebben van deze bestralingstoepassing. Uit de analyse blijkt verder dat hoewel met 'gating' doelvolumina met meer dan 50% kunnen worden gereduceerd in vergelijking met het gebruik van standaard marges, slechts 15% van de patiënten aan dit criterium voldoet.

In **Hoofdstuk 5** worden enkele belangrijke veranderingen gerapporteerd, die kunnen optreden tussen de verschillende sessies van een complete behandeling stereotactische radiotherapie voor het stadium I niet-kleincellig longcarcinoom. Deze bestaan uit zowel een verandering in grootte, als een verandering in positie van het doelvolume. Er werd een significante afname in grootte van het doelvolume waargenomen in de vierde week van de behandeling. Verandering in de positie van het doelvolume van meer dan 5 mm werden waargenomen bij tot wel 43% van de patiënten. Dit onderschrijft het belang om tijdens de behandeling rekening te houden met dergelijke trends. Dit kan bijvoorbeeld geschieden door het herhalen van de gehele planningsprocedure waarbij gebruik wordt gemaakt van een nieuwe plannings-CT scan of door middel van adequate verificatie van het doelvolume op het bestralingstoestel.

Bij een minderheid van de patiënten met niet-kleincellig longcarcinoom wordt de ziekte in een vroeg stadium (stadium I) gediagnostiseerd. De meeste patiënten die worden behandeld met hooggedoseerde radiotherapie, hebben de ziekte in een verder gevorderd stadium (stadium III). Van gelijktijdige behandeling met chemotherapie en radiotherapie bij het stadium III niet-kleincellig longcarcinoom is aangetoond dat dit een hogere locale tumorcontrole geeft en de overleving van deze patiëntengroep verbetert, in vergelijking met sequentiële behandeling met deze twee modaliteiten. Daar staat echter tegenover dat gelijktijdige toepassing van deze behandelingen aanzienlijk meer toxiciteit veroorzaakt. In **Hoofdstuk 6** wordt beschreven wat het dosimetrische voordeel is wanneer 'respiratory gating' wordt toegepast bij dit type tumoren, gezien het feit dat deze manier van bestralen het mogelijk maakt om kleinere doelvolumes te behandelen. De analyse die in dit hoofdstuk is uitgevoerd, toonde opnieuw aan dat het gebruik van standaard marges veel onnauwkeurigheid met zich meebrengt. Daarnaast werd aangetoond dat relatief geringe, doch wel statistisch significante, dosimetrische (zowel in V_{20} als in de gemiddelde longdosis) verbeteringen konden worden bereikt met het toepassen van 'respiratory gating'. Dit gold in het bijzonder voor tumoren welke gelokaliseerd waren in de midden- en onderkwab.

Dankwoord

Een proefschrift schrijven kun je niet alleen. Ik wil hier dan ook iedereen bedanken die ook maar enigszins heeft bijgedragen aan de totstandkoming hiervan met een extra paar handen, extra ideeën of simpelweg wat afleiding. Een aantal van hen wil ik in het bijzonder bedanken voor hun inzet en bijdrage. Gedurende mijn onderzoeksperiode op de afdeling radiotherapie van het VUMC hebben meerdere mensen, direct of indirect, hun medewerking verleend. Het is dus niet ondenkbaar dat ik iemand vergeet en bij voorbaat wil ik hiervoor mijn excuses aanbieden.

Allereerst wil ik mijn beide promotoren, prof. dr. S. Senan en prof. dr. B.J. Slotman bedanken. Beste Suresh, jouw interesse voor de snelle implementatie van 4DCT scanning in de kliniek heeft ervoor gezorgd, dat ik in hoog tempo dit promotie onderzoek kon uitvoeren. Dit was mede mogelijk door jouw scherp inzicht en sturing die je aan het onderzoek gegeven hebt. Tevens ben ik ontzettend onder de indruk geraakt van de onvoorstelbare database aan literatuur, die in jouw hoofd zit. Het zal een grote (en waarschijnlijk onmogelijke) uitdaging zijn voor mij om dit te evenaren. Ook wil ik mijn dank uitspreken voor je flexibele houding ten opzichte van mijn werktijden tijdens de voorbereidingen van mijn huwelijk met Ashra.

Beste Ben, jij hebt mij de mogelijkheid geboden om te werken op de afdeling radiotherapie van het VUMC en een groot deel van mijn AGNIO periode te wijden aan wetenschappelijk onderzoek. Als opleider en hoofd van de afdeling, en alle nevenactiviteiten die daarbij horen, ben je daarbij meer op de achtergrond betrokken geweest. Desalniettemin heb ik altijd veel gehad aan je snelle en kritische commentaar. Heel veel dank daarvoor en ik hoop ook de rest van mijn opleiding met veel plezier en wijsheid af te ronden.

Verder ben ik zeer veel dank verschuldigd aan mijn co-promotor dr. F.J. Lagerwaard. Beste Frank, het is voor een heel groot deel aan jou te danken dat dit '4D' proefschrift er ligt. Onder jouw kundige begeleiding zijn de meeste artikelen geschreven en samen met jou heb ik heel wat data vergaard in de afgelopen jaren. Dankzij de vele discussies en jouw zeer concrete inbreng zijn mijn wetenschappelijke schrijfstijl en denkpatroon enorm vooruit gegaan. Jouw promotie gedurende mijn onderzoeksperiode was voor mij een inspiratiebron om hetzelfde te bewerkstelligen.

De vele uren die we op de 'F' hebben doorgebracht, hebben dan ook zeker hun vruchten (en conditie) afgeworpen! Wellicht dat hier in de toekomst weer wat tijd voor is.

Daarnaast was er ook de zeer aangename en intensieve samenwerking met dr. J.R. van Sörnsen de Koste. Beste John, jij hebt mij getoond wat er allemaal mogelijk is met ruwe data. In een handomdraai toverde jij de mooiste figuren tevoorschijn voor artikelen, posters en powerpoint presentaties. Dankzij jou heb ik geleerd dat er in de wetenschap meerdere wegen naar Rome leiden en dat het niet erg is om halverwege een ingeslagen weg om te draaien en een andere te kiezen. Ook jouw promotie heeft mij uiteraard gemotiveerd om mijn onderzoeksperiode hiermee te bezegelen. Tevens heb je me veel tips gegeven die het maken van de lay-out van dit proefschrift hebben vergemakkelijkt. Heel hartelijk dank hiervoor.

Ik dank alle co-auteurs voor hun hulp en commentaar en natuurlijk ook al mijn collega's van de afdeling radiotherapie van het VUMC voor de getoonde belangstelling voor de voortgang van mijn onderzoek. Ik hoop ook in de toekomst nog heel prettig met jullie samen te werken.

Ik wil alle leden van de leescommissie danken voor het doorlezen en beoordelen van dit proefschrift.

Verder dank ik alvast mijn paranimfen, Ralph Mebus en Jan Underberg voor de morele steun tijdens mijn verdediging.

Mijn ouders wil ik heel erg bedanken voor alle mogelijkheden en steun die ze me hebben gegeven tijdens mijn studie en loopbaan tot nu toe. Heel veel dank voor deze uitstekende start. Jullie stonden, staan nog steeds, en zullen altijd voor mij klaarstaan als ik jullie nodig heb, ook wanneer ik het zelf niet besef. Ik kan alleen maar hopen dat ik zelf ook zo'n goede ouder zal zijn!

Tenslotte grote dank aan de allerbelangrijkste persoon in mijn leven. Lieve Ash, getrouwd met jou door het leven gaan, is de beste keus die ik ooit gemaakt heb. Jouw geduld, steun en begrip zijn werkelijk grenzeloos, getuige alle keren dat ik 's avonds achter de computer verdween. Dank je voor het feit dat je mij met veel praten door

een moeilijke periode hebt gesleept. Met elkaar gaan wij de toekomst met veel plezier tegemoet. Laten we beginnen met een lange vakantie. Wat dacht je van……Nieuw-Zeeland?

Curriculum vitae

René Widjai Marcel Underberg werd geboren op 7 april 1978 te Gainesville, Florida, USA. Na zijn basisschool periode ('De Beiaard' in Utrecht) en het afronden van het Gymnasium aan het College Blaucapel te Utrecht, startte hij in 1996 zijn opleiding geneeskunde aan de Vrije Universiteit te Amsterdam. Tijdens het keuzevak oncologie had hij zijn eerste ontmoeting met de radiotherapie in de vorm van een introductiecollege (door prof. dr. Slotman). In november 2002 werd het artsexamen behaald en kort hierop (januari 2003) startte hij zijn werkzaamheden als AGNIO op de afdeling radiotherapie van het VU medisch centrum te Amsterdam. Na een klinische periode van 10 maanden ving hij zijn promotie onderzoek aan in oktober 2003. Daar de afdeling radiotherapie kort daarna een eigen CT scanner kreeg met de mogelijkheid tot het vervaardigen van 4DCT scans, was de richting van het onderzoek al snel bepaald en het onderzoek verliep dan ook in hoog tempo. Zijn fulltime onderzoeksperiode eindigde op 1 maart 2005, waarna hij een half jaar stage liep op de afdeling interne-oncologie van het Zaans Medisch Centrum te Zaandam. Inmiddels is hij gestart met zijn opleiding tot radiotherapeut-oncoloog.

List of publications

1. **Underberg RWM**, Crul M, Beijnen JH, Schellens JHM. Farnesyltransferaseremmers: een nieuwe klasse oncolytica. *Pharm Weekbl* 2001;136:260-265

2. Crul M, Schoemaker NE, Pluim D, Maliepaard M, **Underberg RW**, Schot M, Sparidans RW, Baas P, Beijnen JH, van Zandwijk N, Schellens JHM. Randomized phase I clinical and pharmacologic study of weekly versus twice-weekly dose-intensive cisplatin and gemcitabine in patients with advanced non-small cell lung cancer. *Clin Cancer Res* 2003;1:3526-3533

3. **Underberg RW**, Lagerwaard FJ, Cuijpers JP, Slotman BJ, van Sörnsen de Koste JR, Senan S. Four-dimensional CT scans for treatment planning in stereotactic radiotherapy for stage I lung cancer. *Int J Radiat Oncol Biol Phys* 2004;15;60:1283-1290

4. **Underberg RW**, Lagerwaard FJ, Slotman BJ, Cuijpers JP, Senan S. Benefit of respiration-gated stereotactic radiotherapy for stage I lung cancer: An analysis of 4DCT datasets. *Int J Radiat Oncol Biol Phys* 2005;62:554-560

5. **Underberg RW**, Lagerwaard FJ, Slotman BJ, Cuijpers JP, Senan S. Use of maximum intensity projections (MIP) for target volume generation in 4DCT scans for lung cancer. *Int J Radiat Oncol Biol Phys* 2005;63:253-260

6. van Sörnsen de Koste JR, Senan S, **Underberg RW**, Oei SS, Elshove D, Slotman BJ, Lagerwaard FJ. Use of CD-ROM-based tool for analyzing contouring variations in involved-field radiotherapy for Stage III NSCLC. *Int J Radiat Oncol Biol Phys* 2005;63:334-339

7. **Underberg RW**, Lagerwaard FJ, van Tinteren H, Cuijpers JP, Slotman BJ, Senan S. Time trends in target volumes for stage I non-small-cell lung cancer after stereotactic radiotherapy. *Int J Radiat Oncol Biol Phys* 2006;64:1221-122

8. van der Geld YG, Senan S, van Sörnsen de Koste JR, van Tinteren H, Slotman BJ, **Underberg RW**, Lagerwaard FJ. Evaluating mobility for radiotherapy planning of lung tumors: A comparison of virtual fluoroscopy and 4DCT. *Lung Cancer* 2006;53:31-37

9. **Underberg RW**, van Sörnsen de Koste JR, Lagerwaard FJ, Vincent A, Slotman BJ, Senan S. A dosimetric analysis of respiration-gated radiotherapy in patients with stage III lung cancer. *Radiat Oncol* 2006;1:8